Analysis of Glycosaminoglycan Biosynthetic Intermediates and Development of Comparative Quantification Method Using Novel β-Xylosides

June 2018

Yuya Otsuka

A Thesis for the Degree of Ph.D. in Engineering

Analysis of Glycosaminoglycan Biosynthetic Intermediates and Development of Comparative Quantification Method Using Novel β-Xylosides

June 2018

Graduate School of Science and Technology
Keio University

Yuya Otsuka

Abstract

Glycosaminoglycans (GAGs) are linear and anionic polysaccharides found in extracellular matrices, and are related to several intracellular biological phenomena. Their structure is highly heterogeneous in terms of their chain length and modification, and this structural diversity is closely related to their biological functions. The structure of GAGs is regulated by the biosynthetic mechanisms; hence, a method for evaluating the GAG production capability including their biosynthetic intermediates is needed for the structure-function relationship studies. β-Xylosides have been used artificial acceptors for GAG; however, the structures of β-xylosides appropriate for investigation of GAG intermediates are not yet developed. Therefore, it was the aim of this study to discover a β-xyloside suitable for in-depth analysis of GAG biosynthetic intermediates in cells and to establish a comparative quantification method. The thesis is composed of six sections.

In chapter 1, general information on GAG and the saccharide primer method was summarized, and then issues in GAG related bioscience were clarified. Additionally, the aim of the study was described.

In chapter 2, the synthetic scheme for β-xylosides that have *O*-xylosyl amino acid residues was established using chemoenzymatic condensation.

In chapter 3, the priming abilities of the four β-xylosides in normal human dermal fibroblast (NHDF) cells were examined. By optimization of sample preparation and liquid chromatography-tandem mass spectrometry (LC–MS/MS) conditions, an analytical method for phosphorylated oligosaccharides was established, and then the saccharide primer appropriate for comparative quantification of GAG intermediate was determined.

In chapter 4, a comparative quantification method for elongated oligosaccharides using stable-isotope-labeled saccharide primer was established. The method was validated using GAG biosynthesis inhibitors. The result indicates that the method could clarify differences in the mode of action of the examined GAG inhibitors.

In chapter 5, the effect of exogenous sulfated GAGs on endogenous GAG production was examined by the comparative quantification method. The method revealed that certain sulfated GAGs stimulate NHDF cells to increase endogenous GAG production.

In chapter 6, the results and discussion of the thesis were summarized and the perspective of the method established in the thesis was described.

In the present thesis, the feasibility of saccharide primer method using β-xyloside for quantitative and qualitative studies for the capability of GAG intermediate biosynthesis was demonstrated. The saccharide primer method was applied to evaluate the effect of exogenous GAGs on endogenous GAG production. The effect of exogenous GAG on endogenous GAG production was successfully confirmed by the established method. This method will lead to an understanding of both GAG biosynthetic mechanisms and the structure-activity relationship of the GAG, as well as drive GAG-based drug discovery.

Table of Contents

Chapter 1
General Introduction

1.1 Glycosaminoglycans

1.1.1 General information

Glycosaminoglycans (GAGs), linear and anionic polysaccharides that comprise of alternative disaccharide units, are main components of extra- and pericellular matrices. In accordance with the structure of repeating disaccharide units, GAGs are classified into four species, which are hyaluronan (HA), chondroitin sulfate/dermatan sulfate (CS/DS), heparan sulfate/heparin (HS/Hep), and keratan sulfate (KS). Although GAGs are ubiquitously distributed in tissues and biological fluid, the structures found in tissues are widely varied. Details of the classification, structural features, and main distribution of the GAGs are summarized in Table 1-1.

Table 1-1 Structural and biological features of glycosaminoglycans.[1]

Classification	Disaccharide units	Molecular weight	Sulfation	Distribution
HA	4GlcA1β-3GlcNAc1β-	4–8000 kDa	No sulfated	Synovial fluid, vitreous humor
CS/DS	4GlcA(IdoA)1β-3GalNAc1β-	5–50 kDa	Hydroxyl groups	Cartilage, tendon, skin, ligament
HS/Hep	4GlcA(IdoA)1α-GlcNHR1β- (R = Ac or H)	5–50 kDa	Hydroxyl and amino groups	Blood vessel wall, Intestinal mucosa
KS	4Gal1β-4GlcNAc1β-	4–19 kDa	Hydroxyl groups	Cornea

Except for HA, all GAGs are sulfated on their hydroxyl or amino groups, and are bound to core proteins of proteoglycan side chains. The disaccharide units composing CS/DS and HS are named in accordance with their sulfated pattern. For instance, CS-A unit indicates a -4 glucuronic acid (GlcA) β1-3 *N*-acetylgalactosamine (GalNAc) (4-*O*-sulfate) β1- structure. The nomenclature of disaccharide units is summarized in Figure 1-1. Besides those described above, some minor disaccharide

units regarded to have sulfated of 3-*O*-groups on GlcA residues have been found in CS/DS.[2] Because of their chain length, disaccharide sequences, and sulfation degrees, the GAG chains are basically highly heterogeneous.

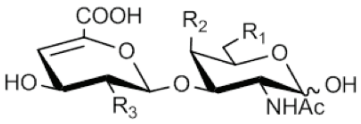

Disaccharide unit	R_1	R_2	R_3
0S (Δdi-0S)	OH	OH	OH
CS-A (Δdi-4S)	OSO_3Na	OH	OH
CS-B (Δdi-SB)	OSO_3Na	OH	OSO_3Na
CS-C (Δdi-6S)	OH	OSO_3Na	OH
CS-D (Δdi-SD)	OH	OSO_3Na	OSO_3Na
CS-E (Δdi-SD)	OSO_3Na	OSO_3Na	OH
TriS (Δdi-triS)	OSO_3Na	OSO_3Na	OSO_3Na

Figure 1-1 The structure of CS disaccharide units. The presented disaccharide unit is an unsaturated disaccharide obtained by CS lyase digestion.

1.1.2 Biological activity

Sulfated GAGs have attracted much interest for several decades because of their unique and wide range of biological functions (Figure 1-2); many studies on sulfated GAGs have been conducted for drug discovery. Specifically, heparin is one of the most investigated GAGs because of its biological function and high potency for therapeutic applications such as anti-coagulants. This bioactivity is mainly attributed to the binding region for anti-coagulant factors such as antithrombin III (Figure 1-3).[3] Moreover, HSs are crucially involved with numerous extracellular signaling events such as cell development and angiogenesis through various growth factors or cytokines.[4,5] For example, HS/Hep allows specific interactions with various growth factors and their receptors. Association of HS with both fibroblast growth factors (FGFs) and FGF receptors (FGFRs) results in an increase in the 1:1 dimer of the FGF–FGFR complex. Consequently, HS and heparin can stabilize the FGF-FGFR complex and enhance the activation of intracellular signaling pathways.[6,7]

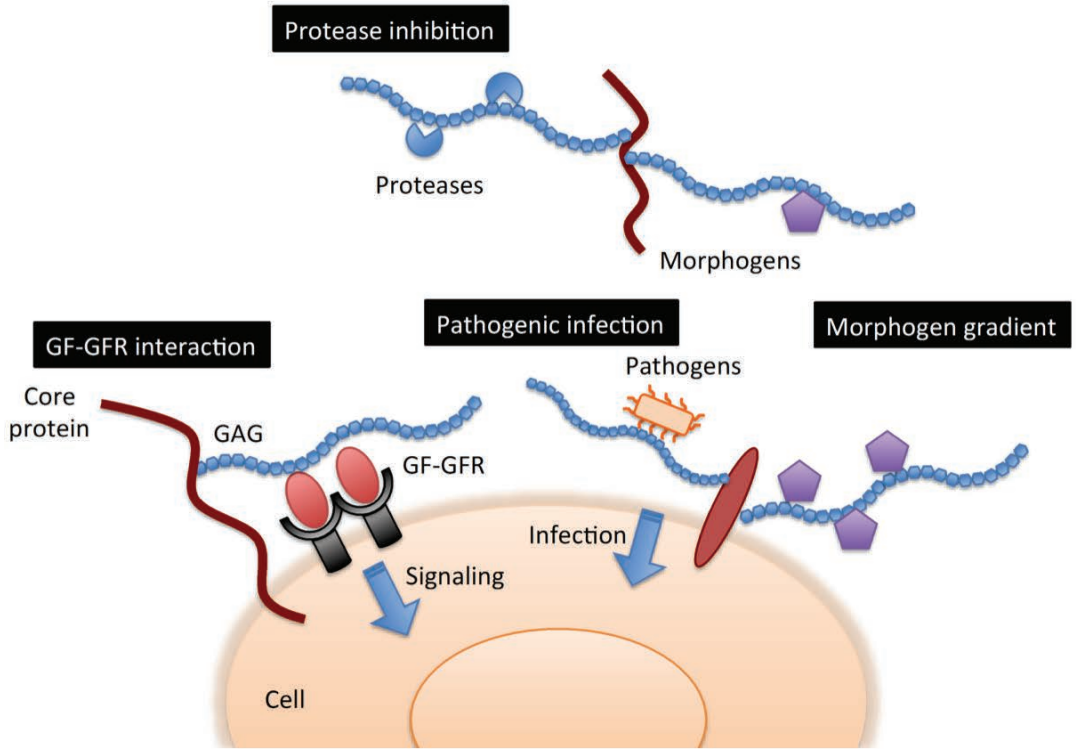

Figure 1-2 Multiple roles of GAGs in biological events.

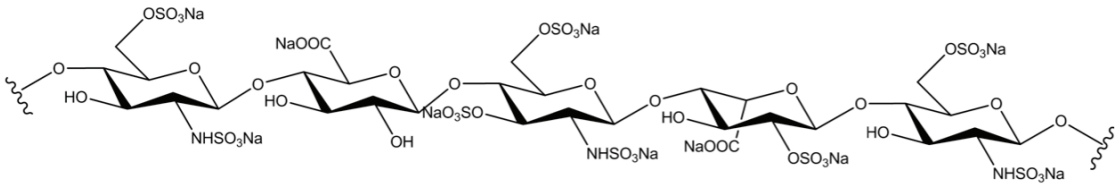

Figure 1-3 Heparin pentasaccharide structure for AT III binding.

CS and DS are also known to contribute to various biological events through non-covalent interaction with growth factors, cytokines, chemokines, morphogens, and small molecules. For example, highly sulfated CSs such as CS-E have been demonstrated to bind to various growth factors such as epidermal growth factors (EGF), FGFs, platelet–derived growth factor (PDGF), vascular endothelial growth factor (VEGF), and transforming growth factor β (TGFβ).[8] Moreover, CSs can associate with microbial pathogens.[9–11] These interactions are due to the sulfated degrees and the sulfated positions and sequences; hence, the characterization of the mechanism of

CS-protein interactions is an issue that needs to be solved in order to understand the biological meaning of the structural variation of the CS chain.

Table 1-2 Some of the putative molecular interactions exhibited by GAGs.[12]

GAGs	ECM proteins	Signaling molecules	Cell adhesion molecules	Others
HS/Hep	Fibronectin; fibrin; collagen types I, III, V; laminin-1; pleiotropin (PTN); tenascins-C, -R; thrombospondin; vitronectin; fibrillin-1; fibulin-2; slit-1, -2	FGF family; HB-EGF; hepatocyte growth factor (HGF)/scatter factor (SF); insulin-like growth factor (IGF)-I, -II; Wnt1, 3a; chordin; Noggin; Slit/Robo; interferon γ; PDGF; VEGF; TGFβ1, 2; midkine; PTN; angiopoietin-3; granulocyte macrophage colony-stimulating factor (GM-CSF); interleukin (IL)-8; IFN-γ-inducible protein of 10 kDa (IP-10); monocyte chemotactic protein (MCP)-1, -4; regulated on activation, normal T cell expressed and secreted (RANTES); tumor necrosis factor (TNF)α,β	Neural cell adhesion molecule (N-CAM); L-selectin; P-selectin; macrophage-1 antigen (MAC-1); platelet endothelial cell adhesion molecule-1 (PECAM-1)	Acetylcholinesterase; thrombin; lipoprotein lipases; heparin cofactor II; neutrophil elastase; plasminogen activator inhibitor; matrix metalloproteinase (MMP)7; apolipoprotein (Apo) B/E; amyloid precursor protein; amyloid precursor-like protein-2; cathepsin-X; viral coat proteins (Tat papilloma virus, cytomegalo virus); microbes and microbial products;
CS	Tenascins-C, -R; cartilage matrix protein (CMP); fibulin-1,-2; fibronectin; fibrillin-1; amphoterin; collagen types V, VI	HB-GAM/PTN; FGF-2, -16, -18; PDGF-AA; angiostatin; midkine; pleiotropin; amphoterin; HB-EGF; VEGF; solute carrier (SLC); IP-10; stromal cell derived factor (SDF)-1β	N-CAM; integrins ($\alpha_5\beta_1/\alpha_4\beta_1$); CD44	PDGFRα; FGF receptor-1, -3; membrane-type-3 (MT3)-MMP; low density lipoprotein (LDL); glycolipids
DS	Collagen types I, II, VI, XII; matrilin 1; tropoelastin; matrix glycoprotein-1; fibronectin; tenascin-X	FGF-1, -2, -7; HGF/SF;TGFβ; PF-4; SLC; IP-10; SDF-1β; RANTES	ICAM-1; L-selectin; P-selectin; CD44	Heparin cofactor II; thrombin; activated protein C; protein C inhibitor; LDL; high density lipoprotein (HDL)
KS	Collagens			

1.1.3 Biosynthesis

Biosynthesis of polysaccharides, known as the third life chain followed by DNA and proteins, are not dictated by the central dogma. Many enzymes such as glycosyltransferases, sulfotransferases, sulfatases, and glycanases play important roles in the makeup of complicated structures of glycans. These enzymes function together in the synthesis of a wide variety of glycan structures. This system enables the modification and adoption of the GAG structure in response to environmental changes. On the other hand, this non-template biosynthesis system is unable to amplify GAG chains unlike DNA and proteins.

Biosynthesis of CS, DS and HS are initiated from the linkage tetrasaccharide, GlcA1β-3 galactose (Gal)1β-3Gal1β-4 xylose (Xyl)1β- construction (Figure 1-4). At first, Xyl-transferation occurs on the seine (Ser) residue on core proteins. Next, two Gal residues are successively elongated on the Xyl. Subsequently, GlcA is attached on the Gal residue. In CS/DS biosynthesis, GalNAc is attached on the GlcA residue in the tetrasaccharides. After that, GalNAc and GlcA are elongated alternatively. During chain elongation, some of the hydroxyl groups are sulfated by various sulfotransferases. For DS biosynthesis, GlcA residues are epimerized to IdoA and the 2-*O* group on the IdoA residues are sulfated.[13] During CS/DS biosynthesis, chondroitin polymerization factors, chondroitin synthases, chondtoitin sulfate GalNAc transferases, dermatan sulfate epimerases, and various sulfatases work in harmony to construct heterogeneous CS/DS chains. For HS/Heparin biosynthesis, the *N*-acetylglucosamine (GlcNAc) residue is attached to the GlcA residue of the tetrasaccharide instead of GalNAc attachment of CS/DS biosynthesis. exostosins (Exts), exostosis-like genes (Extls), *N*-deacetylase-*N*-sulfotransferase (NDST), HS epimerase, and various sulfatases are related to HS/Hep biosynthesis.

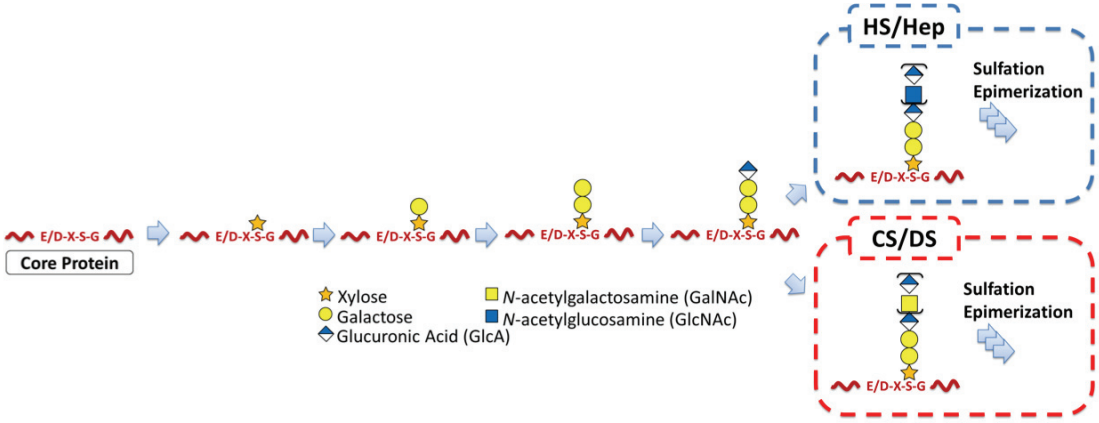

Figure 1-4 Biosynthesis flow of the linkage tetrasaccharide and GAG repeating disaccharide structures.

It has been reported that the phosphorylation/dephosphorylation of the Xyl and sulfation of the GalNAc residue attached to the linkage tetrasaccharide are strongly related to the chain length and amounts of GAG elongated on the tetrasaccharides.[13,14] According to reports, the phosphorylated Xyl residue is required for the construction of the linkage tetrasaccharide, while phosphorylation disrupts CS/DS-type chain elongation on the tetrasaccharide. Therefore, transient phosphorylation is important for the proper construction of GAG chains. In addition, Xyl phosphorylation is related to the sulfation efficiency of the GalNAc residue attached to GlcA of the linage tetrasaccharide.[15] Besides the phosphorylation of Xyl residues, various modifications on the tetrasaccharide have also been reported.[16–18] However, the regulation mechanisms of these modifications and the manner of regulation of the type and sulfation pattern of GAG chains are still unknown.

1.2 Saccharide primers

1.2.1 General information

Glycans have attracted much interest because of their unique and widely varied roles in biological phenomena, so structure–activity relationships of glycans have attracted considerable interest as well.[19] Structural and functional analyses of glycans require large amounts of highly purified samples; however, preparation of these samples

is usually very laborious because of their structural variety. Nevertheless, much effort has been made for the purification of the glycans from biological samples or chemical synthesis. The structural complexity, which is the branching and modification of the glycans, make it difficult to reach this aim. In addition, massive amount of biological resources are needed to purify enough amounts of glycans because the amounts of glycans in cells are much less than those of proteins.

Saccharide primers, which are artificial initiators of glycan biosynthesis, have been used to obtain oligosaccharides synthesized in cells and tissues. The primers have amphiphilic structure comprising hydrophobic groups and saccharide residues. The primers added to the medium are incorporated into cells and tissues, and transported to the endoplasmic reticulum (ER) and the Golgi apparatus where the primers are glycosylated through the glycan biosynthetic pathway. Finally the glycosylated primers are excreted into the medium. The glycosylation occurs according to the capability of glycan biosynthesis by the examined specimen (Figure 1-5). Therefore, saccharide primers have been used to obtain a variety of oligosaccharides and to investigate the glycan biosynthetic potency of the cells and tissues.

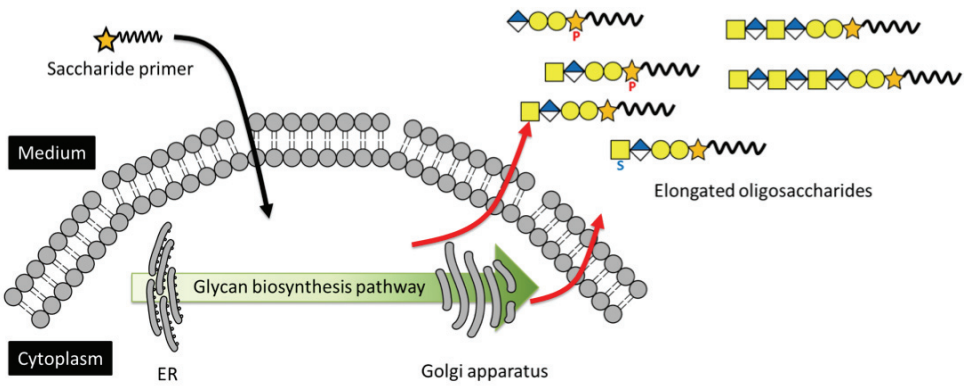

Figure 1-5 Saccharide primers prime oligosaccharides in a manner of glycan biosynthesis machinery.

The types of the elongated glycans are strongly dependent on the structure of saccharide primers. For instance, glycolipid such as gangliosides and lacto/neo-lacto glycolipids are elongated on *O*-alkyl lactosides[20, 21] and *O*-alkyl GlcNAcs[22], respectively.

For glycan side chains of glycoproteins, GAGs and *O*-glycans are elongated on β-xylosides and *O*-serinyl/threonyl-GlcNAcs, respectively. These saccharide primers can be considered as decoys of the biosynthetic initiator of glycoconjugates (Figure 1-6).

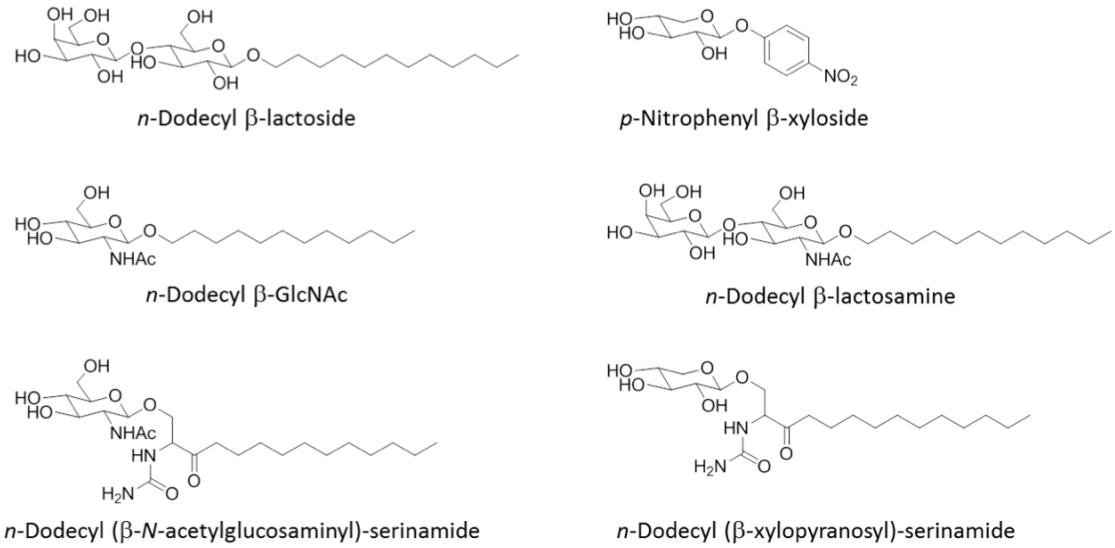

Figure 1-6 The structures of saccharide primers.

1.2.2 β-Xylosides

β-Xylosides have been used to obtain GAG-type glycans because of their priming abilities for GAG oligosaccharides. For example, Okayama *et al*. first showed that *p*-nitrophenyl-β-xylopyranoside (Xyl-*p*NP) can prime GAG-type oligosaccharide when added to chick cartilage cell culture.[23] 4-Methylumbelliphenyl-β-xylopyranoside,[24] β-estradiol-xylopyranoside,[25] naphthol xylopyranosides,[26–29] *C*-xylopyranosides,[30,31] and "click" xylopyranosides[32–35] have also been applied for the elongation of GAG oligosaccharides. These β-xylosides have been used not only as a saccharide primer to obtain the GAG-type oligosaccharides but also as a chemical tool to explore the species of glycans potentially produced by cells and the colocation of glycosyltransferases on the ER and Golgi apparatus.[36] However, the major foci in most of these studies have been on the amount, molecular weight, and GAG types of primed oligosaccharides, whereas there was not much attention has been paid to the intermediates of oligosaccharides primed on the β-xylosides.

1.3 Aims of this study

As described above, GAGs play important roles in several intercellular biological phenomena, whereas their structure–activity relationships remain unclear. The structure of GAG is strongly related to the biosynthetic mechanism and structure of the linkage tetrasaccharide. However, a method for evaluating the GAG production capability including GAG biosynthesis intermediates has not been developed. β-xylosides have been used as artificial initiators of GAG chains but the GAG chain intermediates elongate on them. Therefore, the aim of this thesis is to discover a β-xyloside suitable for in-depth analysis of GAG chain intermediates in cells and to establish a comparative quantification by the saccharide primer method. The thesis is composed of six sections.

The first chapter describes the structures and biological activities, and analytical methods are summarized. Additionally, the aim of the study is described.

The second chapter represents a study on the establishment of a synthetic scheme for β-xylosides that have *O*-xylosyl amino acid residues using chemoemzymatic condensation.

The third chapter represents a study on the priming ability of the four β-xylosides in NHDF cells. In this chapter, the difference in the priming ability including GAG intermediate oligosaccharides is clarified by the optimization of sample preparation and LC–MS/MS conditions.

The forth chapter represents the development of a comparative quantification method for elongated oligosaccharides using stable-isotope-coded saccharide primer. In this chapter, validation of the method was carried out by GAG biosynthesis inhibition assay.

The fifth chapter examines the effect of exogenous sulfated GAGs on endogenous GAGs production by the comparative quantification method.

The sixth chapter summarizes the results and discussions of the thesis. Furthermore, the future perspective of the method established in the study is described.

Chapter 2
Chemical Synthesis of Saccharide Primers by Chemoenzymatic Condensation

2.1 Introduction

N^{α}-lauroyl-*O*-β-D-xylopyranosyl-L-serinamide (Xyl-Ser-C12) showed better GAG oligosaccharide priming ability than did *p*-nitrophenyl xyloside (*p*NP-Xyl) and dodecyl xyloside (Xyl-C12).[37] These results imply that the aglycone structure including amino acid residues could be strongly affected by the priming ability of the xylosides. However, the relationship between the structure of the amino acid in aglycone and the priming ability has not been investigated. One reason for this matter is that the synthetic scheme of Xyl-Ser-C12 for preparing the derivatives on amino acid structures was not appropriate.

In a previous study, Xyl-Ser-C12 was synthesized from the glycosyl donor 2,3,4-tri-*O*-acetyl-D-xylopyranosyl trichloroacetimidate (Figure 2-1). This chemical synthesis requires multiple steps to control the reaction sites and anomeric selectivity of xylose. In addition, de-acetylation process in the final step may cause racemization of the Ser residue. These drawbacks make it difficult to change and modify the amino acid residue. To overcome these concerns, the synthetic scheme using chemoenzymatic condensation was developed.

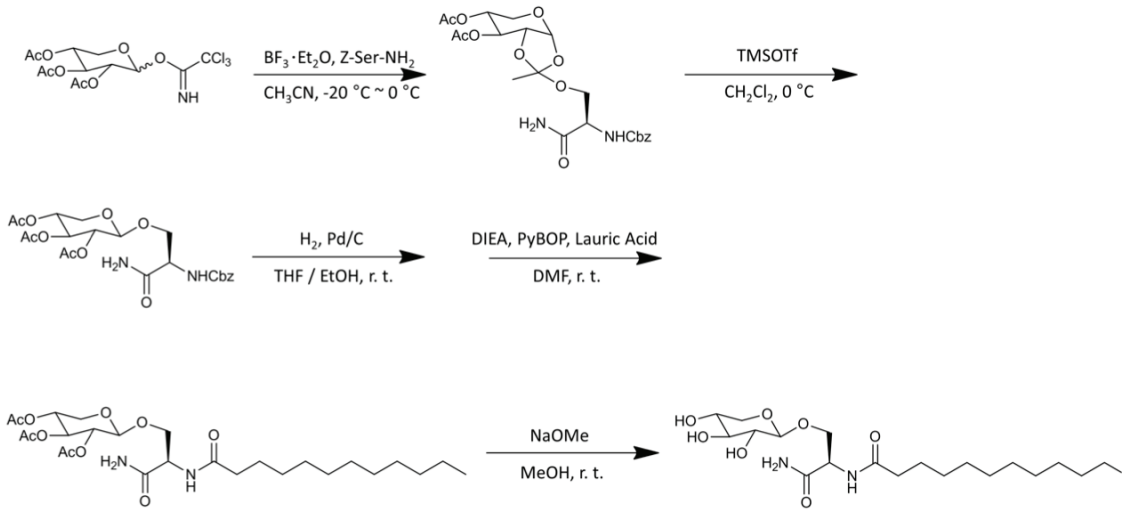

Figure 2-1 Synthesis of Xyl-Ser-C12.[37]

In chemoenzymatic condensation, high selectivity in reaction sites and anomeric configuration can be achieved because of the stereoselectivity of glycosidases used for synthesis.[38] Some studies demonstrated that xylasase, a kind of endo-glycanase, can attach xyloside to alchohols.[39–42] However, there is no information about the chemoenzymatic condensation of xylose with β-hydroxyl amino acids. The author's assumption is that endo-xylosidase catalyzes the condensation of xylose and β-hydroxyl amino acids. Therefore, the chemoenzymatic condensation using endo-xylosidase was examined in this study. Endo-β1-4 xylanase was chosen as an enzyme, xylo-oligosaccharides were chosen as the glycosyl donors, and *N-tert*-butoxycarbonyl serine (Boc-Ser-OH) or *N*-Boc-threonine (Boc-Thr-OH) was chosen as acceptors.

2.2 Materials and methods

Unless otherwise stated, all commercially available reagents and solvent were used without purification. All reactions were carried out at room temperature unless otherwise noted. All nuclear magnetic resonance (NMR) analyses were performed at 300 K with a 500 MHz Bruker Advance DRX 500 spectrometer (Bruker BioSpin, GmbH). The anomeric configuration of the products was confirmed by ^{1}H-NMR spectroscopy. All high resolution mass spectrometory (HRMS) spectra were recorded on a Synapt G2-S (Nihon Waters, Tokyo, Japan). The MS was calibrated by NaI before the experiments and the resolution was set at high resolution mode. Melting points were obtained on a Yanagimoto micro melting point apparatus (Yanagimoto Ltd., Kyoto,

Japan). Optical rotations were measured on a HORIBA SEPA-200A high sensitive polarimeter (Horiba, Tokyo, Japan).

2.2.1 Reverse hydrolysis of xylo-oligosaccharides using xylanases

Chemoenzymatic condensation is a condensation reaction using a reverse reaction of hydrolysis catalyzed by hydrolases. In this study, xylo-oligosaccharides were chosen as glycosyl donor, and Boc-Ser was chosen as an acceptor. As enzymes, endo-β1-4 xylanase (EC 3.2.1.8; *Trichoderma longibrachiatum*), hemicellulose (EC 3.2.1.4; *Aspergills niger*), and cellulose (EC 3.2.1.4; *Aspergills niger*) (Sigma-Aldrich Japan, Osaka, Japan) were screened.

30 mg of xylo-oligosaccharides and 25 mg of Boc-Ser-OH (Wako Pure Chemical Inc. Osaka, Japan) was suspended in 0.5 mL of 10 mM citrate buffer (pH 6.0), then, the pH of the suspension was adjusted to 3.0, 4.0, 5.0, and 6.0 by adding 6 M KOH. The citrate buffer was added into the suspension to adjust the total volume to 1 mL. 4 U of one of the enzymes was added into the solution, and then, the mixture solutions were mildly stirred to dissolve the enzymes completely. The reaction was carried out at 37 ºC. 10 μL of the reaction solutions were diluted with ultra-purified water, heated at 100 ºC for 1 min, filtrated by 0.22 μm filter, and then, subjected to LC–MS analysis.

2.2.2 LC–MS analysis

MS analysis were performed an amaZon speed ETD (iontrap mass spectrometer, Bruker Daltonics, Yokohama, Japan) coupled with a Nexera X2 (Shimadzu, Kyoto, Japan). Instrument control, data acquisition and analysis were performed with Hystar (Bruker Daltonics, Yokohama, Japan). 0.1 % formic acid and 0.1 % formic acid in MeCN were used as mobile phase A and B, respectively. The column temperature was set at 40 ºC. The data were recorded in negative ion mode from 100 to 600 *m/z*. Other ESI conditions were set as follows; Capillary voltage; -3.5 kV, dry gas temperature; 250 ºC, nebulizer; 3.10 psi, dry gas; 9 L/min, target amount; 70000 counts/scan, scan mode; ultra scan mode.

2.2.3 Synthesis of N^{α}-Lauroyl-*O*-*β*-D-xylopyranosyl-L-serinamide (Xyl-Ser-C12) and its derivatives

2.2.3.1 *N*-Boc-*O*-*β*-D-xylopyranosyl-L-serine (5)

1.8 g of Boc-Ser-OH was dissolved in 2 mL of 50 mM ammonium acetate, then, the pH of the solution was adjusted to 5.0 by 6 M KOH. 6.0 g of xylo-oligosccharides was added into the solution and stirred vigorously to dissolve the xylo-ligosaccharide completely. 320 mg of endo-β1-4 xylanase (EC 3.2.1.8; *Trichoderma longibrachiatum*) was suspended in 0.8 mL of 50 mM ammonium acetate, and then added into the solution. The solution was gently stirred by pipetting, and kept stirred with a magnetic stirrer at 40 ºC for 4 days. To quench the reaction, the solution was heated in a boiling water bath for 5 min, followed by removal of precipitate by filtration. The same volume of brine was added into the solution, and then the products was extracted using 40 mL of THF at least 3 times, followed by removal of the solvent by vacuum distillation. The crude product was purified by silica gel chromatography (2.5 cm i.d. × 20 cm, MeCN/water/formic acid = 97/2/1) to obtain *N*-Boc-*O*-β-D-xylopyranosyl-L-serine (5). Yield: 11.1 % (0.327 g). $[\alpha]^{20}$: −31.2 (cell length: 100 mm, c = 0.11 g/dL, λ = 589 nm). ^{1}H-NMR (D_2O): δ 4.39 (m ,1H, Hα), 4.37-4.39 (d, $J_{1,2}$ = 8 Hz, 1H, H-1), 4.24 (m, 1H, H-β_2), 3.93-3.95 (dd, $J_{\alpha,\beta}$ = 5.5 Hz and J_{gem} = 6 Hz, 1H, H-β_2), 3.92-3.95 (dd, $J_{4,5}$ =5.5 Hz and J_{gem} = 6 Hz, 1H, H-5β), 3.57-3.62 (ddd, $J_{4,5} = J_{3,4}$ = 4.5, 5, 5.5 Hz, 1H, H-4), 3.41-3.45 (dd, $J_{3,4} = J_{2,3}$ = 9 Hz, 1H, H-3), 3.27-3.31 (dd, $J_{4,5}$ = 10 Hz and J_{gem} = 11.5 Hz, 1H, H-5α), 3.25-3.29 (dd, $J_{2,3}$ = 8.5 Hz and $J_{1,2}$ = 9 Hz, 1H, H-2), 1.436 (s, 9H, (CH_3)$_3$). ^{13}C-NMR (D_2O); δ 173.94, 165.86, 157.67, 103.21 (C-1), 75.55 (C-3), 72.87 (C-2), 69.39 (C-4), 69.18 (Ser-β), 65.09 (C-5), 54.1 (Ser-α), 27.61 ((CH_3)$_3$). HRMS calcd for $C_{13}H_{23}NO_9Na$ $[M + H]^+$: 360.1265, found: 360.1277.

2.2.3.2 *N*-Boc-*O*-*β*-D-xylopyranosyl-L-serinamide (6)

40 mg (0.12 mmol) of compound 5 was dissolved in 2 mL of MeCN and stirred well, followed by adding 34 mg (0.18 mmol) of 1-(3-Dimethylaminopropyl)-3-ethylcarbodiimide Hydrochloride and 27 mg (0.18

mmol) of 1-hydroxybenzotriazole ammonium salt (HOBt-NH_3). The solution kept stirred for 2 h. After removal of MeCN by vacuum distillation, the reaction mixture was subjected to silica gel chromatography (2.5 cm i.d. × 20 cm, MeCN/water/formic acid = 97/3/0.1) to obtain *N*-Boc-*O*-*β*-D-xylopyranosyl-L-serinamide (6). Yield: 55.7 % (23.2 mg). ^{1}H-NMR (D_2O): δ 4.40-4.41 (d, $J_{1,2}$ = 8 Hz, 1H, H-1), 4.30 (m, 1H, Hα), 4.14-4.16 (m, 1H, H-β2), 3.95-3.98 (dd, $J_{4,5}$ = 5.5, 6 Hz and J_{gem} = 11.5 Hz, 1H, H-5β), 3.88-3.91 (dd, $J_{\alpha,\beta}$ = 4 Hz and J_{gem} = 10.5 Hz, 1H, H-β1), 3.59-3.64 (ddd, $J_{4,5}$ = $J_{3,4}$ = 4.5, 5, 5.5 Hz, 1H, H-4), 3.43-3.47 (dd, $J_{3,4}$ = $J_{2,3}$ = 9 Hz, 1H, H-3), 3.30-3.40 (dd, $J_{4,5}$ = 10.5 Hz and J_{gem} = 11.5 Hz, 1H, H-5α), 3.28-3.31 (dd, $J_{1,2}$ = 8 Hz and $J_{2,3}$ = 9 Hz, 1H, H-2) 1.45 (s, 9H, (CH_3)$_3$). ^{13}C-NMR; δ 175.09, 171.05, 157.67, 103.04 (C-1), 75.56 (C-3), 72.88 (C-2), 69.19 (C-4, Ser-β), 65.16 (C-5), 54.52 (Ser-α), 27.59 ((CH_3)$_3$). HRMS: calcd for $C_{13}H_{24}N_2O_9Na$ $[M + H]^+$: 359.1425, found: 359.1440.

2.2.3.3 *N*$^{\alpha}$-lauroyl-*O*-*β*-D-xylopyranosyl-L-serinamide (1)

24.5 mg (0.073 mmol) of compound 6 was dissolved in 1 mL of 4 mol/L HCl in dioxane and stirred well. After 2 h, the solvent and residual HCl were removed completely under reduced pressure. The residue was dissolved in 3 mL of water, and then 8.0 μL (0.073 mmol) of *N*-methylmorpholine was added. 22 mg (0.11 mmol) of lauric acid dissolved in 2 mL of EtOH was added into the solution, followed by adding 30 mg (0.11 mmol) of 4-(4,6-dimethoxy-1,3,5-triazin-2-yl)-4-methylmorpholinium chloride (DMT-MM). The solution kept stirred at 45 ºC overnight. The next day, saturated aqueous $NaHCO_3$ was added and the reaction mixture was extracted with AcOEt. The organic phase was removed under reduced pressure and the crude product was purified by silica gel column chromatography (1.0 cm i.d. × 20 cm, $CHCl_3$/MeOH = 4/1) to obtain Xyl-Ser-C12 (1) as a white solid. Yield: 63.3 % (19.3 mg). Melting point: 178.9 ºC. $[\alpha]^{20}$: −7.2 (c = 0.047), ^{1}H-NMR (CD_3COOD): δ 4.73-4.75 (dd, $J_{\alpha,\beta}$ = 2 and 5 Hz, 1H, H-α), 4.25-4.26 (d, $J_{1,2}$ = 7.5 Hz, 1H, H-1), 4.02-4.05 (dd, $J_{\alpha,\beta}$ = 4.5 Hz and J_{gem} = 10.5 Hz, 1H, H-β2), 3.84-3.87 (dd, $J_{4,5}$ = 5.3 Hz and J_{gem} = 11.5 Hz, 1H, H-5β), 3.65-3.68 (dd, $J_{\alpha,\beta}$ = 4.5 Hz and J_{gem} = 10.5 Hz, 1H, H-β1), 3.57-3.62 (ddd, $J_{3,4}$ = 5 Hz, $J_{4,5^{\alpha}}$ = 8.5 Hz, $J_{4,5^{\beta}}$ = 10 Hz, 1H, H-4), 3.47-3.50 (dd, $J_{2,3}$ = $J_{3,4}$ = 8.8 Hz, 1H, H-3), 3.27-3.30 (dd, $J_{1,2}$ = $J_{2,3}$ = 8.5 Hz, 1H, H-2), 3.17-3.22 (dd, $J_{4,5}$ = 10 Hz and J_{gem} = 11.5 Hz, 1H, H-5α), 2.19-2.22 (dd, J = 8.8 Hz, 2H, COCH_2), 1.46-1.51 (ddd, J = 7 and 14

Hz, 2H, $COCH_2CH_2(CH_2)_8$), 1.16 (m, 16H, $CH_2(CH_2)_8CH_3$), 0.74-0.77 (t, J = 7 Hz, 3H, $(CH_2)_8CH_3$). ^{13}C-NMR (CD_3COOD): δ 174.26 (amide), 103.21 (C-1), 75.42 (C-3), 72.72 (C-2), 69.02 (C-4, Ser-β), 64.47 (C-5), 52.15 (Ser-α), 35.25 ($COCH_2$), 25.06 ($COCH_2CH_2(CH_2)_8$), 22.04, 28.58, 28.74, 28.82, 28.96, 29.01, 31.37 ($CH_2(CH_2)_8CH_3$), 12.93 ($(CH_2)_8CH_3$). HRMS: Cald for $C_{20}H_{38}N_2O_7$: $[M + Na]^+$, 441,2571. Found: 441.2575.

2.2.3.4 *N*-Boc-*O*-*β*-D-xylopyranosyl-L-threonine (7)

Same method as for compound 5. Purified by silica gel column chromatography (2.5 cm i.d. × 20 cm, MeCN/water/formic acid = 96/3/1) to obtain compound 7. Yield: 12.5 % (0.180 g). $[\alpha]^{20}$: −27.1 (c = 0.1). ^{1}H-NMR (D_2O): d 4.47-4.49 (dd, $J_{\alpha,\beta}$ = 2 Hz and $J_{\beta,\gamma}$ = 6.5 Hz, 1H, H-β), 4.39-4.41 (d, $J_{1,2}$ = 7.5 Hz, 1H, H-1), 4.26 (m, 1H, H-α), 3.86-3.99 (dd, $J_{4,5}$, = 5.5 Hz and J_{gem} = 11.5 Hz, 1H, H-5β), 3.56-3.61 (ddd, $J_{4,5} = J_{3,4}$ = 5, 5.5, 9.5 Hz, 1H, H-4), 3.39-3.43 (dd, $J_{3,4} = J_{2,3}$ = 9.3 Hz, 1H, H-3), 3.22-3.27 (dd, $J_{4,5}$ = 9 Hz and J_{gem} = 11.5 Hz, 1H, H-5α), 3.20-3.23 (dd, $J_{2,3} = J_{1,2}$ = 8 and 9 Hz, 1H, H-2), 1.443 (s, 9H, $(CH_3)_3$), 1.26-1.27 (d, $J_{\beta,\gamma}$ = 6.5 Hz, 3H, H-γ). ^{13}C-NMR; d 173.94, 158.18, 100.07 (C-1), 75.64 (C-3), 74.27 (Thr-β), 72.77 (C-2), 69.27 (C-4), 64.85 (C-5), 58.42 (Thr-α), 27.61 ($(CH_3)_3$) 16.21 (Thr-γ). HRMS calcd for $C_{14}H_{25}NO_9Na$: $[M + Na]^+$, 374.1422. Found: 374.1434.

2.2.3.5 *N*-Boc-*O*-*β*-D-xylopyranosyl-L-threonamide (8)

Same method as for compound 6. Purified by silica gel column chromatography (2.5 cm i.d. × 20 cm, MeCN/water/formic acid = 97/3/0.1) to obtain compound 8. Yield: 75.7 % (39.5 mg). ^{1}H-NMR (D_2O): δ 4.42-4.43 (d, $J_{1,2}$ = 8 Hz, 1H, H-1), 4.37-4.38 (dd, $J_{\alpha,\beta}$ = 5.3 and 11.8 Hz, 1H, H-β), 4.13 (m, 1H, H-α), 3.91-3.95 (dd, $J_{4,5}$ = 5.5 Hz and J_{gem} = 11.8 Hz, 1H, H-5β), 3.58-3.63 (ddd, $J_{4,5}$ and $J_{3,4}$ = 5, 5.5, 9.5 Hz, 1H, H-4), 3.42-3.45 (dd, $J_{3,4}$ and $J_{2,3}$ = 9.3 Hz, 1H, H-3), 3.26-3.30 (dd, $J_{4,5}$ = 9 Hz and J_{gem} = 11 Hz, 1H, H-5α), 3.23-3.26 (dd, $J_{2,3}$ and $J_{1,2}$ = 7.5 and 8.5 Hz, 1H, H-2), 1.457 (s, 9H, $(CH_3)_3$), 1.26-1.27 (d, $J_{\beta,\gamma}$ = 6.5 Hz, 3H, H-γ). ^{13}C-NMR; δ 175.38, 157.87, 100.41 (C-1), 75.65 (C-3), 73.66 (Thr-β), 72.73 (C-2), 69.29 (C-4), 65.02 (C-5), 58.95 (Thr-α), 27.60 ($(CH_3)_3$) 15.83 (Thr-γ). HRMS calcd for $C_{14}H_{26}N_2O_9Na$: $[M + Na]^+$,

373.1581. Found: 373.1595.

2.2.3.6 N^{α}-lauroyl-*O*-*β*-D-xylopyranosyl-L-threonine (2)

Same method as for compound 1. Purified by silica gel column chromatography (1.0 cm i.d. × 20 cm, CH_2Cl_2/MeOH = 5/1) to obtain compound 2 as a white solid. Yield: 44.3 % (13.9 mg). Melting point: 110.3 °C. $[\alpha]^{20}$: −6.8 (c = 0.081). ^{1}H-NMR (CD_3COOD): δ 4.69 (d, $J_{\alpha,\beta}$ = 4 Hz, 1H, H-α), 4.37-4.38 (d, $J_{1,2}$ = 7.5 Hz, 1-H, H-1), 4.15-4.19 (qd, $J_{\alpha,\beta}$ = 4 Hz and $J_{\beta,\gamma}$ = 6.5 Hz, 1H, H-β), 3.84-3.87 (dd, $J_{4,5}$ = 5 Hz and J_{gem} = 11.5 Hz, 1H, H-5β), 3.57-3.62 (ddd, $J_{4,5}$ = 5 and 10 Hz, $J_{3,4}$ = 8.5 Hz, 1H, H-4), 3.49-3.52 (dd, $J_{3,4}$ = $J_{2,3}$ = 8.8 Hz, 1H, H-3), 3.25-3.29 (dd, $J_{2,3}$ = 9 Hz and $J_{1,2}$ = 7.5 Hz, 1H, H-2), 3.20-3.24 (dd, $J_{4,5}$ = 10.5 Hz and J_{gem} = 11.5 Hz, 1H, H-5α), 2.21-2.24 (dd, *J* = 7.5 Hz, 2H, CO*CH*$_2$), 1.47-1.51 (ddd, *J* = 7.5, 7, 6 Hz, 2H, *CH*$_2$(CH_2)$_8$), 1.16 (m, 16H, CH_2(*CH*$_2$)$_8$$CH_3$), 1.07-1.08 (d, $J_{\beta,\gamma}$ = 6.5 Hz, 3H, H-γ), 0.74-0.77 (t, *J* = 6.8 Hz, 3H, (CH_2)$_8$*CH*$_3$). ^{13}C-NMR (CD_3COOD): δ 173.82 (amide), 101.21 (C-1), 75.46 (C-3), 74.01 (Thr-β), 72.69 (C-2), 69.08 (C-4), 55.94 (Thr-α), 35.20 (CO*CH*$_2$), 25.15 (CH_2(*CH*$_2$)$_8$), 22.04, 28.58, 28.73, 28.81, 28.96, 29.09, 31.36 (CH_2(*CH*$_2$)$_8$), 14.73 (Thr-γ), 12.93 ((CH_2)$_8$*CH*$_3$). HRMS calcd for $C_{21}H_{40}N_2O_7Na$: $[M + Na]^+$, 455.2728. Found: 455.2738.

2.2.3.7 *N*-Boc-*O*-*β*-D-xylopyranosyl-L-serinyl glycinamide (9)

40 mg (0.12 mmol) of compound 5 was dissolved in 2 mL of MeCN. 26 mg (0.13 mmol) of glycinamide hydrochrolide, 26 μL (0.26 mmol) of *N*-methylmorpholine, and 39 mg (0.18 mmol) of DMT-MM were added into the solution. The mixture was stirred 2 h, and then the solvent was removed under reduced pressure. The crude residue was purified with silica gel column chromatography (2.5 cm i.d. × 20 cm, MeCN/water/formic acid = 90/10/0.1) to obtain compound 9. Yield: 54.8 % (25.0 mg). ^{1}H-NMR (D_2O): δ 4.39-4.41 (d, $J_{1,2}$ = 8 Hz, 1H, H-1), 4.33-4.35 (dd, $J_{\alpha,\beta}$ = 4.5 Hz, 1H, Ser-α), 4.15-4.18 (dd, $J_{\alpha,\beta}$ = 4.8 Hz and J_{gem} = 10.3 Hz, 1H, Ser-β2), 3.94-3.98 (dd, $J_{4,5}$ = 5.5 and 6.5 Hz, J_{gem} = 11.3 Hz, 1H, H-5β), 3.93 (s, 2H, Gly), 3.90-3.93 (dd, $J_{\alpha,\beta}$ = 3 and 4.5 Hz, J_{gem} = 10.3 Hz, 1H, Ser-β1), 3.58-3.63 (ddd, $J_{4,5}$ = 5.5 and 10.5 Hz, $J_{3,4}$ = 9 Hz, 1H, H-4), 3.42-3.46 (dd, $J_{3,4}$ = $J_{2,3}$ = 9 and 9.5 Hz, 1H, H-3), 3.28-3.33 (dd, $J_{4,5}$ =

11 Hz and J_{gem} = 11.5 Hz, 1H, H-5α), 3.24-3.28 (dd, $J_{1,2}$ = 8 Hz and $J_{2,3}$ = 9.5 Hz, 1H, H-2) 1.44 (s, 9H, $(CH_3)_3$). ^{13}C-NMR (D_2O); δ 174.17, 173.05, 164.92, 157.66, 102.98 (C-1), 75.58 (C-3), 72.94 (C-2), 68.95 (Ser-β), 65.20 (C-4, C-5), 55.01 (Ser-α), 42.21 (Gly), 27.58 ($(CH_3)_3$). HRMS calcd for $C_{15}H_{27}N_3O_9Na$: $[M + Na]^+$, 416.1640. Found: 416.1653.

2.2.3.8 N^{α}-lauroyl -*O*-*β*- D-xylopyranosyl-L-serinyl glycinamide (3)

23 mg (0.059 mmol) of compound 9 was dissolved in 1 mL of trifluoroacetic acid (TFA) and stirred at room temperature, After 15 min, the solvent and TFA was removed completely under reduced pressure. The residue was dissolved in 1 mL of water, followed by adding 13 mg (0.065 mmol) of lauric acid and 18 mg (0.065 mmol) of DMT-MM. The mixture was stirred at 40 ºC for 2 h. Saturated aqueous $NaHCO_3$ was added and the reaction mixture was extracted with AcOEt. The organic phase was removed under reduced pressure and the residue was purified by silica gel column chromatography (1.0 cm i.d. × 20 cm, CH_2Cl_2/MeOH = 4/1). Compound 3 was obtained as a white solid. Yield; 93.1 % (26.0 mg). Melting point: 161.4 ºC. $[\alpha]^{20}$: −14.2 (c = 0.065). ^{1}H-NMR (CD_3COOD): δ 4.75-4.77 (dd, $J_{\alpha,\beta}$ = 5.5 Hz, 1H, Ser-α), 4.26-4.27 (d, $J_{1,2}$ = 7.5 Hz, 1H, H-1), 4.00-4.03 (dd, $J_{\alpha,\beta}$ = 5 Hz and J_{gem} = 10.5 Hz, 1H, Ser-β1), 3.94-3.97 (d, J_{gem} = 17 Hz, 1H, Gly-α), 3.87-3.90 (d, J_{gem} = 17 Hz, 1H, Gly-β), 3.84-3.88 (dd, $J_{4,5}$ = 5.3 Hz, J_{gem} = 12 Hz, 1H, H-5α), 3.68-3.71 (dd, $J_{\alpha,\beta}$ = 6 Hz and J_{gem} = 10.5 Hz, 1H, Ser-β2), 3.57-3.62 (ddd, $J_{4,5^{\alpha}}$ = 5.5 Hz, $J_{4,5^{\beta}}$ = 10 Hz, $J_{3,4}$ = 9 Hz, 1H, H-4), 3.46-3.50 (dd $J_{3,4}$ = $J_{2,3}$ = 9 Hz, 1H, H-3), 3.25-3.28 (dd, $J_{1,2}$ = 7.5 Hz and $J_{2,3}$ 8.5 Hz, 1H, H-2), 3.18-3.22 (dd, $J_{4,5}$ = 10.5 Hz and J_{gem} = 11.5 Hz, 1H, H-5β), 2.18-2.1 (dd, J = 7.5 Hz, 2H, $COCH_2$), 1.47-1.50 (m, 2H, $CH_2(CH_2)_8$), 1.16 (m, 16H, $CH_2(CH_2)_8CH_3$), 0.74-0.77 (t, J = 6.8 Hz, 3H, $(CH_2)_8CH_3$). ^{13}C-HMR (CD_3COOD): δ 174.17, 171.30 (amide), 103, 12 (C-1), 75.48 (C-3), 72.74 (C-2), 69.00 (C-4), 68.85 (Ser-β), 64.58 (C-5), 52.69 (Ser-α), 41.78 (Gly), 35.19 ($COCH_2$), 25.06 ($CH_2(CH_2)_8$), 22.04, 28.58, 28.73, 28.82, 28.95, 29.09, 29.10, 31.36 ($(CH_2)_8CH_3$), 12.93 (CH_3). HRMS calcd for $C_{22}H_{41}N_3O_8Na$: $[M + Na]^+$, 498.2786. Found: 498.2801.

2.2.3.9 *N*-Boc-*O*-*β*-D-xylopyranosyl-L-threonyl glycinamide (10)

Same method as for compound 9. Purified by silica gel chromatography (2.5 cm i.d. × 20 cm, MeCN/water/formic acid = 90/10/0.1) to obtain compound 10. Yield; 70.6 % (41.5 mg). ^{1}H-NMR (D_2O): δ 4.41-4.43 (d, $J_{1,2}$ = 8 Hz, 1H, H-1), 4.38-4.40 (dd, $J_{\alpha,\beta}$ = 3 Hz and $J_{\beta,\gamma}$ = 6 Hz, 1H, Thr-β), 4.18-4.19 (m, 1H, Thr-α), 3.92 (s, 2H, Gly), 3.88-3.92 (dd, $J_{4,5}$ = 5.5 and 8 Hz, J_{gem} = 11.8 Hz, 1H, H-5β), 3.55-3.60 (ddd, $J_{4,5}$ = 5.5 and 9.8 Hz, $J_{3,4}$ = 9.5 Hz, 1H, H-4), 3.41-3.44 (dd, $J_{3,4}$ = $J_{2,3}$ = 9 and 9.5 Hz, 1H, H-3), 3.24-3.29 (dd, $J_{4,5}$ = 11 Hz and J_{gem} = 11 Hz, 1H, H-5α), 3.19-3.23 (dd, $J_{1,2}$ = 8 Hz and $J_{2,3}$ = 9 Hz, 1H, H-2) 1.45 (s, 9H, $(CH_3)_3$), 1.27-1.28 (d, $J_{\beta,\gamma}$ = 6.5 Hz, 3H, Thr-γ). ^{13}C-NMR (D_2O); δ 174.24, 173.39, 157.98, 100.25 (C-1), 75.66 (C-3), 73.53 (Thr-α). 72.90 (C-2), 69.28 (C-4), 63.88 (C-5), 59.52 (Thr-β), 42.33 (Gly), 27.59 ($(CH_3)_3$), 15.73 (Thr-γ). HRMS calcd for $C_{16}H_{30}N_3O_9Na$: $[M + Na]^+$, 430.1796. Found: 430.1801.

2.2.3.10 *N*$^{\alpha}$-lauroyl -*O*-*β*-D-xylopyranosyl-L-threonyl glycinamide (4)

Same method as for compound 3. Purified by silica gel column chromatography (1.0 cm i.d. × 20 cm, CH_2Cl_2/MeOH = 5/1) to obtain compound 4 as a white solid. Yield: 57.3 % (21.4 mg). Melting point: 151.7 ºC. $[\alpha]^{20}$: −16.8 (c = 0.087). ^{1}H-NMR (CD_3COOD): d 4.72-4.73 (d, $J_{\alpha,\beta}$ = 4 Hz, 1H, Thr-α), 4.36-4.38 (d, $J_{1,2}$ = 7.5 Hz, 1-H, H-1), 4.16-4.21 (qd, $J_{\alpha,\beta}$ = 4.5 Hz and $J_{\beta,\gamma}$ = 6.5 Hz, 1H, Thr-β), 3.93-3.97 (d, J_{gem} = 17.5 Hz, 1H, Gly-α), 3.88-3.91 (d, J_{gem} = 17 Hz, 1H, Gly-β), 3.84-3.88 (dd, $J_{4,5}$ = 5 Hz and J_{gem} = 11.5 Hz, 1H, H-5α), 3.58-3.63 (ddd, $J_{4,5}$ = 5 and 10 Hz, $J_{3,4}$ = 8.5 Hz, 1H, H-4), 3.48-3.52 (dd, $J_{3,4}$ = $J_{2,3}$ = 9 Hz, 1H, H-3), 3.24-3.27 (dd, $J_{2,3}$ = 9 Hz and $J_{1,2}$ = 7.5 Hz, 1H, H-2), 3.21-3.25 (dd, $J_{4,5}$ = 10.5 Hz and J_{gem} = 11.5 Hz, 1H, H-5β), 2.21-2.24 (dd, J = 7.5 Hz, 2H, $COCH_2$), 1.48-1.51 (ddd, J = 6 and 7 Hz, 2H, $CH_2(CH_2)_8$), 1.16 (m, 16H, $CH_2(CH_2)_8CH_3$), 1.07-1.09 (d, $J_{\beta,\gamma}$ = 6.5 Hz, 3H, Thr-γ), 0.74-0.77 (t, J = 6.8 Hz, 3H, $(CH_2)_8CH_3$). ^{13}C-NMR (CD_3COOD): δ 174.31, 170.88 (amide), 101.06 (C-1), 75.51 (C-3), 74.09 (Thr-β), 72.72 (C-2), 69.05 (C-4), 64.65 (C-5), 56.61 (Thr-α), 41.80 (Gly), 35.16 ($COCH_2$), 25.14 ($CH_2(CH_2)_8$), 22.04, 28.58, 28.72, 28.81, 28.96, 29.08, 31.36 ($CH_2(CH_2)_8$), 14.60 (Thr-γ), 12.93 ($(CH_2)_8CH_3$). HRMS calcd for $C_{23}H_{43}N_3O_8Na$: $[M + Na]^+$, 512.2942. Found: 512.2949.

2.3 Results and discussion

2.3.1 Synthetic strategy for Xyl-Ser-C12 and its derivatives

The proposed synthesis strategy of Xyl-Ser-C12 and its derivatives is shown in Figure 2-2. In this scheme, the derivatives could be easily synthesized from these amino acid derivatives through Boc-chemistry once *N*-Boc-*O*-Xyl-amino acids were prepared.

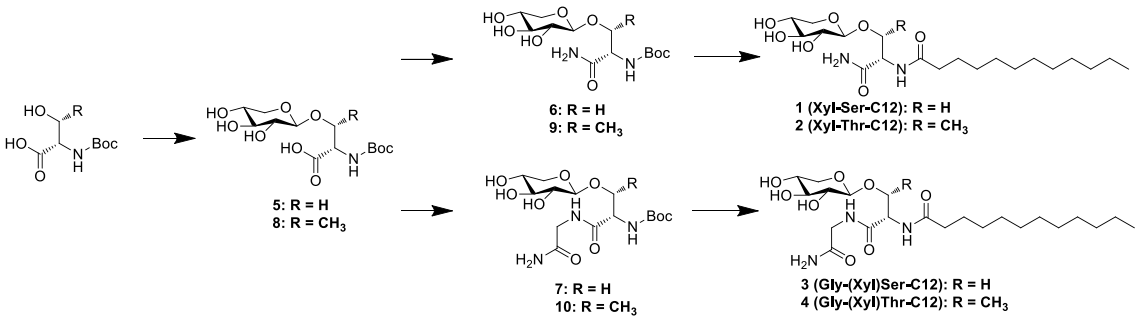

Figure 2-2 Chemoenzymatic synthesis of Xyl-Ser-C12 and its derivatives (2-4).

2.3.2 Optimization for chemoenzymatic condensation

Various β-xylosides such as alkyl xylosides also have been synthesized by the chemoenzymatic condensation; however, to the author's best knowledge, there are no reports about the chemoenzymatic condensation of β-hydroxyl amino acids and xylose. Therefore, optimization of chemoenzymatic condensation between Ser and Xyl was first carried out.

Figure 2-3 shows the extracted ion chromatogram (EIC) (*m/z* 336.12) chromatograms of the reaction solutions with the endo-β1-4 xylanase. In the EICs, the peaks around 2.5 min were clearly observed. The peak intensity was the highest when pH 5.0 buffer was used. The reason for the peak shapes split is the very large amount of Boc-Ser-OH was eluted at about 2.5 min. The same peaks were also observed in the EICs of the samples reacted with both the hemicellulase and the cellulose; however, the peak intensity of the peaks were much lower than those of the endo-β1-4 xylanase (data not shown). From this result, endo-β1-4 xylanase was chosen as the enzyme for the next experiment.

Next, the reaction times at various temperatures were investigated. The condensations were carried out at 30, 40, and 50 ºC in pH 3.0 or 5.0 buffer. An aliquot of the reaction solutions was subjected to LC–MS analyses at 0, 3, 6, 24, 48, and 96 h.

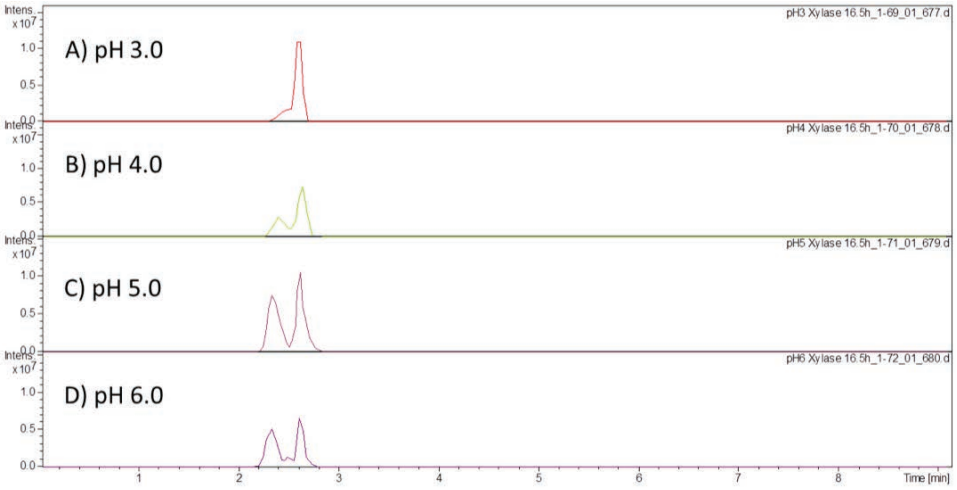

Figure 2-3 EICs of the reaction solutions with the endo-β1-4 xylanase (*m/z* 336.12): (A) pH 3.0, (B) pH 4.0, (C) pH 5.0, and (D) pH 6.0. LC–MS conditions are described below. A 2.1 mm i.d. × 50 mm ACQUITY UPLC BEH130 C18, 1.7 μm (Nihon Waters, Tokyo, Japan) was used for separation. The column was equilibrated with 5 % B, and the sample was eluted with a 5–15 % B linear gradient for 5 min at a flow rate of 0.5 mL/min.

As an example, Figure 2-4 shows the LC–MS chromatograms of the reaction solution (40 ºC, pH 5.0, 96 hours). Boc-Ser-OH, Xyl-Boc-Ser-OH, Hex-Boc-Ser-OH, and Xyl_2-Boc-Ser-OH were monitored with *m/z* 204 ($[M - H]^-$), *m/z* 336 ($[M - H]^-$), *m/z* 366 ($[M - H]^-$), and *m/z* 468 ($[M - H]^-$), respectively. The acceptor and the glycosylated products were clearly separated and discriminated by individual EIC channels. Two other glycosylated products could be detected. Xyl_2-Boc-Ser-OH might be synthesized from the condensation of xylobiose and the acceptor. Hex-Boc-Ser-OH might be caused by hexoses in the xylo-oligosaccharides. This result implies that the endo-β1-4 xylanase has both xylanase and hexosidase activities, or that hexosidases are contaminated in the endo-1-4 xylanase.

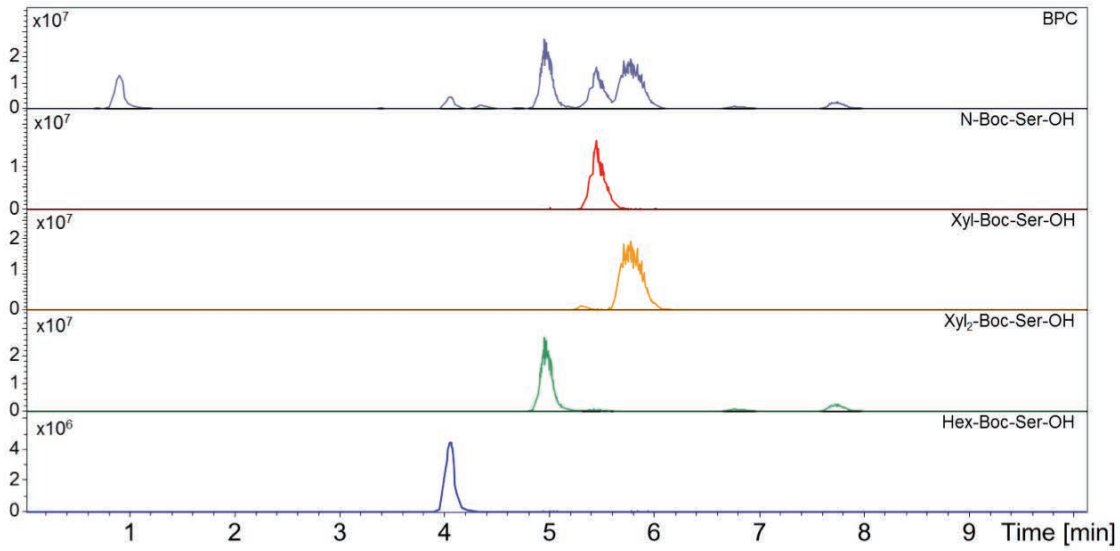

Figure 2-4 LC-MS chromatograms of the reactant mixture solution (pH 5, 40 °C, 96 h). LC–MS conditions are described below. A 2.0 mm i.d. × 150 mm UK-C18 (3 μm; Imtakt, Kyoto, Japan) was used for separation. The column equilibration and sample elution were carried out with a 10%B isocratic mode. The flow rate was set at 0.4 mL/min.

To investigate the time courses of the reaction, the peak areas of the products were plotted on the graphs (Figure 2-5). Figure 2-5A indicates the time course of the Xyl-Boc-Ser-OH production at each condition. The production mostly reached plateau at 40 and 50 ºC in pH 5.0 buffers. Although the production at 30 ºC increased according to the reaction time, the production was not as much as that at 40 or 50 ºC. The production was much lower in pH 3.0 buffers. In particular, the production at 50 ºC in pH 3.0 peaked at 6 h and gradually decreased for 96 h. This result suggests that the enzyme was inactivated in 6 h at 50 ºC in pH 3.0 buffers.

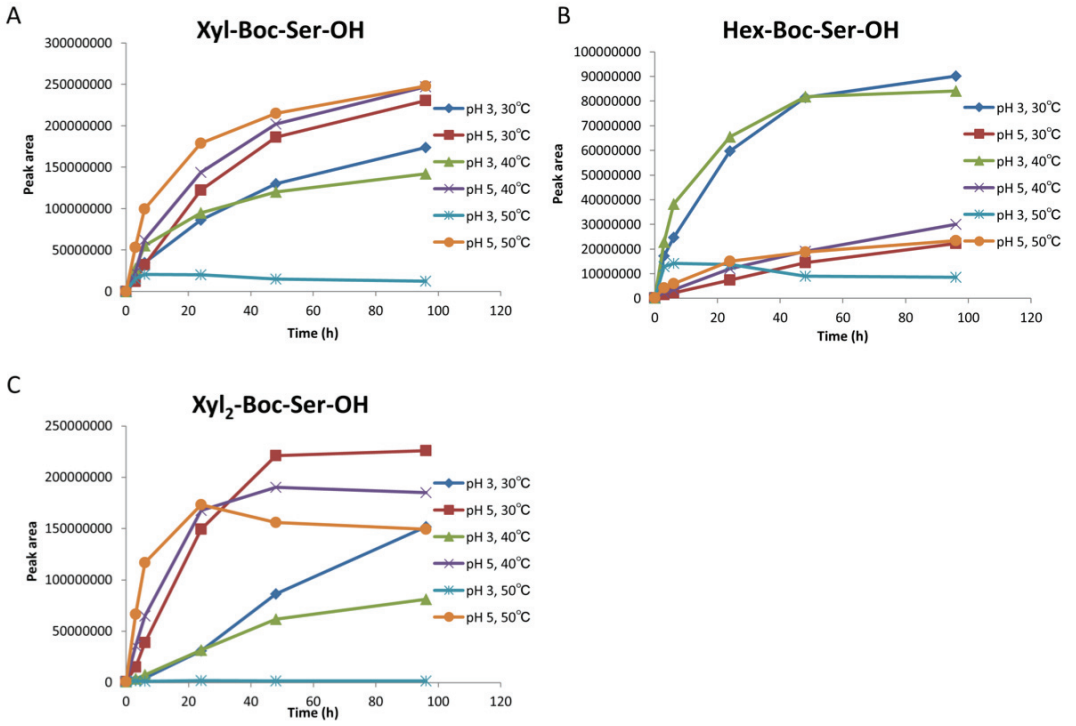

Figure 2-5 Time courses of the peak areas of the reaction products in several conditions. (A) Xyl-Boc-Ser-OH, (B) Hex-Boc-Ser-OH, and (C) Xyl_2-Boc-Ser-OH.

As shown in Figure 2-5C, the production of Xyl_2-Boc-Ser-OH was similar to that of Xyl-Boc-Ser-OH. In contrast, the production of Hex-Boc-Ser-OH was higher in pH 3.0 buffer than in pH 5.0 buffer (Figure 2-5B). This result means that the hexosidase activity in endo-β1-4 xylanase increases at lower-pH buffer. To maximize the Xyl-Boc-Ser-OH production and to minimize the byproducts, the chemoenzymatic condensation was determined be carried out at 40 ºC in pH 5.0 buffer for 96 h.

To confirm the structure of Xyl-Boc-Ser-OH obtained by the condensation, the product was purified by liquid extraction and silica gel chromatography. The peaks of the anomeric protons at around 4.37 ppm in the ^{1}H-NMR spectra of the purified product are shown. The coupling constants were 7.5 Hz (Figure 2-6). Therefore, it was confirmed that the purified products have β-anomer configuration. The yields of the chemoenzymatic condensations were 11.1 % for Xyl-Boc-Ser-OH. This yield was similar to the cases of other chemoenzymatic condensations using glycosidase.[38]

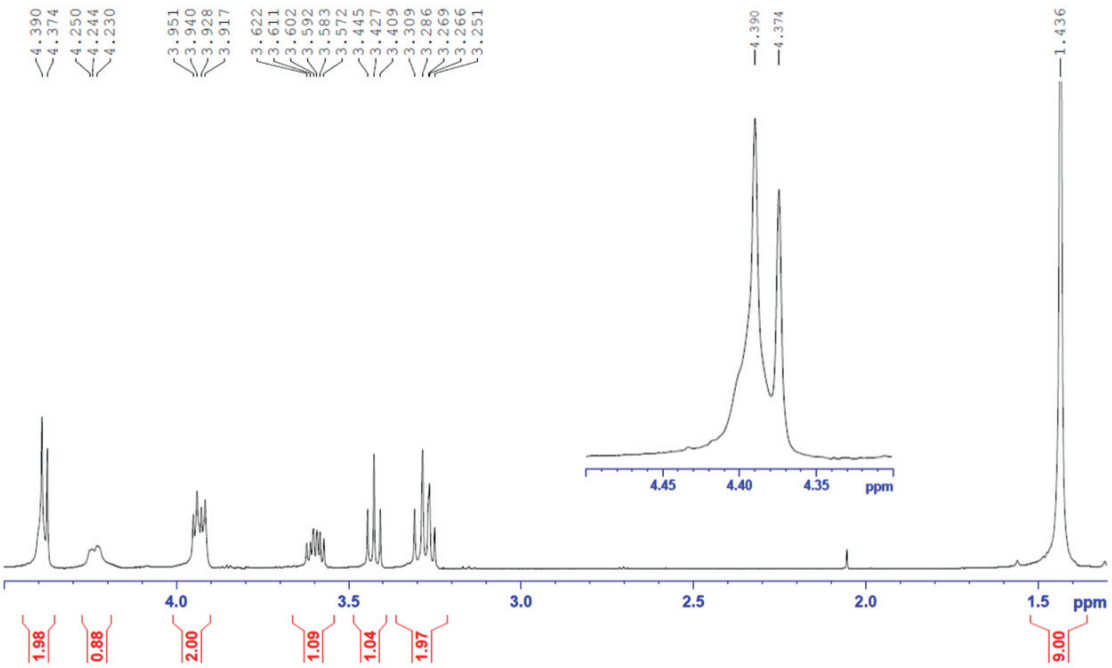

Figure 2-6 ^{1}H NMR spectrum of Xyl-Boc-Ser-OH. The inset is the enlarged around 4.37 ppm.

Conversion of Xyl-Boc-Ser-OH into the final products was carried out in accordance with *N*-Boc chemistry for peptide synthesis. For conversion of carboxy groups into amides, the reactions were carried out using HOBt-NH_3 and EDCI.[43] Condensation with lauric acid was carried out with two-step synthesis involving the removal of the *N*-Boc group with acid catalysts (4 M HCl in dioxane) and condensation using DMT-MM. The overall yields of the final products were 4.10 % for Xyl-Ser-C12. From comparison with the results of the previous report, the number of synthesis steps was reduced from 10 to 3.

To expand the structural variety of the β-xylosides, the Xyl-Thr-C12, Gly-(Xyl)Ser-C12, and Gly-(Xyl)Thr-C12 were synthesized chemoenzymatically. In the same manner, *N*-Boc-*O*-*β*-D-xylopyranosyl-L-threonine (8) was synthesized by the chemoenzymatic condensation using *N*-Boc-Thr-OH as an acceptor, and the yield of the condensation was 12.5 %. This result demonstrates the utility of the condensation using the xylanase, which can be applied to primary hydroxyl groups but also to secondary ones. In the same manner, Xyl-Ser-C12, Xyl-Thr-C12 could be synthesized in

accordance with *N*-Boc chemistry for peptide synthesis. The total yield of Xyl-Thr-C12 was 4.91 %, which was comparable to that of Xyl-Ser-C12. For Gly-(Xyl)Ser-C12 and Gly-(Xyl)Thr-C12 syntheses, the primary amidation steps were substituted by condensation of glycinamide using DMT-MM. The total yields were 5.66 % for Gly-(Xyl)Ser-C12 and 5.06 % for Gly-(Xyl)Thr-C12.

Consequently, the synthetic schemes using chemoenzymatic condensation is less laborious. Furthermore, *N*-Boc-Ser and *N*-Boc-Thr can be useful as a building block for xylosylated glycopeptides by *N*-Boc chemistry, since the result shows that the β-xyloside group was sufficiently durable for peptide bond construction chemistry. Hence, our synthetic strategy for β-xyloside is applicable to the synthesis of various xylosylated peptides.

2.4. Conclusion

In this part, the synthetic schemes for Xyl-Ser-C12 and its derivatives were established. In particular, the chemoenzymatic condensation using endo-β1-4 xylanase was useful because it is low-cost, time-effective, and versatile for both primary and secondary hydroxyl amino acids.

Chapter 3
Evaluation of GAG Priming Ability of the Saccharide Primers

3.1 Introduction

As described in chapter 1, β-xylosides have been used as artificial initiators of GAG biosynthesis. These β-xylosides have been applied to obtain GAG oligosaccharides, investigate GAG biosynthetic mechanism, and clarify the localization of glycan transferases on ER or Golgi apparatus.[36] The types of oligosaccharides elongated on β-xylosides are deeply related to their aglycone structures, and there are many literatures that reported the relationship between the aglycone structure of β-xylosides and the GAG chain elongated on thereof.[24,27,44–49] Most of these studies have paid much attention to the amount, molecular weight, and GAG types of primed oligosaccharides, whereas not much attention was paid to the intermediates of oligosaccharides primed on the β-xylosides.

In previous study, it is reported that a novel β-xyloside, Xyl-Ser-C12, which was designed to resemble the consensus sequence of proteoglycan (PG), showed excellent GAG-type oligosaccharides priming ability including various intermediates of the linkage tetrasaccharides.[37] Form these results, it is possible that the amino acid residues in the aglycone affect strongly the priming ability of the β-xyloside, and a proper β-xyloside can be used as a chemical probe for investigation of GAG biosynthesis. However, any other investigation about the relationship between the structure of the amino acid and the priming ability has not been examined, and intermediates of GAG oligosaccharides like phosphorylated ones have not been found in the glycosylated products. The reasons given for this include poor recovery of the phosphorylated products from the cell culture,[50–53] incomparability of the analytical apparatus and conditions for the phosphorylated products, and difficulty in distinguishing the phosphorylated and sulfated products due to their equivalent nominal molecular weights. In other words, it is possible to find the phosphorylated oligosaccharides in the glycosylated products when a proper analytical condition is applied.

In this chapter, the glycosylated products of Xyl-Ser-C12 and its derivatives were investigated to examine their priming abilities. The analytical procedure, from

solid phase extraction (SPE) to LC–MS analyses, was optimized to detect the phosphorylated products efficiently. The structure of glycosylated products was deduced by MS/MS spectra and enzymatic digestion. The priming abilities of the β-xylosides were compared, and the relationship between the aglycones and priming abilities is discussed.

3.2 Materials and methods

3.2.1 Materials

Unless otherwise stated, all commercially available reagents and solvent were used without purification.

3.2.2 GAG priming in cells

NHDF cells (Kurabo Co., Osaka, Japan) were cultured in Medium 106 (Thermofisher Scientific, Yokohama, Japan) with NHDF growth supplements, gentamicin, and amphotericin B (Kurabo Co., Osaka, Japan) at 37 ºC in a humidified atmosphere containing 5 % CO_2.

NHDF cells (4 x 10^5) in a six-well plate were seeded with FibroLife® S2 Medium Complete kit (Kurabo Co., Osaka, Japan) containing 25 μM Xyl-Ser-C12, Xyl-Thr-C12, Gly-(Xyl)Ser-C12, or Gly-(Xyl)Thr-C12 for 48 h.

3.2.3 Purification of glycosylated products

Purification of glycosylated products was carried out in the previous report, with some modification.[37] Briefly, the glycosylated products were collected from the culture medium using a SPE cartridge. First, 1 mL of 7.5 M Urea was added into the culture medium (about 1.5 mL) and stirred well to dissolve precipitate completely in the medium, followed by addition of 2.5 mL of 20 mM tetrabutylammonium hydrogensulfate (TBA-HSO_4). Next, the solution was applied to the cartridge (Strata-X, 60 mg, 3 mL; Phenomenex, CA) that was conditioned with methanol and equilibrated with 10 mM TBA-HSO_4. After the cartridge was washed with 2 mL of water and 2 mL of 30 % MeOH, the glycosylated products were eluted with 1 mL of 50 % MeOH, 70 % of MeOH, and 1 mL of 90 % MeOH. The eluent fractions were collected and the solvent was removed under reduced vacuum condition. In order to remove excess

amount of TBA, the residues were dissolved with 200 μL of water/MeOH/*i*PrOH (1/1/1, v/v) and passed through 200 μL of cation exchange resin (Muromachi Chemica, Tokyo, Japan) that was washed with MeOH and protonated with 2 % formic acid. After removal of the solvent by vacuum distillation, the residues were stored at −20 ºC.

3.2.4 LC–ESI–MS of glycolsylated products

All solvents and reagents used for LC–MS experiment were LC–MS grade. The glycosylated products and the digested samples were subjected to LC–MS analysis. MS analysis were performed a Synapt G2-S (quadruple/time-of-flight mass spectrometer equipped with ion mobility cell) coupled online by an ACQUITY UPLC H-Class Bio (Nihon Waters, Tokyo, Japan). Instrument control, data acquisition and analysis were performed with MassLynx software v.4.1. The samples were dissolved in water/MeCN (1/3, v/v) and load onto 2.1 mm i.d. × 150 mm ACQUITY UPLC BEH Glycan, 1.7 μm (Nihon Waters, Tokyo, Japan). Fifty mM ammonium formate buffer (pH 7.8) was used as mobile phase A, MeCN as mobile phase B, and 20 mM phosphoric acid in 50 % MeCN as mobile phase C. Before every analysis, the high-performance liquid chromatography (HPLC) system and the column were flushed with mobile phase C at 0.3 mL/min for 3 min so as to avoid undesirable absorption of phosphorylated compounds, and then, washed with mobile phase A: mobile phase B = 50:50 solution at 0.3 mL/min for 2 min. The column was equilibrated with 95 %B then the sample was eluted with a 95-50 %B linear gradient for 40 min at a flow rate of 0.4 mL/min. The column temperature was set at 60 ºC. The *m/z* recorded ranged from 50 to 1500. The MS calibration was carried out using NaI, and the lock mass spray was setup with Leu-enkephalin (*m/z* 554.2615: $[M - H]^-$). The quadrupole profile was optimized not to detect background phosphate ion. The resolution was set to resolution mode (approximately 25,000 at *m/z* 554). Other electrospray ionization (ESI) conditions were set as follows; Capillary voltage; −1.5 kV, cone voltage; 30 V, sample offset; 60 V, source temperature; 120 ºC, desolvation temperature; 500 ºC, cone gas; 50 L/h, trap collision energy (CE); 2 V.

3.2.5 Enzymatic digestion of the glycosylated products

Chondrotinase ABC (C-ABC), chondroitinase ACII (C-ACII), heparitinase I, heparitinase II, and heparitinase III were purchased from Seikagaku Corporation (Tokyo,

Japan). β-D-galactosidase was purchased from Wako Pure Chemical Industries (Osaka, Japan). α2-3 sialidase was purchased from Takara Bio (Shiga, Japan). α2,3-6 sialidase was purchased from Nakarai Tesque (Kyoto, Japan). To determine the structure of glycosylated products elongated on the primers, the glycosylated products were digested with GAG lyases and glycosidases. The glycosylated products extracted from the medium were dissolved in 100 μL of water. For CS/DS digestion, 100 μL of 100 mM Tris-HCl buffer (pH 8.0) containing 250 mU chondroitinase ABC, 25 mU chondroitinase ACII, and 0.005 % bovine serum albumin (BSA) was added. For CS digestion, 100 mM sodium acetate buffer (pH 6.0) containing 250 mU chondroitinase ACII and 0.005 % BSA was added. For HS digestion, 100 mM sodium acetate, 50 mM calcium acetate (pH 7.0) containing 250 mU heparitinase I, II, and III was added. For β-galactosidase digestion, 100 μL of 100 mM phosphate buffer (pH 7.3) containing 1000 U β-D-galactosidase was added. For α2-3 sialidase digestion, 100 mM sodium acetate buffer (pH 5.5) and 10 μL of α2-3 sialidase were added. For α2,3-6 sialidase digestion, 100 mM sodium acetate buffer (pH 5.0) containing 2000 mU α2,3-6 sialidase was addwd. The mixture solutions kept 37 ºC for 10 min (α2-3 sialidase), 2 h (C-ABC, ACII), or 17 h (HSases, β-galactosidase, α2,3-6 sialidase digestion). All the reactions were quenched by heating for 30 sec in boiling water bath. The samples were passed through 200 μL of cation exchange resin, concentrated, and stored at −20 ºC before use.

3.2.6 Statistical analysis

All values are given as the mean ± standard deviation (SD). Statistical analyses were performed using the Student's t-test available in Microsoft Excel 2010, and the level of significance is indicated in figures when more than three independent experiments were performed.

3.3 Results and discussion

3.3.1 Method optimization and structure analysis of phosphorylated products

In advance with evaluation of the priming abilities of the β-xylosides, the protocol to extract the phosphorylated products was optimized.

For the glycosylated products analysis by LC–MS, hydrophilic interaction chromatography (HILIC) mode was applied for separation with amide column. The

glycosylated products were separated in accordance with the number of saccharide residues and sulfate groups. However, the phosphorylated products gave extremely broad peaks or were not detected at all. For example, Figure 3-1A shows EICs of the phosphorylated products under conventional HILIC conditions. Even though the non-phosphorylated products (HexNAc-HexA-Hex-Hex-Xyl-Ser-C12) gave the shape peak around 20 min, the all phosphorylated products were not observed. This result is probably due to the absorption of the phosphate groups on the stainless steel surface; because it is well known that phosphorylated compounds are easily absorbed on surface of LC system and it result in poor peaks shapes of the phosphorylated compounds. Adding a few amount of phosphoric acid into the mobile phases,[54] using ammonium bicarbonate buffer in mobile phases,[55] and washing LC apparatus with ethylenediaminetetraacetic acid (EDTA) solution were taken to solve this problem.[56] Tried these conditions; nevertheless they were not effective to prevent the absorption of the phosphorylated products. Finally, the LC system was flushed with phosphoric acid solution before every analysis. By flushing LC–MS system with 20 mM phosphoric acid in 50 % MeCN, the peak shapes of the phosphorylated products were dramatically improved without changing their retention times, peak shapes, and sensitivities of other glycosylated products (Figure 3-1B).

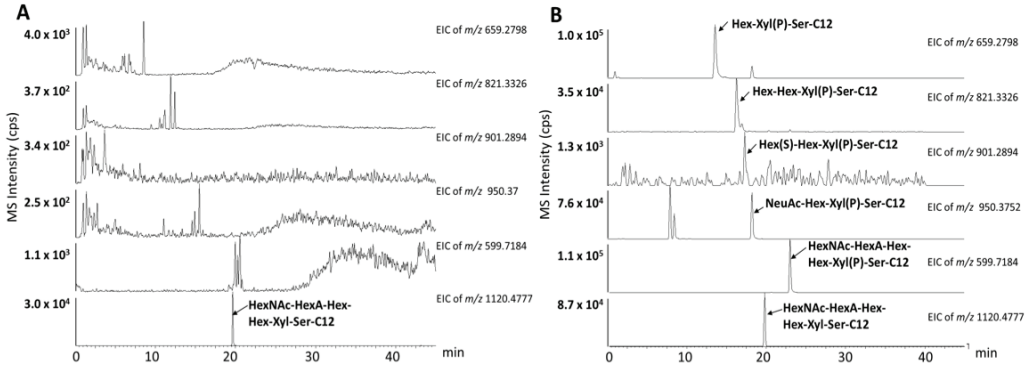

C

Glycosylated products	Ion type	*m/z*
Hex-Xyl(P)-Ser-C12	$[M - H]^-$	659.2798
Hex-Hex-Xyl(P)-Ser-C12	$[M - H]^-$	821.3326
Hex(S)-Hex-Xyl(P)-Ser-C12	$[M - H]^-$	901.2894
NeuAc-Hex-Xyl(P)-Ser-C12	$[M - H]^-$	950.3752
HexNAc-HexA-Hex-Hex-Xyl(P)-Ser-C12	$[M - 2H]^{2-}$	599.7184
HexNAc-HexA-Hex-Hex-Xyl-Ser-C12	$[M - H]^-$	1120.4777

Figure 3-1 EICs of the phosphorylated products. (A) Before phosphoric acid wash. (B) After phosphoric acid wash. (C) The ion types and *m/z* values of monitored glycosylated products. S and P described in the glycosylated products indicate sulfate and phosphate groups,

Next, to maximize recovery of the phosphorylated products, several solid phase extraction cartridges and additives were screened. Formic acid (FA), NaCl, or TBA-HSO_4 were added into the medium, and then, SPE were carried out. The recoveries were compared in accordance with the relative intensities of the glycosylated products in EICs. A part of the results is shown in Figure 3-2. Among the additives, TBA-HSO_4 demonstrated the highest recovery for both sulfated and phosphorylated products.

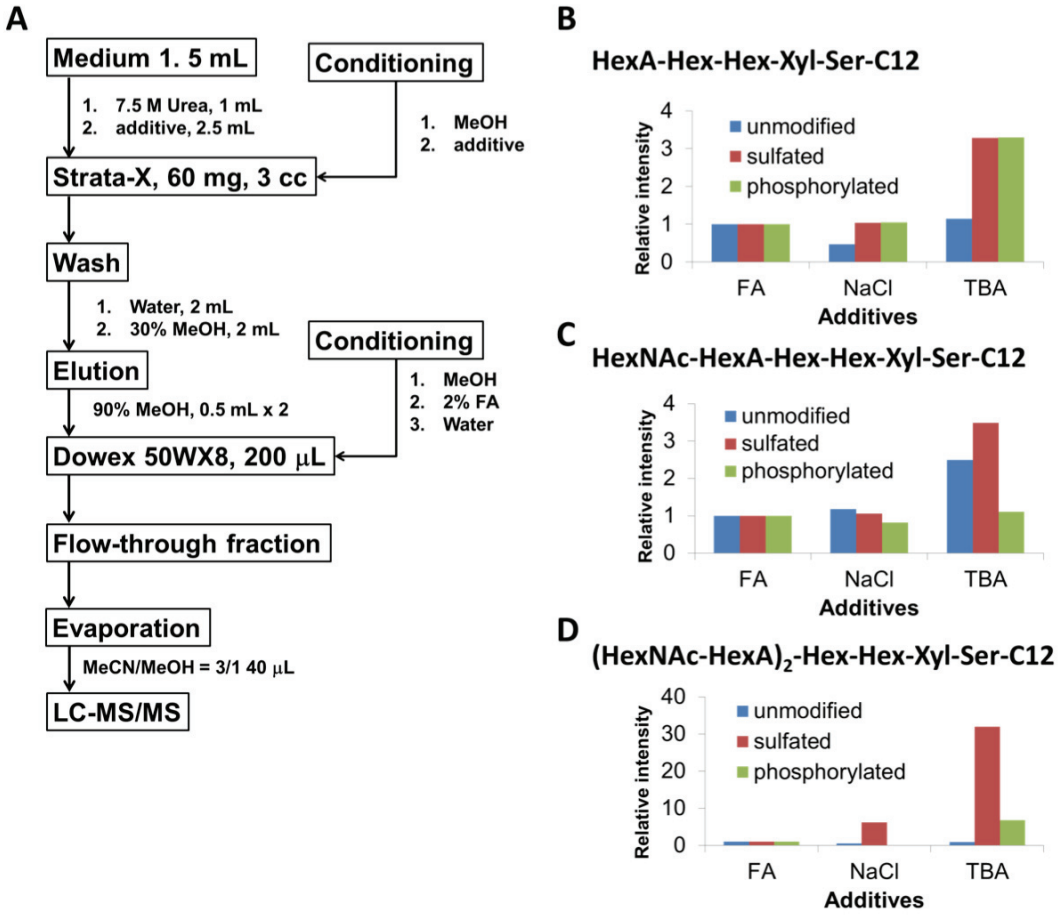

Figure 3-2 Comparison of the recovery of the phosphorylated and sulfated products obtained by SPE. (A) SPE protocols examined in the study. Each additive was used for dilution of the medium and the conditioning of SPE cartridge. (B) The tetrasaccharides. (C) The pentasaccharides. (D) The heptasaccharides.

The glycosylated products obtained from the NHDF cell culture were prepared and analyzed by the optimized method. Table 3-1 and Table 3-2 show the structure, *m/z* value, ion type, retention time, proportions, and fragment ions of the MS/MS spectrum of the detected glycosylated product. The structures of the glycosylated products were deduced from the MS/MS spectra and the results of enzymatic digestion. In particular, phosphorylated and sulfated products were determined by accurate *m/z* values and observation of *m/z* 78.9585 ($[PO_3]^-$) in the MS/MS spectra.[57]

Twenty-nine glycosylated products were detected from 1.5 mL of the NHDF cell culture, of which 11 were considered to be phosphorylated products.

Table 3-1 Detected glycosylated products elongated on Xyl-Ser-C12. The glycosylated products that had identical *m/z* values but differed in their retention times were distinguished by the numbers after underscore. Hex; hexose, HexNAc; *N*-acetylhexosamine, HexA; hexuronic acid, NeuAc; *N*-acetylneuraminic acid.

Glycosylated products	Ion type	Calculated *m/z*	Observed *m/z*	Error (ppm)	R. T.[a] (min)
Hex-Xyl-R	$[M - H]^-$	579.3134	579.3116	-3.11	6.90
Hex(S)-Xyl-R	$[M - H]^-$	659.2703	659.2704	0.15	8.66
Hex-Hex-Xyl-R	$[M - H]^-$	741.3663	741.3636	-3.64	11.24
Hex(S)-Hex-Xyl-R	$[M - H]^-$	821.3231	821.3158	-8.89	11.99
Hex-Hex(S)-Xyl-R	$[M - H]^-$	821.3231	821.3193	-4.63	12.55
Hex-Xyl(P)-R	$[M - H]^-$	659.2798	659.2767	-4.70	13.34
NeuAc-Hex-Xyl-R	$[M - H]^-$	870.4089	870.4049	-4.60	13.41
Hex-Hex-Xyl(P)-R	$[M - H]^-$	821.3326	821.3297	-3.53	16.06
NeuAc-Hex-Hex-Xyl-R	$[M - H]^-$	1032.4617	1032.4546	-6.88	16.35
Hex(S)-Hex-Xyl(P)-R	$[M - H]^-$	901.2894	901.2847	-5.21	17.04
NeuAc-Hex-Xyl(P)-R	$[M - H]^-$	950.3752	950.376	0.84	17.96
HexA-Hex-Hex-Xyl-R	$[M - H]^-$	917.3978	917.398	0.22	18.17
HexA(S)-Hex-Hex-Xyl-R	$[M - H]^-$	997.3552	997.3514	-3.81	18.35
NeuAc-NeuAc-Hex-Xyl-R	$[M - H]^-$	1161.5043	1161.4995	-4.13	18.28
HexNAc-HexA-Hex-Hex-Xyl-R_1	$[M - H]^-$	1120.4777	1120.4736	-3.66	19.52
HexNAc-HexA-Hex-Hex-Xyl-R_2	$[M - H]^-$	1120.4777	1120.4736	-3.66	19.69
HexNAc(S)-HexA-Hex-Hex-Xyl-R	$[M - 2H]^{2-}$	599.7148	599.7127	-3.50	19.96
NeuAc-Hex-Hex-Xyl(P)-R	$[M - H]^-$	1112.4280	1112.4242	-3.42	20.13
HexA-Hex-Hex-Xyl(P)-R	$[M - H]^-$	997.3647	997.3585	-6.22	21.72
HexA(S)-Hex-Hex-Xyl(P)-R	$[M - 2H]^{2-}$	538.1578	538.1541	-6.88	21.96
HexNAc-HexA-Hex-Hex-Xyl(P)-R	$[M - 2H]^{2-}$	599.7184	599.7173	-1.83	22.83
NeuAc-NeuAc-Hex-Hex-Xyl(P)-R_1	$[M - 2H]^{2-}$	701.2581	701.2564	-2.42	22.86
NeuAc-NeuAc-Hex-Hex-Xyl(P)-R_2	$[M - 2H]^{2-}$	701.2581	701.2554	-3.85	23.41
HexA-HexNAc-HexA-Hex-Hex-Xyl-R	$[M - 2H]^{2-}$	647.7513	647.7484	-4.48	24.39
$(HexNAc\text{-}HexA)_2$-Hex-Hex-Xyl-R_HS[b]	$[M - 2H]^{2-}$	749.2910	749.2877	-4.40	24.45
$(HexNAc\text{-}HexA)_2$-Hex-Hex-Xyl-R_CS[c]	$[M - 2H]^{2-}$	749.2910	749.2887	-3.07	24.97
HexNAc(S)-HexA-HexNAc-HexA-Hex-Hex-Xyl-R	$[M - 2H]^{2-}$	789.2694	789.2659	-4.43	25.21
$(HexNAc\text{-}HexA)_2$-Hex-Hex-Xyl(P)-R	$[M - 2H]^{2-}$	789.2741	789.2722	-2.41	27.31
$(HexNAc\text{-}HexA)_3$-Hex-Hex-Xyl-R	$[M - 2H]^{2-}$	938.8467	938.8445	-2.34	28.90

[a] Retention time.

[b] The products digested by heparitinases.

[c] The products digested by C-ABC.

Table 3-2 MS/MS assignments of the glycosylated products.

Glycosylated products	Fragment ions
Hex-Xyl-R	267.2083 (Z_0), 161.0441 (B_1)
Hex(S)-Xyl-R	391.0555 (C_2), 241.0023 (B_1), 96.9610 ($[HSO_4]^-$)
Hex-Hex-Xyl-R	395.1242 ($^{2,5}A_3$), 383.1205 ($^{2,4}A_3$), 323.0990 (B_2), 267.2075 (Z_0), 263.0779 ($^{2,5}A_2$), 221.0665 ($^{2,4}A_2$)
Hex(S)-Hex-Xyl-R	553.1039 (C_3), 403.0630 (B_2), 241.0020 (B_1), 96.9598 ($[HSO_4]^-$)
Hex-Hex(S)-Xyl-R	659.2714 (Y_2), 553.1146 (C_3), 403.0518 (B_2), 96.9564 ($[HSO_4]^-$)
Hex-Xyl(P)-R	497.2288 (Y_1), 391.0667 (C_2), 373.0561 (B_1), 259.0222 ($[Hex + PO_3]^-$), 241.0112 ($[Hex - H_2O + PO_4]^-$), 78.9585 ($[PO_4]^-$)
NeuAc-Hex-Xyl-R	649.3218 ($^{0,2}X_3$), 602.1959 (C_3), 480.1747 ($^{2,5}A_3 - CO_2$), 468.1740 ($^{2,4}A_3 - CO_2$), 408.1616 ($B_3 - CO_2$), 290.0983 (B_1), 267.2126 (Z_0)
Hex-Hex-Xyl(P)-R	659.2807 (Y_2), 553.1211 (C_3), 535.1099 (B_3), 497.2257 (Y_1), 421.0768 ($[Hex + Hex + PO_3]^-$), 78.9583 ($[PO_3]^-$)
NeuAc-Hex-Hex-Xyl-R	811.3792 ($^{0,2}X_3$), 642.2279 ($^{2,5}A_3 - CO_2$), 570.2025 ($B_2 - CO_2$), 395.1175 ($^{2,5}A_3/Y_3$), 383.1174 ($^{2,4}A_3/Y_3$), 323.0972 (B_2/Y_3), 290.0881 (B_1), 267.2068 (Z_0)
Hex(S)-Hex-Xyl(P)-R	821.3353 ($[M - H - SO_3]^-$), 659.2846 (Y_2), 553.1113 ($C_3 - SO_3$), 535.1119 ($B_3 - SO_3$), 240.9993 (B_1), 78.9557 ($[PO_3]^-$)
NeuAc-Hex-Xyl(P)-R	906.3903 ($[M - H - CO_2]^-$), 659.2913 (Y_2), 497.2286 (Y_1), 391.0692 (C_3/Y_2), 373.0564 (B_3/Y_2), 78.9587 ($[PO_3]^-$)
HexA-Hex-Hex-Xyl-R	649.1868 (C_4), 589.1686 ($^{0,2}A_4$), 517.1450 (C_3), 455.1406 (B_4/Y_3), 395.1209 ($^{2,5}A_4/Y_3$), 337.0771 (B_2), 323.1008 (B_3/Y_3), 267.2066 (Z_0)
HexA(S)-Hex-Hex-Xyl-R	917.4081 ($[M - H - SO_3]^-$), 729.1453 (C_4), 649.1871 ($C_4 - SO_3$), 267.2077 (Z_0), 254.9880 (B_1), 210.9911 ($B_1 - CO_2$), 96.9594 ($[HSO_4]^-$)
NeuAc-NeuAc-Hex-Xyl-R	870.4119 (Y_3), 581.1873 (B_2), 537.1964 ($B_2 - CO_2$), 290.0938 (B_1), 267.2074 (Z_0)
HexNAc-HexA-Hex-Hex-Xyl-R_1	899.3929 (Z_4), 509.1490 ($^{2,5}A_5/Z_4 - CO_2$), 437.1272 ($C_4/Z_4 - CO_2$), 267.2029 (Z_0)
HexNAc-HexA-Hex-Hex-Xyl-R_2	899.3914 (Z_4), 855.4024 ($Z_4 - CO_2$), 852.2647 (C_5), 509.1566 ($^{2,5}A_5/Z_4 - CO_2$), 437.1315 ($C_4/Z_4 - CO_2$), 267.2079 (Z_0)
HexNAc(S)-HexA-Hex-Hex-Xyl-R	932.2285 (C_5), 852.2615 ($C_5 - SO_3$), 800.1821 (C_4), 720.2226 (C4- SO_3), 638.1266 (C_3), 558.1722 ($C_3 - SO_3$), 476.0723 (C_2), 458.0573 (B_2), 396.1162 ($C_2 - SO_3$), 300.0408 (C_1), 267.2064 (Z_0)
NeuAc-Hex-Hex-Xyl(P)-R	1068.4458 ($[M - H - CO_2]^-$), 821.3354 (Y_3), 659.2799 (Y_2), 553.1210 (C_4/Y_3), 535.1100 (B_4/Y_3), 497.2289 (Y_1), 290.0853 (B_1), 79.9585 ($[PO_3]^-$)
HexA-Hex-Hex-Xyl(P)-R	821.3367 (Y_3), 729.1527 (C_4), 659.2758 (Y_2), 553.1232 (C_4/Y_2), 535.1155 (B_4/Y_2), 497.2288 (Y_1), 78.9577 ($[PO_3]^-$)
HexA(S)-Hex-Hex-Xyl(P)-R	821.3328 (Y_3), 254.9837 (B_1), 78.9596 ($[PO_3]^-$)
HexNAc-HexA-Hex-Hex-Xyl(P)-R	979.3587 (Z_4), 935.3710 ($Z_4 - CO_2$), 821.3344 (Y_3), 803.3246 (Z_3), 659.2821 (Y_2), 553.1206 (C_5/Y_3), 535.1094 (B_5/Y_3), 497.2276 (Y_1), 355.0439 (B_5/Z_2), 78.9583 ($[PO_3]^-$)
NeuAc-NeuAc-Hex-Hex-Xyl(P)-R_1	821.3374 (Y_3), 290.0917 (B_1), 78.9576 ($[PO_3]^-$)
NeuAc-NeuAc-Hex-Hex-Xyl(P)-R_2	821.3371 (Y_3), 290.0862 (B_1), 78.9579 ($[PO_3]^-$)
HexA-HexNAc-HexA-Hex-Hex-Xyl-R	1028.2963 (C_6), 896.2433 (C_5), 734.1983 (C_4), 572.1512 (C_3), 509.1527 ($^{2,5}A_6/Z_4 - CO_2$), 396.1161 (C_2), 267.2080 (Z_0), 193.0338 (C_1)
$(HexNAc-HexA)_2$-Hex-Hex-Xyl-R_HS	1234.4941 ($Z_6 - CO_2$), 899.4190 (Z_4), 757.2145 (B_4), 599.1989 (C_3), 509.1496 ($^{2,5}A_7/Z_4 - CO_2$), 480.1401 ($^{2,5}A_3$), 396.1109 (C_2), 267.2070 (Z_0)
$(HexNAc-HexA)_2$-Hex-Hex-Xyl-R_CS	1234.5146 ($Z_6 - CO_2$), 1231.3741 (C_7), 1010.2892 (C_7/Z_6), 966.3002 ($C_7/Z_6 - CO_2$), 899.3911 (Z_4), 757.2137 (B_4), 599.1954 (C_3), 509.1534 ($^{2,5}A_7/Z_4 - CO_2$), 396.1157 (C_2), 267.2076 (Z_0)
HexNAc(S)-HexA-HexNAc-HexA-Hex-Hex-Xyl-R	1120.4812 (Y_5), 1010.2779 (C_7/Z_6), 917.4000 (Y_4), 899.3916 (Z_4), 757.2137 ($B_4 - SO_3$), 679.1526 (C_3), 599.1962 ($C_3 - SO_3$), 509.1509 ($^{2,5}A_7/Z_4 - CO_2$), 458.0632 (B_2), 396.1171 ($C_2 - SO_3$), 300.0399 (C_1), 282.0290 (B_1), 267.2072 (Z_0)
$(HexNAc-HexA)_2$-Hex-Hex-Xyl(P)-R	1234.5221 ($Z_6 - CO_2 - HPO_3$), 997.3666 (Y_4), 979.3548 (Z_4), 935.3652 ($Z_6 - CO_2$), 821.3378 (Y_3), 659.2739 (Y_2), 396.1106 (C_2), 78.9588 ($[PO_3]^-$)
$(HexNAc-HexA)_3$-Hex-Hex-Xyl-R	1278.5253 (Z_6), 1120.4763 (Y_5), 978.3136 (C_5), 917.4018 (Y_4), 899.3984 (Z_4), 775.2314 (C_4), 757.2167 (B_4), 599.1964 (C_3), 509.1504 ($^{2,5}A_9/Z_4 - CO_2$), 396.1187 (C_2), 267.2078 (Z_0)

Figure 3-3 shows the structural analysis of the disaccharide (*m/ z* 659.2798) as an example. In the MS/MS spectrum (Figure 3-3A), $[PO_3]^-$ (*m/z* 78.9601) was clearly observed and hence the disaccharide was considered to be phosphorylated. In addition, *m/z* 497.2288 (Y_1), 391.0667 (C_2), and 373.0561 (B_1) meant glycoside bond cleavage ions, suggesting that the phosphorylation occurred on the Xyl. However, in the phosphorylated product, peaks at *m/z* 241.0112 and 259.0222 were also clearly observed (shown by arrows in Figure 3-3A). These ions implied the existence of a phosphorylated hexose residue in the products, a phenomenon inconsistent with the existence of the phosphorylated Xyl residue. To clarify this point, the glycosylated products were digested by β-galactosidase, followed by the LC−MS/MS analysis. Figure 3-3B shows the EICs of *m/z* 659.2798 and 497.2270 (Xyl(P)-Ser-C12) before and after β-galactosidase digestion, respectively. The peak height at 11.5 min on the EIC of *m/z* 659.2798 (Hex- Xyl(P)-Ser-C12) decreased considerably after digestion, whereas that at 5.7 min on the EIC of *m/z* 497.2270 (Xyl(P)-Ser- C12) largely increased after digestion. On the basis of these results, the major component of the phosphorylated disaccharide (*m/z* 659.2798) was deduced to be Galβ-Xyl(P)-Ser-C12. The fragment ions *m/z* 241.0112 and 259.0222 in the MS/MS may have been detected due to migration of the phosphate group during MS/MS excitation [58] or co-elution of Gal(P)β-Xyl-Ser-C12.

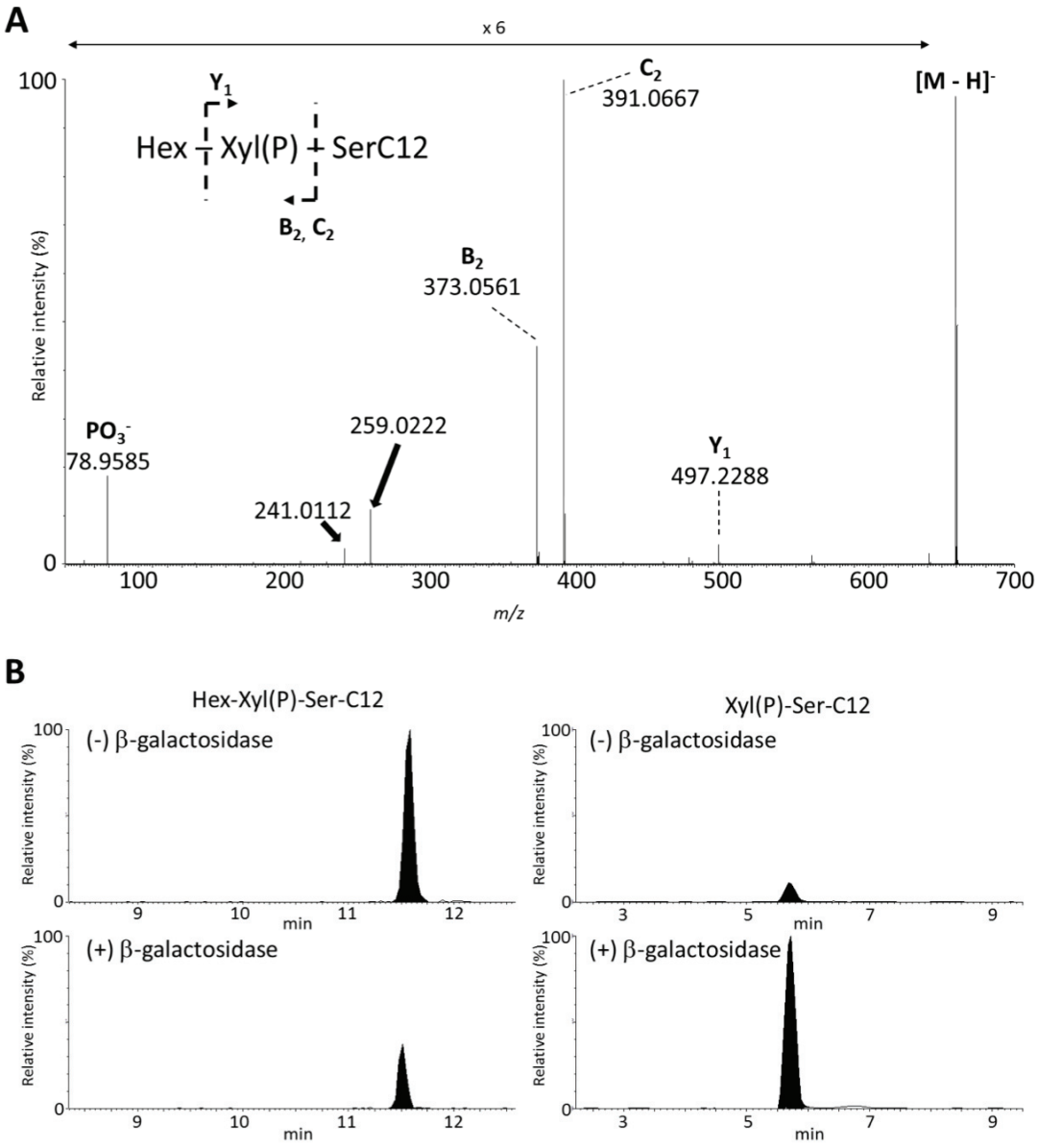

Figure 3-3 Structure analysis of the phosphorylated disaccharide (*m/z*; 659.2798). (A) MS/MS spectrum of *m/z* 659.2798. The y-axis was enlarged 6 times in the *m/z* range of 50-650. Assignment of the fragment ions is described in the figure. Arrows indicate *m/z* 241.0112 and 259.0222. (B) Comparison of EIC profiles before and after β-galactosidase digestion. The ranges of the vertical axis are set equal.

As in the case of the phosphorylated disaccharide, other glycosylated products that gave $[PO_3]^-$ ions in their MS/MS spectra were considered to be phosphorylated products. These phosphorylated products were deduced to be phosphorylated on the Xyl

residue because Y_1 (*m/z* 497.23) or Y_2 (*m/z* 659.28) ions were observed in their MS/MS spectra (Table 3-2). Thus, the phosphorylated products were concluded to be intermediates of the linkage tetrasaccharide and GAG oligosaccharides. The major reason why the phosphorylated products were not detected in previous studies is probably due to the absorption of these products. This result demonstrates the feasibility of Xyl-Ser-C12 for use as a chemical probe to investigate the GAG biosynthesis mechanism.

Interestingly, not only Xyl-phosphorylated di-, tri-, and tetra- oligosaccharides but longer phosphorylated pentasaccharides (*m/z* 599.7184 and 701.2581) and a heptasaccharide (*m/z* 789.2741) were also detected. The phosphorylated pentasaccharide (*m/z* 599.7184) could be partly digested by heparitinases (Figure 3-4A); the major structure of the phosphorylated pentasaccharide was deduced to be GlcNAcα1-4HexA-Hex-Hex-Xyl(P)-Ser-C12. In contrast, the phosphorylated heptasaccharide (*m/z* 789.2741) could be digested by C-ABC and C-ACII but was not digested by heparitinases (Figure 3-4B). Therefore, the structure of the heptasaccharide would be GalNAcβ1-4GlcAβ1-3GalNAcβ1-4GlcA-Hex-Hex-Xyl(P)-Ser-C12. Izumikawa *et al*. demonstrated the phosphorylated linkage oligosaccharides to be an intermediate of the immature GAG chain resulting from an imbalance of GAG xylosylkinase-named family with sequence similarity 20, member B (FAM20B), xylose phosphatase, and chondroitin *N*-acetylgalactosaminyltransferase-1.[15] Their results indicate that the phosphorylation on Xyl residues may be a discrimination tag to sort the linkage oligosaccharides into GAG chain elongation or termination and that these enzymes work in harmony to regulate the number, length, and amount of GAG chains elongated on PGs. In this study, both phosphorylated and nonphosphorylated oligosaccharides that have a linkage tetrasaccharide structure were detected. Thus, the ratio of phosphorylated and nonphosphorylated oligosaccharides probably represents the capability of GAG biosynthesis of the examined cells.

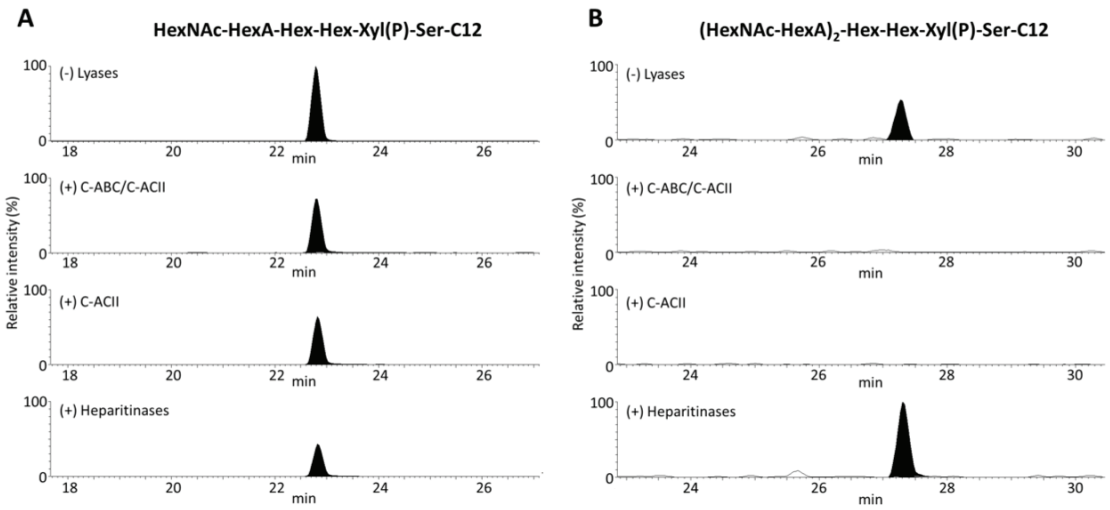

Figure 3-4 Comparison of EIC profiles before and after GAG lyase digestion. (A) EIC profiles of phosphorylated pentasaccharide (HexNAc-HexA-Hex-Hex-Xyl(P)-Ser-C12; *m/z* 599.7184). (B) EIC profiles of phosphorylated heptasaccharide (HexNAc-HexA-HexNAc-HexA-Hex-Hex-Xyl(P)-Ser-C12; *m/z* 789.2741). The ranges of the vertical axis are set equal.

3.3.2 Structural analysis of the glycosylated products by GAG lyase digestion

To determine the GAG types of the elongated oligosaccharides, the glycosylated products were digested by GAG lyases, followed by the LC−MS/MS analysis. (Figure 3-5) shows the structural analysis of heptasaccharides (*m/z* 749.2910). In the chromatograms (Figure 3-5A), the untreated sample gave a minor peak at 24.49 min and a major peak at 25.97 min. After digestion with C-ABC/C-ACII, the major peak completely disappeared, whereas the minor peak remained intact. In contrast, the minor peak completely disappeared by heparitinase digestion, whereas the entire major peak remained. In addition, the cross-ring cleavage ion, $^{2,5}A_3$ (*m/z* 480.1401), was observed in the MS/MS spectra of *m/z* 749.2910 at the minor peak (Figure 3-5B), indicating the existence of the -HexA1-4HexNAc- structure in the sequence. The cross-ring cleavage ion was not observed in the spectra at the major peak (Figure 3-5C). Other oligosaccharides composed of repeating disaccharide units were digested by C-ABC/C-ACII but not by heparitinase (Figure 3-4B and Figure 3-6). Therefore, the heptasaccharide at the minor peak and major peak were considered to be an HS-type oligosaccharide and a CS-type oligosaccharide, respectively.

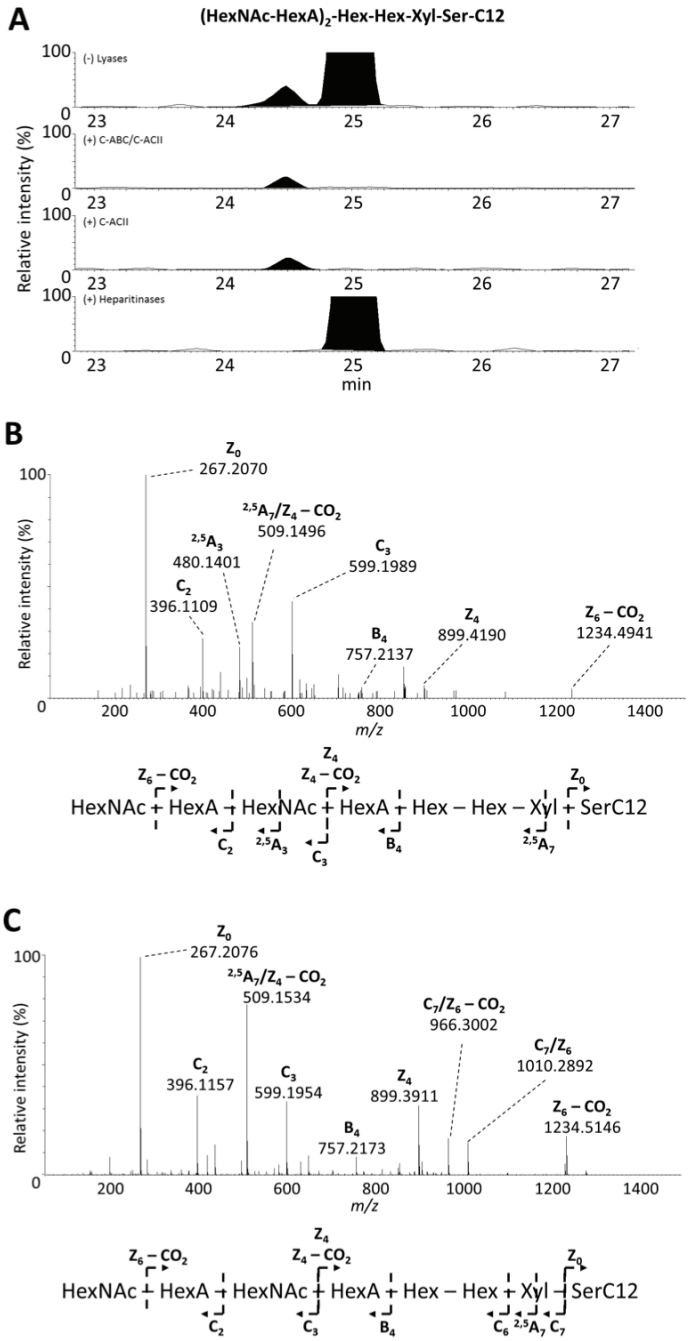

Figure 3-5 Structural analysis of the heptasaccharides (*m/z* 749.2910). (A) EIC profiles of the heptasaccharides. The ranges of the vertical axis are set equal. (B) The MS/MS spectrum of the heptasaccharide at 24.4 min. (C) The MS/MS spectrum of the heptasaccharide at 24.9 min.

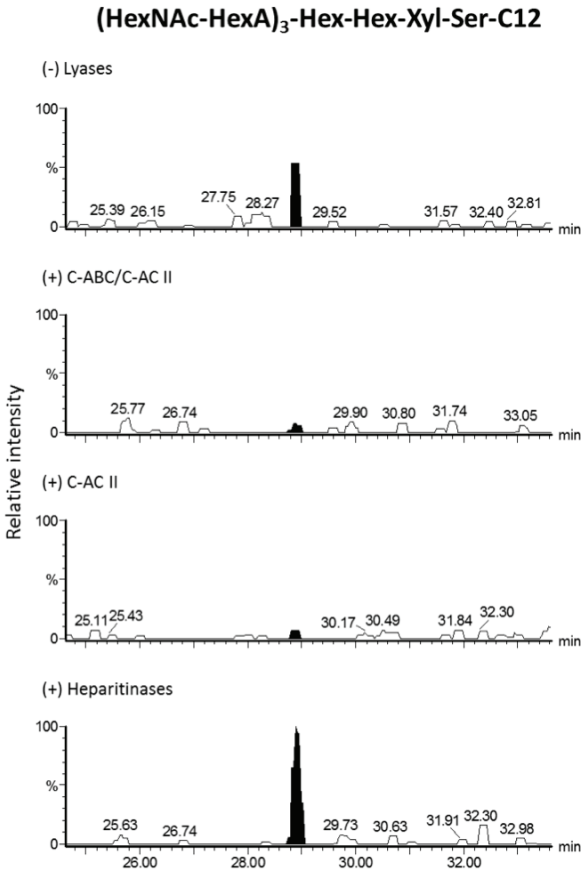

Figure 3-6 GAG lyase digestion of the nonasaccharide $(HexNAc\text{-}HexA)_3$-Hex-Hex-Xyl-Ser-C12.

3.3.3 Structure analysis of sialylated products

Besides GAG-type oligosaccharides, many sialyloligosaccharides are found in the glycosylated products. Among these sialyloligosaccharides, α2-3 sialosides are considered to be an unnatural type of oligosaccharides, resulting from misrecognition of β-xylosides by the glycolipid biosynthesis pathway or an end- capping structure instead of phosphorylated Xyl.[15,36] To confirm the structure of the sialoside bond of the glycosylated products, they were digested by α2-3 sialidase or α2-3,6 sialidase and then analyzed by LC−MS/MS. The result is shown in Figure 3-7. NeuAc-Hex-Xyl-Ser-C12 (*m/z* 870.4089), the most abundant sialyloligosaccharide, completely disappeared by digestion with both sialidases (Figure 3-7A). Similarly, NeuAc-Hex-Xyl(P)-Ser- C12 (*m/z* 950.3752) and NeuAc-Hex-Hex-Xyl-Ser-C12 (*m/z* 1032.4617) were digested by both sialidases (Figure 3-7B,C), so the sialoside bonds of these products were determined to be an α2-3 sialoside bond. In contrast, NeuAc-Hex-Hex-Xyl(P)-Ser- C12 (*m/z* 1112.4280) was digested only by α2-3,6 sialidase and not by α2,3 sialidase (Figure

3-7D). This result suggests the structure to be an α2-6 sialoside.

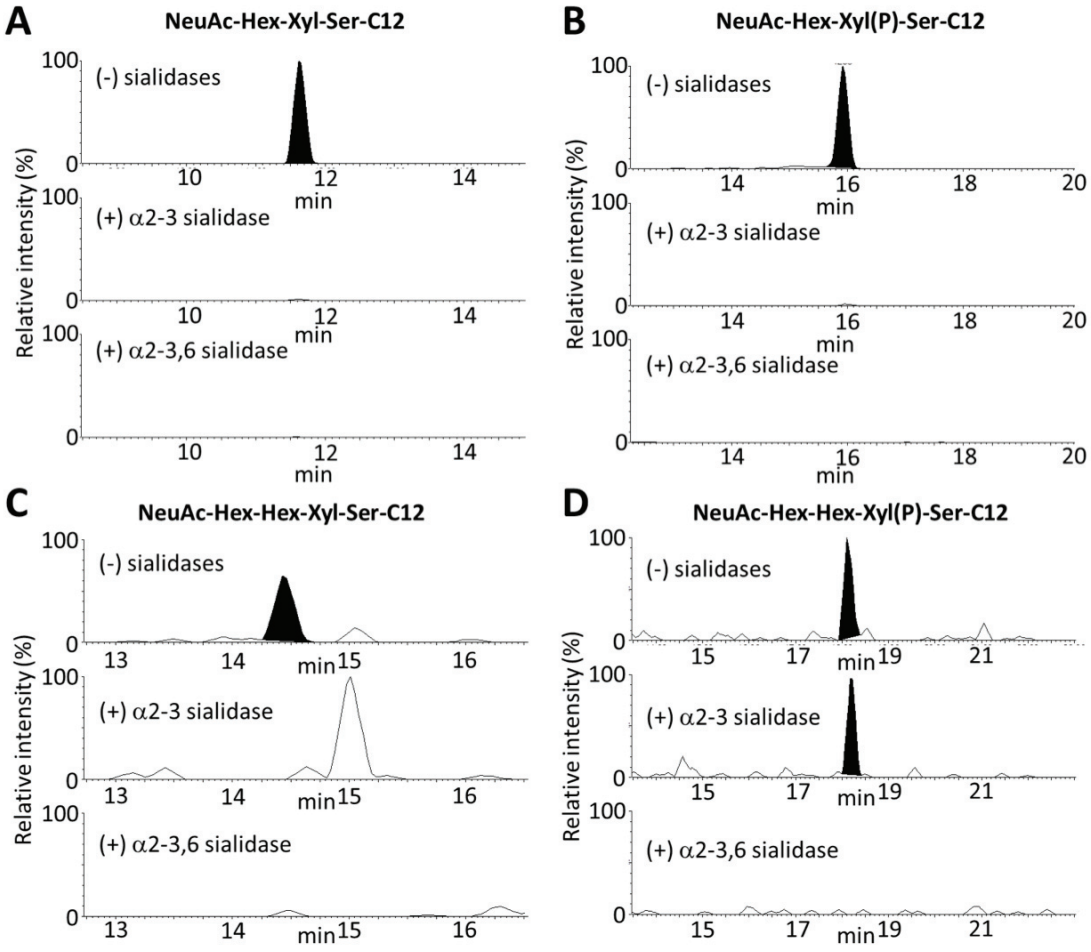

Figure 3-7 Comparison of EIC profiles before and after sialidase digestion. (A) EIC profiles of NeuAc-Hex-Xyl-Ser-C12; *m/z* 870.4089). (B) EIC profiles of NeuAc-Hex-Xyl(P)-Ser-C12; *m/z* 950.3752). (C) EIC profiles of NeuAc-Hex-Hex-Xyl-Ser-C12; *m/z* 1032.4617). (D) EIC profiles of NeuAc-Hex-Hex-Xyl(P)-Ser-C12; *m/z* 1112.4280). The ranges of the vertical axis are set equal.

NeuAcα2-3Hex-Xyl is regarded as an end-capping structure when disaccharide structure Hex-Xyl is not phosphorylated properly by FAM20B.[59] Therefore, the proportions of this sialyloligosaccharide show a tendency of Xyl-Ser-C12 to not be incorporated into the GAG biosynthetic pathway. Moreover, NeuAcα2-3Hex-Hex-Xyl is also considered to be an end-capping structure because the C3 position of the nonreducing end, Hex, where GlcA should be attached, was occupied by sialic acid. In contrast, some sialyloligosaccharides that were phosphorylated on the Xyl residue were

also detected. This result did not agree with the GAG biosynthesis mechanism controlled by FAM20B, suggesting that the sialylation might occur by a different biosynthesis mechanism.

In addition, the sialyltetrasaccharide (NeuAcα2-6Hex-Hex-Xyl(P)-Ser-C12) had another sialoside bond structure. Recently, sialylation on the Gal residue of the linkage tetrasaccharide in the human inter-α-trypsin inhibitor was reported.[16,60] This implies that α2-6 sialoside might be added on the Gal residues of the linkage tetrasaccharide during GAG biosynthesis. Therefore, NeuAcα2-6-Hex-Hex-Xyl(P)-Ser-C12 might be a novel intermediate structure of GAG biosynthesis. On the basis of these results, sialylation on the β-xyloside might be a key factor to understanding the GAG biosynthetic mechanism. In this regard, Xyl-Ser-C12 could be a powerful tool to investigate the GAG biosynthetic mechanism because Xyl-Ser-C12 is able to prime phosphorylated, GAG-type, and sialyloligosaccharides all at the same time.

3.3.4 Quantitative analysis of the glycosylated products obtained from the β-xylosides

To confirm the relationship between the structure and priming ability of each β-xyloside, the proportions of the glycosylated products were calculated and compared. In the same manner as that for the glycosylated products of Xyl-Ser-C12, those of other β-xylosides were deduced by LC–MS/MS and enzymatic digestion. The proportions were calculated from the peak areas of the glycosylated products. The results are shown in Table 3-3, Table 3-4, Table 3-5, Table 3-6, Table 3-7, Table 3-8, Table 3-9, and Figure 3-8.

Table 3-3 Detected glycosylated products elongated on Xyl-Thr-C12. The glycosylated products that had identical *m/z* values but differed in their retention times were distinguished by the numbers after underscore.

Glycosylated products	Ion type	Calculated m/z	Observed m/z	Error (ppm)	R. T. (min)
Hex-Xyl-R	$[M - H]^-$	593.3291	593.327	-3.54	6.55
Hex(S)-Xyl-R	$[M - H]^-$	673.2859	673.2861	0.30	8.24
Hex-Hex-Xyl-R	$[M - H]^-$	755.3819	755.3796	-3.04	10.86
Hex(S)-Hex-Xyl-R	$[M - H]^-$	835.3387	835.3408	2.51	11.62
Hex-Hex(S)-Xyl-R	$[M - H]^-$	835.3387	835.3404	2.04	12.18
Hex-Xyl(P)-R	$[M - H]^-$	673.2954	673.2926	-4.16	13.10
NeuAc-Hex-Xyl-R	$[M - H]^-$	884.4245	884.4214	-3.51	13.07
Hex-Hex-Xyl(P)-R	$[M - H]^-$	835.3483	835.343	-6.34	15.79
NeuAc-Hex-Hex-Xyl-R_1	$[M - H]^-$	1046.4773	1046.474	-3.34	16.03
NeuAc-Hex-Hex-Xyl-R_2	$[M - H]^-$	1046.4773	1046.479	1.24	16.59
NeuAc-Hex-Xyl(P)-R	$[M - H]^-$	964.3908	964.3877	-3.21	17.72
HexA-Hex-Hex-Xyl-R	$[M - H]^-$	931.414	931.4171	3.33	17.86
NeuAc-NeuAc-Hex-Xyl-R	$[M - H]^-$	1175.5199	1175.516	-3.74	17.96
HexA(S)-Hex-Hex-Xyl-R	$[M - H]^-$	1011.3708	1011.365	-5.34	18.13
HexNAc-HexA-Hex-Hex-Xyl-R	$[M - H]^-$	1134.4934	1134.495	1.76	19.41
HexNAc-HexA-Hex-Hex-Xyl(P)-R	$[M - 2H]^{2-}$	606.7262	606.7252	-1.65	22.63
$(HexNAc-HexA)_2$-Hex-Hex-Xyl-R_CS[a]	$[M - 2H]^{2-}$	756.2988	756.2974	-1.85	24.73

[a] The product digested by C-ABC.

Table 3-4 MS/MS assignments of the glycosylated products elongated on Xyl-Thr-C12.

Glycosylated products	Fragment ions
Hex-Xyl-R	281.2258 (Z_0), 221.0660 ($^{2,4}A_2$), 198.1859, 161.0447 (B_1)
Hex(S)-Xyl-R	391.0567 (C_2), 373.0455 (B_2), 331.0346 ($^{0,2}A_2$), 241.0018 (B_1), 96.9589 ($[HSO_4]^-$)
Hex-Hex-Xyl-R	455.1394 (B_3), 395.1252 ($^{2,5}A_3$), 383.1207 ($^{2,4}A_3$), 323.0990 (B_2), 281.2235 (Z_0), 263.0781 ($^{2,5}A_2$), 221.0672 ($^{2,4}A_2$)
Hex(S)-Hex-Xyl-R	553.1016 (C_3), 241.0021 (B_1)
Hex-Hex(S)-Xyl-R	673.2898 (Y_2), 655.2886 (Z_2), 553.1129 (C_3), 403.0582 (B_2), 96.9565 ($[HSO_4]^-$)
Hex-Xyl(P)-R	511.2414 (Y_1), 391.0656 (C_2), 373.0551 (B_1), 78.9577 ($[PO_3]^-$)
NeuAc-Hex-Xyl-R	663.3362 ($^{0,2}X_3$), 480.1759 ($^{2,5}A_3 - CO_2$), 468.1745 ($^{2,4}A_3 - CO_2$), 408.1597 ($B_3 - CO_2$), 290.0987 (B_1), 281.2275 (Z_0)
Hex-Hex-Xyl(P)-R	673.2966 (Y_2), 535.1110 (B_3), 493.2395 (Z_1), 78.9577 ($[PO_3]^-$)
NeuAc-Hex-Hex-Xyl-R_1	825.3888 ($^{0,2}X_3$), 755.3824 (Y_2), 642.2266 ($^{2,5}A_3 - CO_2$), 570.2068 ($B_2 - CO_2$), 408.1534 ($B_2 - CO_2$), 290.0888 (B_1), 281.2232 (Z_0)
NeuAc-Hex-Hex-Xyl-R_2	884.3812 (Y_{3a}), 825.3921 ($^{0,2}X_{3b}$), 764.2452 (C_4), 630.2259 ($^{2,4}A_3 - CO_2$), 570.2018 ($B_3 - CO_2$), 290.0879 (B_{1b}), 281.2239 (Z_0)
NeuAc-Hex-Xyl(P)-R	920.4038 ($[M - H - CO_2]^-$), 673.2972 (Y_2), 511.2444 (Y_1), 391.0633 (C_3/Y_2), 373.0567 (B_3/Y_2), 78.9585 ($[PO_3]^-$)
HexA-Hex-Hex-Xyl-R	649.1827 (C_4)
NeuAc-NeuAc-Hex-Xyl-R	884.4279 (Y_3), 581.1866 (B_2), 537.1963 ($B_2 - CO_2$), 408.1520 ($B_3 - CO_2/Y_3$), 290.0967 (B_1), 281.2235 (Z_0)
HexA(S)-Hex-Hex-Xyl-R	931.4188 ($[M - H - SO_3]^-$), 755.3876 (Y_3), 649.1839 ($C_4 - SO_3$), 281.2242 (Z_0), 254.9826 (B_1), 96.9589 (HSO_4^-)
HexNAc-HexA-Hex-Hex-Xyl-R	913.4067 (Z_4), 869.4172 ($Z_4 - CO_2$), 509.1534 ($^{2,5}A_4 - CO_2$), 437.1306 ($C_4/Z_4 - CO_2$), 281.2218 (Z_0)
HexNAc-HexA-Hex-Hex-Xyl(P)-R	993.374082 (Z_4), 37 (Z_4), 949.3834 ($Z_4 - CO_2$), 835.3521 (Y_3), 673.2985 (Y_2)
$(HexNAc-HexA)_2$-Hex-Hex-Xyl-R_CS	1292.5101 (Z_6), 1248.5308 ($Z_6 - CO_2$), 1010.2892 (C_7/Z_6), 913. 869.4188 ($Z_4 - CO_2$), 599.1979 (C_3), 509.1470 ($^{2,5}A_7/Z_4 - CO_2$), 396.1150 (C_2), 281.2193 (Z_0)

Table 3-5 Detected glycosylated products elongated on Gly-(Xyl)Ser-C12. The glycosylated products that had identical *m/z* values but differed in their retention times were distinguished by the numbers after underscore.

Glycosylated products	Ion type	Calculated. m/z	Observed m/z	Error (ppm)	R. T. (min)
Hex-Xyl-R	$[M - H]^-$	636.3349	636.332	-4.56	8.25
Hex(S)-Xyl-R	$[M - H]^-$	716.2917	716.2874	-6.00	9.72
Hex-Hex-Xyl-R	$[M - H]^-$	798.3877	798.3846	-3.88	12.28
Hex(S)-Hex-Xyl-R	$[M - H]^-$	878.3446	878.3359	-9.90	12.90
Hex-Xyl(P)-R	$[M - H]^-$	716.3012	716.2989	-3.21	13.59
NeuAc-Hex-Xyl-R	$[M - H]^-$	927.4303	927.4276	-2.91	14.13
Hex-Hex-Xyl(P)-R	$[M - H]^-$	878.3541	878.3506	-3.98	16.28
NeuAc-Hex-Hex-Xyl-R	$[M - H]^-$	1089.4832	1089.4813	-1.74	16.93
Hex(S)-Hex-Xyl(P)-R	$[M - H]^-$	958.3109	958.308	-3.03	17.31
NeuAc-Hex-Hex-Xyl-R	$[M - H]^-$	1089.4832	1089.479	-3.86	17.41
NeuAc-Hex-Xyl(P)-R_1	$[M - H]^-$	1007.3967	1007.3915	-5.16	18.07
NeuAc-Hex-Xyl(P)-R_2	$[M - H]^-$	1007.3967	1007.3936	-3.08	18.49
NeuAc-NeuAc-Hex-Xyl-R	$[M - H]^-$	1218.5257	1218.5222	-2.87	18.70
HexA-Hex-Hex-Xyl-R	$[M - H]^-$	974.4198	974.4104	-9.65	18.76
HexA(S)-Hex-Hex-Xyl-R	$[M - H]^-$	1054.3766	1054.3696	-6.64	18.94
HexNAc-HexA-Hex-Hex-Xyl-R	$[M - H]^-$	1177.4992	1177.4915	-6.54	20.22
NeuAc-Hex-Hex-Xyl(P)-R	$[M - 2H]^{2-}$	1169.4495	1169.4434	-5.22	20.25
HexNAc(S)-HexA-Hex-Hex-Xyl-R_1	$[M - H]^-$	628.2244	628.225	0.96	20.35
HexNAc(S)-HexA-Hex-Hex-Xyl-R_2	$[M - H]^-$	628.2244	628.2261	2.71	20.70
NeuAc-Hex-Hex-Xyl(P)-R	$[M - 2H]^{2-}$	1169.4495	1169.4434	-5.22	20.25
HexNAc-HexA-Hex-Hex(S)-Xyl-R	$[M - 2H]^{2-}$	628.2244	628.2234	-1.59	21.00
HexA-Hex-Hex-Xyl(P)-R	$[M - 2H]^{2-}$	1054.3862	1054.3904	3.98	21.86
NeuAc-NeuAc-Hex-Hex-Xyl(P)-R	$[M - 2H]^{2-}$	729.7688	729.7632	-7.67	22.87
HexNAc-HexA-Hex-Hex-Xyl(P)-R	$[M - 2H]^{2-}$	628.2291	628.2271	-3.18	22.90
HexNAc(S)-HexA-Hex-Hex-Xyl(P)-R	$[M - 2H]^{2-}$	668.2028	668.2012	-2.39	23.14
HexA-HexNAc-HexA-Hex-Hex-Xyl-R	$[M - 2H]^{2-}$	676.262	676.2669	7.25	24.77
$(HexNAc-HexA)_2$-Hex-Hex-Xyl-R_HS[a]	$[M - 2H]^{2-}$	777.8017	777.7968	-6.30	24.87
$(HexNAc-HexA)_2$-Hex-Hex-Xyl-R_CS[b]	$[M - 2H]^{2-}$	777.8017	777.7999	-2.31	25.31
HexNAc(S)-HexA-HexNAc-HexA-Hex-Hex-Xyl-R	$[M - 2H]^{2-}$	817.7801	817.7741	-7.34	25.55
$(HexNAc-HexA)_2$-Hex-Hex-Xyl(P)-R_1	$[M - 2H]^{2-}$	817.7847	817.7824	-2.81	26.87
$(HexNAc-HexA)_2$-Hex-Hex-Xyl(P)-R_2	$[M - 2H]^{2-}$	817.7847	817.7863	1.96	27.38
$(HexNAc-HexA)_3$-Hex-Hex-Xyl-R	$[M - 2H]^{2-}$	967.3574	967.3547	-2.79	29.14

[a] The product digested by heparitinases.

[b] The product digested by C-ABC.

Table 3-6 MS/MS assignments of the glycosylated products elongated on Gly-(Xyl)Ser-C12.

Glycosylated products	Fragment ions
Hex-Xyl-R	474.2065 (Y_1), 324.2345 (Z_0), 281.2223
Hex(S)-Xyl-R	391.0525 (C_2), 324.2342 (Z_0), 281.2221, 240.9982 (B_1)
Hex-Hex-Xyl-R	395.1241 ($^{2,5}A_3$), 324.2359 (Z_0), 263.0779 ($^{2,5}A_2$), 221.0665 ($^{2,4}A_2$)
Hex(S)-Hex-Xyl-R	553.1105 (C_3), 241.0020 (B_1)
Hex-Xyl(P)-R	554.2509 (Y1), 391.0663 (C2), 373.0561 (B2), 259.0221 ([Hex + PO_3]$^-$), 241.0128 ([Hex – H_2O + PO_3]$^-$), 78.9597 ([PO_3]$^-$)
NeuAc-Hex-Xyl-R	706.3425 ($^{0,2}X_3$), 602.1965 (C_3), 468.1745 ($^{2,4}A_3$ – CO_2), 408.1541 (B_3 – CO_2), 324.2336 (Z_0), 290.0983 (B_1)
Hex-Hex-Xyl(P)-R	716.3032 (Y_2), 698.2935 (Z_2), 554.2469 (Y_1), 553.1216 (C_3), 535.1114 (B_3), 221.0654 ($^{2,4}A_2$) (Y_1), 78.9583 ([PO_3]$^-$)
NeuAc-Hex-Hex-Xyl-R	868.4003 ($^{0,2}X_3$), 764.2661 (C_4), 746.2454 (B_4), 642.2231 ($^{2,5}A_3$ – CO_2), 630.2277 ($^{2,4}A_4$ – CO_2), 570.2067 (B_2 – CO_2), 324.2283 (Z_0), 290.0880 (B_1)
Hex(S)-Hex-Xyl(P)-R	716.3085 (Y_2), 535.1090 (B_3 – SO_3), 78.9564 ([PO_3]$^-$)
NeuAc-Hex-Hex-Xyl-R	324.2256 (Z_0), 290.0848 (B_1)
NeuAc-Hex-Xyl(P)-R_1	963.4118 ([M – H - CO_2]$^-$), 716.3090 (Y_2), 554.2497 (Y_1), 391.0662 (C_3/Y_2), 373.0558 (B_3/Y_2), 78.9587 ([PO_3]$^-$)
NeuAc-Hex-Xyl(P)-R_2	963.4065 ([M – H - CO_2]$^-$), 716.3043 (Y_2), 554.2424 (Y_1), 391.0651 (C_3/Y_2), 373.0610 (B_3/Y_2), 78.9557 ([PO_3]$^-$)
NeuAc-NeuAc-Hex-Xyl-R	927.4344 (Y_3), 581.1848 (B_2), 537.1937 (B_2 – CO_2), 290.0846 (B_1)
HexA-Hex-Hex-Xyl-R	649.1876 (C_4), 355.0899 (C_2), 324.2288 (Z_0)
HexA(S)-Hex-Hex-Xyl-R	878.3483 (Y_3), 649.1840 (C_4 – SO_3), 589.1661 ($^{0,2}A_4$ – SO_3), 324.2288 (Z_0), 254.9818 (B_1), 96.9594 ([HSO_4]$^-$)
HexNAc-HexA-Hex-Hex-Xyl-R	956.4141 (Z_4), 852.2656 (C_5), 631.1741 (C_5/Z_4), 509.1529 ($^{2,5}A_5/Z_4$ – CO_2), 437.1303 (B_4/Z_3), 324.2306 (Z_0)
NeuAc-Hex-Hex-Xyl(P)-R	1125.4596 ([M – H – CO_2]$^-$), 878.3582 (Y_3), 716.3001 (Y_2), 554.2384 (Y_1), 553.1182 (C_4/Y_3), 535.1071 (B_4/Y_3), 79.9585 ([PO_3]$^-$)
HexNAc(S)-HexA-Hex-Hex-Xyl-R_1	932.2158 (C_5), 852.2451 (C_5 – SO_3), 324.2274 (Z_0), 282.0317 (B_1), 96.9598 ([HSO_4]$^-$)
HexNAc(S)-HexA-Hex-Hex-Xyl-R_2	932.2403 (C_5), 852.2678 (C_5 – SO_3), 458.0599 (B_2), 324.2285 (Z_0), 282.0282 (B_1)
NeuAc-Hex-Hex-Xyl(P)-R	878.3549 (Y_3), 716.2964 (Y_2), 78.9587 ([PO_3]$^-$)
HexNAc-HexA-Hex-Hex(S)-Xyl-R	932.3071 (C_5), 852.2667 (C_5 – SO_3), 553.1079 (C_5/Y_3), 324.2297 (Z_0)
HexA-Hex-Hex-Xyl(P)-R	878.3560 (Y_3), 729.1508 (C_4), 716.3100 (Y_2), 554.2518 (Y_1), 553.1188 (C_4/Y_3), 535.1071 (B_4/Y_3), 324.2299 (Z_0), 193.0365 (C_1), 78.9610 ([PO_3]$^-$)
NeuAc-NeuAc-Hex-Hex-Xyl(P)-R	878.3586 (Y_3), 716.3123 (Y_2), 553.1178 (C_5/Y_3), 290.0872 (B_1), 78.9602 ([PO_3]$^-$)
HexNAc-HexA-Hex-Hex-Xyl(P)-R	1036.3807 (Z_4), 992.3937 (Z_4 – CO_2), 878.3574 (Y_3), 716.3028 (Y_2), 554,2504 (Y_1), 509.1519 ($^{2,5}A_6/Z_4$ – CO_2), 324.2303 (Z_0), 78.9590 ([PO_3]$^-$)
HexNAc(S)-HexA-Hex-Hex-Xyl(P)-R	878.3730 (Y_3), 716.3028 (Y_2), 458.0674 (B_2), 282.0251 (B_1)
HexA-HexNAc-HexA-Hex-Hex-Xyl-R	1028.2915 (C_6), 396.1104 (C_2), 324.2293 (Z_0), 193.0374 (B_1)
(HexNAc-HexA)$_2$-Hex-Hex-Xyl-R_HS	1231.3788 (C_7), 1010.2853 (C_7/Z_6), 956.4163 (Z_3), 599.2028 (C_3), 509.1603 ($^{2,5}A_7/Z_4$ – CO_2), 480.1440 ($^{2,5}A_3$), 396.1121 (C_2), 324.2312 (Z_0)
(HexNAc-HexA)$_2$-Hex-Hex-Xyl-R_CS	1291.5408 (Z_6 – CO_2), 1231.3706 (C_7), 1099.3533 (C_6), 1010.2803 (C_7/Z_6), 956.4081 (Z_3), 937.2877 (C_5), 757.2130 (B_4), 599.1923 (C_3), 509.1527 ($^{2,5}A_7/Z_4$ – CO_2), 396.1154 (C_2), 324.2301 (Z_0)
HexNAc(S)-HexA-HexNAc-HexA-Hex-Hex-Xyl-R	1177.5214 (Y_5), 974.4074 (Y_4), 956.4096 (Z_4), 757.2216 (B_4 – SO_3), 679.1537 (C_3), 599.1962 (C_3 – SO_3), 509.1535 ($^{2,5}A_9/Z_4$ – CO_2), 458.0644 (B_2), 396.1151 (C_2 – SO_3), 324.2307 (Z_0), 282.0278 (B_1)
(HexNAc-HexA)$_2$-Hex-Hex-Xyl(P)-R_1	992.3873 (Z_4 – CO_2 – HPO_3), 878.3685 (Y_3), 757.2396 (B_4), 599.1926 (C_3), 396.1138 (C_2), 78.9561 ([PO_3]$^-$)
(HexNAc-HexA)$_2$-Hex-Hex-Xyl(P)-R_2	1036.3835 (Z_4 – HPO_3), 992.38794 (Z_4 – CO_2 – HPO_3), 878.3558 (Y_3), 757.2181 (B_4), 716.3064 (Y_3), 599.1977 (C_3), 535.1083 (B_7/Y_3), 396.1116 (C_2), 324.2238 (Z_0), 78.9566 ([PO_3]$^-$)
(HexNAc-HexA)$_3$-Hex-Hex-Xyl-R	1291.5387 (Z_6 – CO_2), 956.4130 (Z_3), 775.2224 (C_4), 757.2167 (B_4), 599.1960 (C_3), 396.1157 (C_2), 324.2293 (Z_0)

Table 3-7 Detected glycosylated products elongated on Gly-(Xyl)Thr-C12. The glycosylated products that had identical *m/z* values but differed in their retention times were distinguished by the numbers after underscore.

Glycosylated products	Ion type	Calculated m/z	Observed m/z	Error (ppm)	R. T. (min)
Hex-Xyl-R	$[M - H]^-$	650.3506	650.3489	-2.61	7.72
Hex(S)-Xyl-R	$[M - H]^-$	730.3074	730.3035	-5.34	9.21
Hex-Hex-Xyl-R	$[M - H]^-$	812.4034	812.3988	-5.66	11.79
Hex(S)-Hex-Xyl-R	$[M - H]^-$	892.3602	892.3544	-6.50	12.42
Hex-Hex(S)-Xyl-R	$[M - H]^-$	892.3602	892.3576	-2.91	12.76
NeuAc-Hex-Xyl-R	$[M - H]^-$	941.446	941.442	-4.25	13.62
Hex-Hex-Xyl(P)-R	$[M - H]^-$	892.3697	892.366	-4.15	15.96
NeuAc-Hex-Hex-Xyl-R_1	$[M - H]^-$	1103.4988	1103.4927	-5.53	16.63
NeuAc-Hex-Hex-Xyl-R_2	$[M - H]^-$	1103.4988	1103.4988	0.00	16.93
HexA-Hex-Hex-Xyl-R	$[M - H]^-$	988.4355	988.4283	-7.28	18.35
HexA(S)-Hex-Hex-Xyl-R	$[M - H]^-$	1068.3923	1068.3832	-8.52	18.59
NeuAc-NeuAc-Hex-Hex-Xyl-R	$[M - 2H]^{2-}$	696.7935	696.7921	-2.01	20.17
HexNAc-HexA-Hex-Hex-Xyl(P)-R	$[M - 2H]^{2-}$	635.237	635.2363	-1.10	22.66
$(HexNAc-HexA)_2$-Hex-Hex-Xyl-R_CS[a]	$[M - 2H]^{2-}$	784.8095	784.8046	-6.24	25.04

[a] The product digested by C-ABC.

Table 3-8 MS/MS assignments of the glycosylated products elongated on Gly-(Xyl)Thr-C12

Glycosylated products	Fragment ions
Hex-Xyl-R	470.2883 (Z_1), 338.2532 (Z_0), 295.2387, 255.2072, 238.1812
Hex(S)-Xyl-R	391.0558 (C_2), 338.2440 (Z_0), 241.0016 (B_1), 96.9598 ($[HSO_4]^-$)
Hex-Hex-Xyl-R	650.3516 (Y_2), 488.3006 (Y_1), 470.2904 (Z_1), 395.1242 ($^{2,5}A_3$), 338.2516 (Z_0), 263.0780 ($^{2,5}A_2$), 221.0670 ($^{2,4}A_2$)
Hex(S)-Hex-Xyl-R	241.0012 (B_1)
Hex-Hex(S)-Xyl-R	730.3107 (Y_2), 712.2971 (Z_2), 553.1126 (C_3), 403.0578 (B_2), 96.9590 ($[HSO_4]^-$)
NeuAc-Hex-Xyl-R	720.3580 ($^{0,2}X_2$), 650.3522 (Y_2), 602.1957 (C_3), 480.1743 ($^{2,5}A_3 - CO_2$), 468.1739 ($^{2,4}A_3 - CO_2$), 408.1553 ($B_3 - CO_2$), 338.2506 (Z_0), 290.0973 (B_1)
Hex-Hex-Xyl(P)-R	730.3204 (Y_2), 553.1226 (C_3), 78.9567 ($[PO_3]^-$)
NeuAc-Hex-Hex-Xyl-R_1	882.4208 ($^{0,2}X_3$), 812.4063 (Y_2), 650.3469 (Y_1), 338.2456 (Z_0), 290.0888 (B_1)
NeuAc-Hex-Hex-Xyl-R_2	290.0892 (B_1)
HexA-Hex-Hex-Xyl-R	649.1846 (C_4), 338.2415 (Z_0)
HexA(S)-Hex-Hex-Xyl-R	892.3639 (Y_3), 650.1973 (Y_2), 338.2427 (Z_0), 254.9814 (B_1), 96.9549 ($[HSO_4]^-$)
NeuAc-NeuAc-Hex-Hex-Xyl-R	1103.5037 (Y_4), 1011.3585 ($C_5 - CO_2$), 882.4087 ($^{0,2}X_3$), 338.2447 (Z_0), 290.0885 (B_1)
HexNAc-HexA-Hex-Hex-Xyl(P)-R	892.3714 (Y_3), 874.3593 (Z_3), 730.3190 (Y_2), 568.2643 (Y_1), 78.9585 ($[PO_3]^-$)
$(HexNAc-HexA)_2$-Hex-Hex-Xyl-R_CS	1231.4858 (C_7), 599.1954 (C_3), 509.1525 ($^{2,5}A_7/Z_4 - CO_2$), 396.1138 (C_2), 338.2453 (Z_0)

Table 3-9 Proportions of glycosylated products obtained from NHDF cells. The average values were obtained from three individual experiments. S. D. means standards deviations.

Glycosylated products	Average				S.D. (n = 3)			
	Xyl-Ser-C12	Xyl-Thr-C12	Gly-(Xyl) Ser-C12	Gly-(Xyl) Thr-C12	Xyl-Ser-C12	Xyl-Thr-C12	Gly-(Xyl) Ser-C12	Gly-(Xyl) Thr-C12
Hex-Xyl-R	7.41	45.09	7.70	50.80	0.41	5.00	0.57	5.80
Hex(S)-Xyl-R	0.44	0.29	0.04	0.31	0.48	0.08	0.01	0.21
Hex-Hex-Xyl-R	11.86	25.25	18.66	40.36	0.87	2.10	0.47	4.92
Hex(S)-Hex-Xyl-R	1.28	0.40	0.12	0.78	1.47	0.10	0.04	0.81
Hex-Hex(S)-Xyl-R	0.72	0.20	-	0.30	0.82	0.08	-	0.22
NeuAc-Hex-Xyl-R	10.24	26.12	2.76	6.29	3.70	7.46	0.04	1.83
Hex-Xyl(P)-R	17.85	0.75	6.69	-	0.60	0.17	0.21	-
Hex-Hex-Xyl(P)-R	6.22	0.18	10.68	0.19	0.65	0.06	0.17	0.03
Hex(S)-Hex-Xyl(P)-R	0.07	-	0.03	-	0.05	-	0.00	-
NeuAc-Hex-Hex-Xyl-R_1	0.13	0.15	0.07	0.11	0.01	0.02	0.01	0.05
NeuAc-Hex-Hex-Xyl-R_2	-	0.05	-	0.04	-	0.01	-	0.03
NeuAc-Hex-Xyl(P)-R_1	5.81	0.18	2.72	-	0.36	0.02	0.26	-
NeuAc-Hex-Xyl(P)-R_2	-	-	0.09	-	-	-	0.03	-
HexA-Hex-Hex-Xyl-R	1.35	0.08	1.00	0.07	0.08	0.05	0.11	0.02
HexA(S)-Hex-Hex-Xyl-R	1.32	0.24	0.70	0.14	0.21	0.11	0.18	0.05
NeuAc-NeuAc-Hex-Xyl-R	0.05	0.06	0.01	-	0.02	0.02	0.01	-
HexNAc-HexA-Hex-Hex-Xyl-R_1	0.09	-	-	-	0.01	-	-	-
HexNAc-HexA-Hex-Hex-Xyl-R_2	10.62	0.40	7.02	-	1.90	0.05	0.16	-
NeuAc-NeuAc-Hex-Hex-Xyl-R	-	-	-	0.22	-	-	-	0.16
HexNAc(S)-HexA-Hex-Hex-Xyl-R_1	0.09	-	0.08	-	0.02	-	0.05	-
HexNAc(S)-HexA-Hex-Hex-Xyl-R_2	-	-	0.05	-	-	-	0.03	-
NeuAc-Hex-Hex-Xyl(P)-R	0.31	-	0.40	-	0.04	-	0.02	-
HexA-Hex-Hex-Xyl(P)-R	0.30	-	0.34	-	0.01	-	0.04	-
HexA(S)-Hex-Hex-Xyl(P)-R	0.37	-	-	-	0.16	-	-	-
HexNAc-HexA-Hex-Hex-Xyl(P)-R	20.91	0.53	36.75	0.38	3.25	0.21	0.26	0.06
NeuAc-NeuAc-Hex-Hex-Xyl(P)-R_1	0.63	-	1.23	-	0.13	-	0.15	-
NeuAc-NeuAc-Hex-Hex-Xyl(P)-R_2	0.03	-	-	-	0.01	-	-	-
HexA-HexNAc-HexA-Hex-Hex-Xyl-R	0.05	-	0.04	-	0.02	-	0.00	-
$(HexNAc\text{-}HexA)_2$-Hex-Hex-Xyl-R_HS	0.03	-	0.04	-	0.00	-	0.01	-
$(HexNAc\text{-}HexA)_2$-Hex-Hex-Xyl-R_CS	0.91	0.04	0.93	0.03	0.17	0.01	0.08	0.00
HexNAc(S)-HexA-HexNAc-HexA-Hex-Hex-Xyl-R	0.36	-	0.31	-	0.05	-	0.04	-
$(HexNAc\text{-}HexA)_2$-Hex-Hex-Xyl(P)-R_1	-	-	0.05	-	-	-	0.01	-
$(HexNAc\text{-}HexA)_2$-Hex-Hex-Xyl(P)-R_2	0.49	-	0.78	-	0.07	-	0.02	-
$(HexNAc\text{-}HexA)_3$-Hex-Hex-Xyl-R	0.05	-	0.04	-	0.02	-	0.01	-

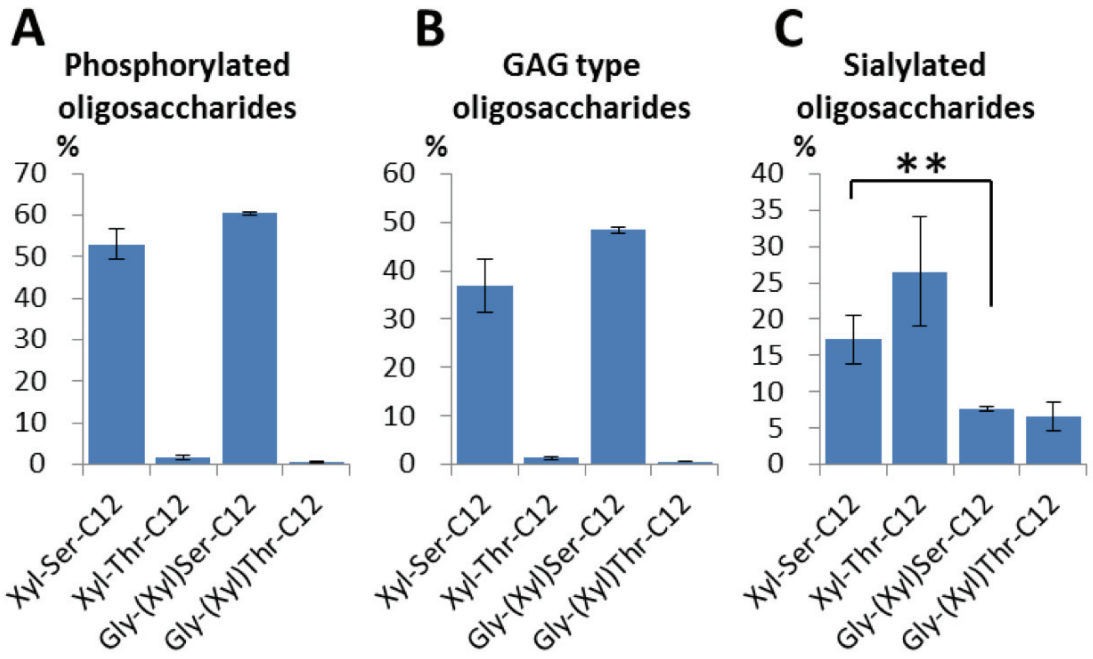

Figure 3-8 Total proportion of (A) phosphorylated, (B) GAG type, and (C) sialyloligosaccharides elongated on the β-xylosides. Double asterisk (**) denotes $p < 0.01$ in Student's t-test.

Among the β-xylosides, Xyl-Ser-C12 primed the maximum amount of glycosylated products (Table 3-9). Among the glycosylated products of Xyl- Ser-C12, the most abundant product was a phosphorylated pentasaccharide (HexNAc-HexA-Hex-Hex-Xyl(P)-Ser-C12) (20.91 %). The sum of the proportion of phosphorylated products obtained from Xyl-Ser-C12 is about 50 %. These phosphorylated products have not been detected in previous studies (Figure 3-8).[37,61] These results suggest that Xyl-Ser-C12 works as an appropriate substrate for Xyl phosphorylation, and the phosphorylated products were easily excreted into the medium. Furthermore, the sum of the proportion of GAG-type oligosaccharides, which were composed of the linkage tetrasaccharides, was about 40 % (Figure 3-8B). Taking into consideration the fact that the phosphorylated products were the intermediates of GAG biosynthesis, a large part of Xyl-Ser- C12 was incorporated into the GAG biosynthesis pathway. The total proportion of the sialyloligosaccharides was approximately 17 %. Therefore, some part of Xyl-Ser-C12 taken by NHDF cells may be recognized by sialyltransferases.

Similar to Xyl-Ser-C12, Gly-(Xyl)Ser-C12 also initiated mainly GAG-type

oligosaccharides. The most abundant product was the phosphorylated pentasaccharide (HexNAc-HexA-Hex-Hex-Xyl(P)-GlySer-C12) (36.75 %). In comparison with Xyl-Ser-C12, phosphorylated products and GAG-type oligosaccharides were slightly but not significantly increased (Figure 3-8A, B). In addition, it is notable that the amount of sialyloligosaccharides elongated on Gly-(Xyl)Ser-C12 was significantly lower than that on Xyl-Ser-C12 (Figure 3-8C). These results suggest that the Gly residue flanked by the Ser residue in Gly-(Xyl)Ser-C12 affects the efficiency of Xyl phosphorylation and sialylation. Gly-(Xyl)Ser-C12 would be a better primer to construct GAG-like oligosaccharide libraries because α2-3 sialylated oligosaccharides, which are the end-capping structure, were undesirable to obtain phosphorylated and GAG-type oligosaccharides.

Xyl-Thr-C12 and Gly-(Xyl)Ser-C12 gave fewer species of elongated oligosaccharides than either Xyl-Ser-C12 or Gly-(Xyl)Ser-C12 (Table 3-9). They initiated large amounts of sialyloligosaccharides, such as NeuAcα2-3Hex-Xyl-R, and small amounts of both phosphorylated and GAG-type oligosaccharides (Figure 3-8A–C). Therefore, these β-xylosides, which are composed of a Xyl-Thr residue, are unlikely to work well for Xyl phosphorylation.

3.4 Conclusion

In this study, we established an analytical method for phosphorylated oligosaccharides elongated on the saccharide primers, by which a wide variety of oligosaccharides could be observed using LC–MS/MS. Most of these oligosaccharides seemed to be synthesized in accordance with the GAG biosynthetic pathway (Figure 3-9). These results indicate that the β-xylosides prime phosphorylated GAG-type oligosaccharides in living cells. In addition, the comparison of the relative amounts of these oligosaccharides revealed that the proportions of phosphorylated oligosaccharides and sialylated oligosaccharides were completely different between the primers. To our best knowledge, this is the first report to demonstrate that the amino acid residues around the Xyl attachment position strongly affect phosphorylation efficiency. Taking into consideration the GAG biosynthetic pathway, our results suggest that both phosphorylation and α2-3 sialylation are related to the GAG priming ability of the

primers. Notably, these oligosaccharides included phosphorylated α2-6 sialyloligosaccharides, implying that both sialylation and Xyl phosphorylation might orchestrate the GAG biosynthesis mechanism. However, the function of the α2-6 sialylation in the GAG biosynthesis mechanism remains to be discussed further, thus in-depth analysis of the phosphorylated sialyloligosaccharides is needed.

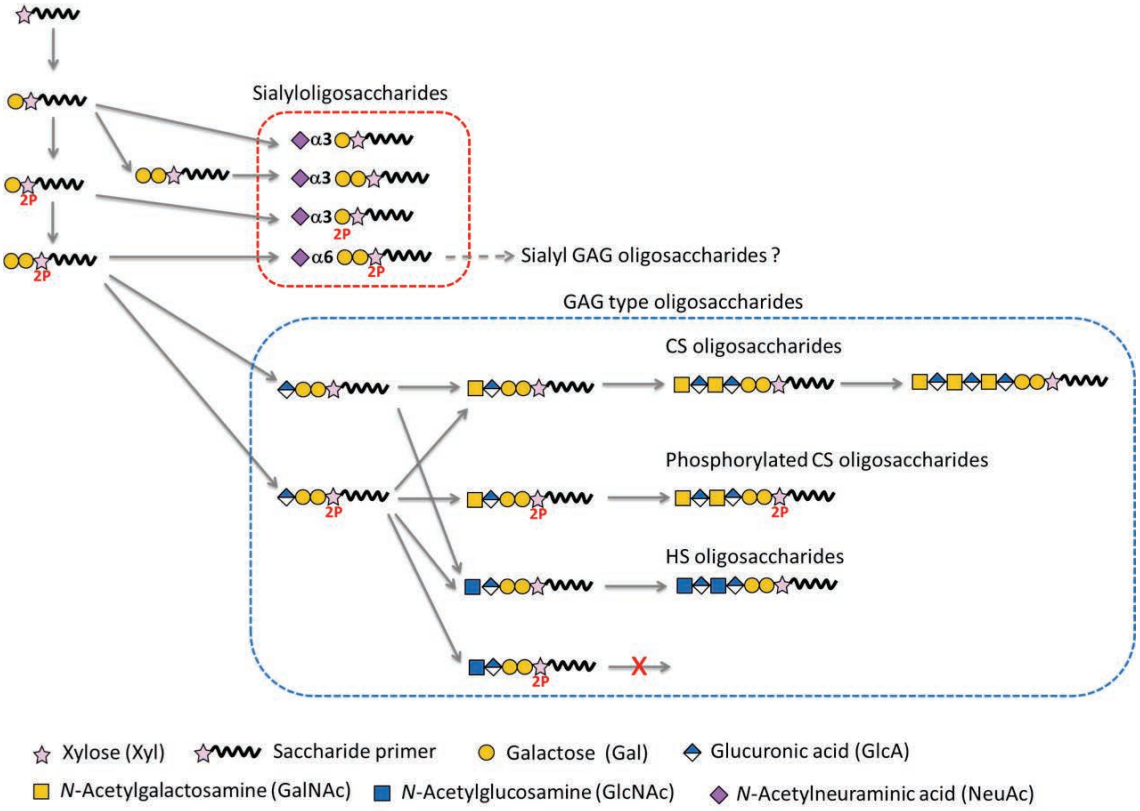

Figure 3-9 Speculated biosynthesis pathways of glycosylated products elongated on saccharide primer. The biosynthesis is initiated with galactosylation on the Xyl. The disaccharide is phosphorylated for GAG-type oligosaccharide biosynthesis. The phosphorylated disaccharide is used as an intermediate of GAG biosynthetic pathway. Dephosphorylation can be occurred during both GlcA addition on the phosphorylated trisaccharide and GalNAc addition on the phosphorylated tetrasaccharide. The phosphorylated trisaccharide can be modified by α2-6 linked NeuAc for sialyl GAG synthesis. Without the Xyl phosphorylation, the disaccharide can be capped by α2-3 linked NeuAc. Gal, HexA, and HexNAc residues can be sulfated during the biosynthesis.

β-Xylosides with amino acid residues in their aglycone were synthesized by chemoenzymatic synthesis to examine the effect of the aglycone structure on the

priming ability. The amino acid residues strongly affect the structure of oligosaccharides, especially phosphorylated oligosaccharides. The β-xylosides synthesized in this study demonstrated high priming ability for a wide variety of oligosaccharides, providing a chemical tool not only to obtain GAG-type oligosaccharides but also to investigate the GAG biosynthesis mechanism. This study is an important step in the development of a new methodology using β-xylosides to clarify the GAG biosynthesis mechanism and for the comparison of glycosaminoglycomics between different cells and tissues.

Chapter 4
Method Development for Comparative Quantification for Priming Oligosaccharides Using a Stable Isotope Labeled Saccharide Primer.

4.1 Introduction

There are several reports of the use of saccharide primers for comparative glycomics studies.[30,61] Comparison of the glycosylated products has been carried out by several analytical techniques such as high-performance thin-layer chromatography,[20,62] HPLC,[63] and LC–MS.[37,61,64] However, accurate comparative quantification remains challenging because experimental processes such as solid phase extraction, LC separation and MS detection may cause experimental errors. Therefore, a more accurate comparative quantification method for glycosylated products is required.

In the MS field, the isotope-labeling strategy is a promising approach for relative quantification and is widely used in omics studies.[65–67] There are two approaches for stable isotope labeling: metabolic labeling and chemical modification. Specifically, metabolic labeling approaches like stable isotope labeling using amino acids in cell culture (SILAC) in proteomics are highly reliable for comparative proteomics because these methods can circumvent experimental bias caused by the chemical modification process.[68–71] In regards to glycomics research, several isotope-labeling methods have been developed.[72] For example, reductive amination,[73–75] reducing end modification,[76] and permethylation[77] have been used for the chemical labeling approach. On the other hand, there are a few studies focusing on the metabolic labeling approach in the glycomics field. For instance, isotopic detection of aminosugars with glutamine (IDAWG) is a metabolic labeling technique using amide-^{15}N Gln to introduce ^{15}N into hexosamines.[78] In this approach, "heavy" glycans are increased 1 Da in their molecular weight per amino sugar residue. However, this increase is not sufficient to discriminate "light" and "heavy" products because the MS peaks of "light" glycans could overlap the peaks of "heavy" glycans. This overlap might result in inaccurate quantification. Hence, a more accurate and reliable approach is required to compare the amounts of glycosylated products elongated on saccharide primers.

Here, we established a relative quantification method for comparative glycomics research using an isotope-labeled saccharide primer. In this method, a pair of deuterium-labeled and non-labeled saccharide primers is used for comparison of GAG biosynthesis in cells. In order to demonstrate the feasibility of this method for comparative glycomics study, effects of known GAG biosynthesis inhibitors for living cells were confirmed using the method.

4.2 Materials and methods

4.2.1 Materials

NHDF cells were purchased from Kurabo Industries Ltd. (Osaka, Japan). DMEM GlutaMax, and DMEM without phenol red were purchased from Thermo Fisher Scientific (Yokohama, Japan). Lauric acid-d_5 was purchased from Sigma-Aldrich Japan (Tokyo, Japan). All other chemical reagents were purchased from Sigma-Aldrich Japan (Tokyo, Japan), Wako Pure Chemical Industries Ltd. (Osaka, Japan), and Tokyo Chemical Industries Co., Ltd. (Tokyo, Japan). Unless otherwise stated, reagents and solvents were used without purification.

4.2.2 Chemical synthesis of Gly-(Xyl)Ser-C12-d5 (heavy primer)

23 mg (0.059 mmol) of *N*-Boc-*O*-*β*-D-xylopyranosyl-L-serinyl glycinamide was dissolved in 1 mL of TFA and stirred at room temperature. After 15 min, TFA was removed completely under reduced pressure. The residue was dissolved in 1 mL of water, followed by the addition of 13 mg (0.065 mmol) of lauric acid-d5 and 18 mg (0.065 mmol) of DMT-MM. The mixture was stirred at 40 °C for 2 h. Saturated aqueous sodium bicarbonate was added and the reaction mixture was extracted with ethyl acetate. The organic phase was removed under reduced pressure and the residue was purified by silica gel column chromatography (1.0 cm i.d. × 20 cm, chloroform/methanol = 4/1). Gly-(Xyl)Ser-C12-d_5 was obtained as a white solid. Yield: 93.1 % (26.0 mg). Melting point: 161.4 °C. $[\alpha]^{20}$: -14.2 (c = 0.065). ^{1}H-NMR (CD_3COOD): d 4.75-4.77 (dd, $J_{\alpha,\beta}$ = 5.5 Hz, 1H, H-α), 4.26-4.27 (d, $J_{1,2}$ = 7.5 Hz, 1H, H-1), 4.00-4.03 (dd, $J_{\alpha,\beta}$ = 5 Hz and J_{gem} 10.5 Hz, 1H, H-β_1), 3.94-3.97 (d, J_{gem} = 17 Hz, 1H, CH_2(Gly)α), 3.87-3.90 (d, J_{gem} = 17 Hz, 1H, CH_2(Gly)β), 3.84-3.88 (dd, $J_{4,5}$ = 5.3 Hz and J_{gem} = 12 Hz, 1H, H-5α), 3.68-3.71 (dd, $J_{\alpha,\beta}$ = 6 Hz and J_{gem} = 10.5 Hz, 1H, H-β_2), 3.57-3.62 (ddd, $J_{4,5^\alpha}$ = 5.5 Hz, $J_{4,5^\beta}$ = 10 Hz, $J_{3,4}$ = 9 Hz, 1H, H-4), 3.46-3.50 (dd

$J_{3,4} = J_{2,3}$ = 9 Hz, 1H, H-3), 3.25-3.28 (dd, $J_{1,2}$ = 7.5 Hz and $J_{2,3}$ = 8.5 Hz, 1H, H-2), 3.18-3.22 (dd, $J_{4,5}$ = 10.5 Hz and J_{gem} = 11.5 Hz, 1H, H-5β), 2.18-2.1 (dd, J = 7.5 Hz, 2H, COCH_2), 1.47-1.50 (m, 2H, $CH_2(CH_2)_7CD_2CD_3$), 1.12-1.15 (m, 14H, $CH_2(CH_2)_7CD_2CD_3$). ^{13}C-NMR (CD_3COOD): 18.50, 18.66, 18.82, 18.87, 18.97, 19.03, 19.14, 25.05, 28.58, 28.73, 28.79, 28.95, 29.10, 31.08, 35.19, 41.78, 52.69, 64.58, 68.85, 69.00, 72.74, 75.48, 103.12, 171.31, 174.17, 175.69. HRMS calculated for $C_{22}H_{41}N_3O_8Na$: $[M + Na]^+$, 503.3100. Found: 503.3106.

4.2.3 Priming of elongated-oligosaccharides on the saccharide primers

The primers were purified by reverse phase HPLC in advance. NHDF cells were cultured and expanded in DMEM GlutaMax medium with 10 % fetal bovine serum and 1% penicillin-streptomycin solution in a humidified atmosphere containing 5 % CO_2.

To confirm differences in the priming abilities, NHDF cells (4 x 10^6) were seeded onto a 15 cm dish and cultured for 18 h to 80 % confluence. After washing with PBS, the cells were incubated with 10 mL of phenol red-free DMEM containing 25 μM of the light or heavy primer for 3 days. For the linearity test, NHDF cells (4 x 10^5) were seeded onto the wells of a six-well plate and cultured for 18 h to 80 % confluence. After washing with phosphate-buffered saline (PBS), the cells were incubated with 1 mL of phenol red-free DMEM containing 25 μM of the light primer for 3 days. When examining GAG biosynthesis inhibition, phenol red-free DMEM containing 10 or 100 μM of each inhibitor was used. After 3 days incubation, the media and cells were harvested. When the media were transferred to tubes, the wells and plates were washed with 0.5 mL and 3 mL of PBS, respectively, and the PBS wash solutions were combined with the respective media. The cells were removed by centrifugation, and then each medium was transferred to a 5 mL tube. The medium containing the heavy primer was collected in the same manner and transferred to a 15 mL tube. The collected medium was store at −80 °C until use.

4.2.4 Sample preparation

In the experiment, the elongated oligosaccharides on the heavy primer were used internal standards. A 0.75-mL aliquot of the “heavy” medium was added into the same volume of the “light” medium collected from a well and mixed. The glycosylated

products in the mixed medium were extracted using a solid-phase extraction cartridge. A 45-μL aliquot of 0.5 mol/L dibutylammonium acetate (DBAA) solution was added into 1.5 mL of the culture medium and stirred well. The mixed solution was applied to a Strata-X cartridge (60 mg, 3 mL, Phenomenex, Torrance, CA), which had been washed with methanol and equilibrated with 20 mM DBAA in advance. After the cartridge was washed with 2 mL of water and then 2 mL of 30 % MeOH, the glycosylated products were eluted with 0.5 mL of 90 % MeOH twice. The eluted fractions were subjected to centrifugal evaporation to remove the solvent. The residues were dissolved in 30 μL of MeCN/MeOH/5 mM $(NH_4)_2HPO_4$ (15/3/2) and filtrated using 0.22 μm filters. The filtrated solutions were subjected to LC–MS/MS analysis.

4.2.5 LC–MS/MS analysis

LC–MS/MS analysis was performed using a Synapt G2-S coupled to an Acquity UPLC H-Class Bio (Nihon Waters, Tokyo, Japan). The glycosylated products were separated by Acquity UPLC BEH Glycan (2.1 mm x 150 mm, 1.7 μm) at 60°C. A 50-mM concentration of ammonium formate buffer (pH 7.8) was used as solvent A and pure acetonitrile was used as solvent B. The flow rate was set at 0.2 mL/min. The glycosylated products were eluted in a linear gradient (95 % B to 60 % B in 40 min). The data were recorded in MS mode for quantification and MS/MS mode for structure analysis. The polarity was in negative ion mode. For all analyses, the resolution was set to sensitivity mode (resolution approximately 10,000 at *m/z* 554). MS recording range was 400-1500 in MS mode and 50-1500 in MS/MS mode. Other MS parameters are shown below. Capillary voltage: −0.3 kV, cone voltage: 20 V, source offset: 20 V, source temperature: 350 °C, desolvation gas flow: 1200 L/h, desolvation gas temperature: 600 °C, nebulizer gas: 6.0 L/min, trap CE: 20 V at low CE and 70 V at high CE, transfer CE: 2 V. All LC–MS data were analyzed using MassLynx software ver. 4.1 (Waters).

4.2.6 Data analysis for comparative quantification

The light/heavy rate of elongated oligosaccharides was calculated based on EIC chromatograms generated by MassLynx software ver. 4.1. The relative peak area (Rp_i) of a glycosylated product was calculated using the following equation.

$$Rp_i = \frac{Lp_i}{Hp_i}$$

Where Lp_i and Hp_i are the peak area of a glycosylated product elongated on the light primer and that of the heavy primer, respectively. To compare the effects of GAG biosynthesis inhibitors, the relative amount of a glycosylated product obtained from each GAG inhibitor-added medium was calculated by dividing the Rp_i of each inhibitor by the average of Rp_i obtained from the control media. Statistical analyses were performed with a Student's t test using Microsoft Excel 2010.

4.2.7 Structural analysis of the glycosylated products

Determination of compositions of the glycosylated products and assignment of fragmentation ions in MS/MS spectra was accomplished using GlycoWorkbench version 2.1[79] and ChemDraw Std 12.0. Briefly, saccharide composition of the glycosylated products was determined according to the *m/z* values of MS spectra. Assignments of fragment ions in MS/MS spectra were carried out according to the nomenclature introduced by Domon and Costello.[80] The confirmation of the glycosylated products elongated on the primers was based on diagnostic fragment ions related to the aglycone structure such as Z_0 and $Z_0 - H_2O$. Glycan sequences were deduced by the fragment ions caused by the glycoside bond cleavage. Discrimination of sulfated or phosphorylated products was carried out relying on the observation of $[HSO_4]^-$ ion and $[PO_3]^-$ ion in MS/MS spectra. The diagnostic fragment ions and neutral losses are shown below.

Table 4-1 Diagnostic fragment ions observed in the MS/MS spectra for the glycosylated products elongated on the light primer.

Structure	Fragment ions	Ionic formula	*m/z*
GlySerC12	Z_0	$C_{18}H_{34}N_3O_2^-$	324.27
	$Z_0 - H_2O$	$C_{18}H_{32}N_3O^-$	308.27
	-	$C_{16}H_{29}N_2O_2^-$	281.22
	-	$C_{14}H_{27}N_2O_2^-$	255.21
	-	$C_{14}H_{24}NO_2^-$	238.18
Hex	$[Hex - H]^-$	$C_6H_{11}O_6^-$	179.06
	$[Hex - H_2O - H]^-$	$C_6H_9O_5^-$	161.05
HexNAc	$[HexNAc - H]^-$	$C_8H_{14}NO_6^-$	220.08
	$[HexNAc - H_2O - H]^-$	$C_8H_{12}NO_5^-$	202.07
HexA	$[HexA - H]^-$	$C_6H_9O_7^-$	193.04
	$[HexA - H_2O - H]^-$	$C_6H_7O_6^-$	175.02
	$[C_5H_5O_3]^-$	$C_5H_5O_3^-$	113.02
NeuAc	$[NeuAc - H_2O - H]^-$	$C_{11}H_{16}NO_8^-$	290.09
	$[C_3H_3O_3]^-$	$C_3H_3O_3^-$	87.01
Phosphate	$[PO_3]^-$	PO_3^-	78.96
	$[H_2PO_4]^-$	$H_2PO_4^-$	96.97
Sulfate	$[HSO_4]^-$	HSO_4^-	96.96

Table 4-2 Diagnostic neutral losses observed in the MS/MS spectra for the glycosylated products elongated on the light primer.

Structure	Neutral losses	Compositional formula	$\Delta m/z$
GlySerC12	GlySerC12 − H_2O	$C_{18}H_{35}N_3O_2$	325.27
Xyl	Xyl − H_2O	$C_5H_8O_4$	132.04
	Xyl	$C_5H_{10}O_5$	150.05
Hex	Hex − H_2O	$C_6H_{10}O_5$	180.06
	Hex	$C_6H_{12}O_6$	162.05
HexA	HexA − H_2O	$C_6H_8O_6$	176.03
	HexA	$C_6H_{10}O_7$	194.04
HexNAc	HexNAc − H_2O	$C_8H_{13}NO_5$	203.08
	HexNAc	$C_8H_{15}NO_6$	221.09
NeuAc	NeuAc − H_2O	$C_{11}H_{17}NO_8$	291.10
Phosphate	HPO_3	HPO_3	79.97
Sulfate	SO_3	SO_3	79.96
Carboxylate	CO_2	CO_2	43.99

4.3 Results and discussion

4.3.1 Strategy for comparative quantification of the elongated oligosaccharides

Figure 4-1 illustrates the strategy used in the comparative quantification experiment. The pair of primers can be synthesized from *N*-Boc-*O*-*β*-D-xylopyranosyl-L-serinyl glycinamide by a one-pot reaction (Figure 4-1A, B). The primers were added into the cell culture media individually and incubated to obtain each glycosylated product separately. After glycosylation, the heavy medium was added into the light medium, the mixtures are extracted by solid phase extraction and then subjected to LC–MS analysis (Figure 4-1C). This procedure can offset experimental errors related to sample preparation and LC–MS detection. In addition, the glycosylated products gave doublet peaks in the MS spectra. In accordance with the MS signal intensities of heavy products and light products, relative amounts of the glycosylated products were calculated. Moreover, this feature helps to discriminate the peaks of glycosylated products from background signals related to medium components.

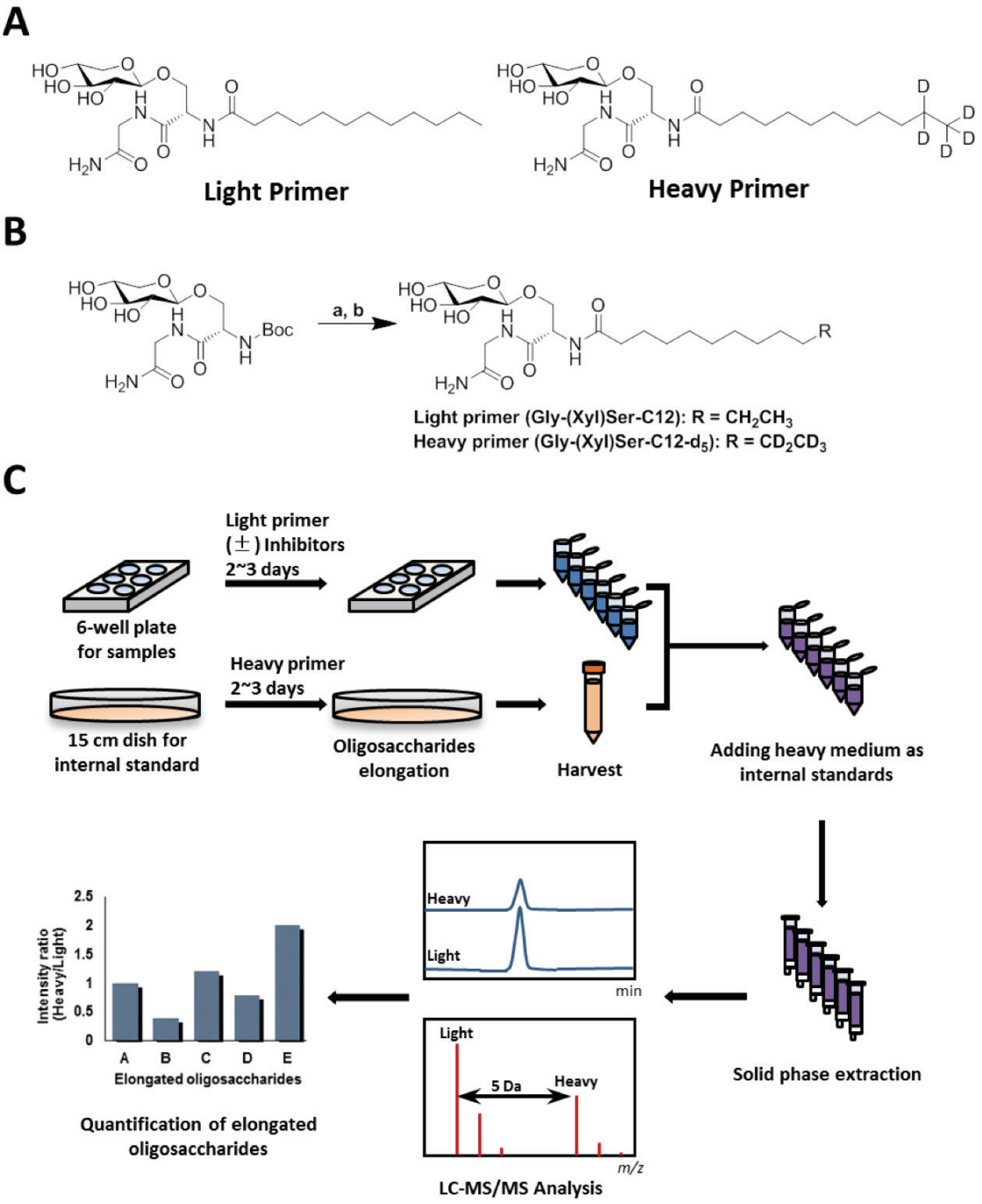

Figure 4-1 Comparative quantification strategy using isotope-labeled saccharide primers. (A) The saccharide primers used in this study. The heavy primer is deuterated in the fatty chain. (B) Synthetic scheme of the primers. Conditions and reagents; (a) TFA, r.t., 15 min. (b) Lauric acid, DMT-MM, EtOH/H_2O, 40 °C, 2 h. (C) Schematic flow chart for the comparative quantification.

4.3.2 Structure analysis of elongated oligosaccharides by LC–MS/MS

Analysis of the sample extracted from the light medium revealed 32 glycosylated products detected by LC–MS. In chapter 3, the glycosylated products elongated on Gly-(Xyl)Ser-C12 were identified using MS/MS and enzymatic digestion. In reference to the previous result, the structures of the glycosylated products detected in this study could be deduced with the MS/MS spectra (Table 4-3).

Table 4-3 Theoretical *m/z* values, experimental *m/z* values, and errors of glycosylated products elongated on the primers. The glycosylated products that had identical *m/z* values but differed in their retention times were distinguished by the numbers after underscore.

Glycosylated products	Charge	Theoretical *m/z*		Experimental *m/z*		Error (ppm)	
		Light	Heavy	Light	Heavy	Light	Heavy
Hex-Xyl-R	-1	636.3349	641.3663	636.3336	641.3640	2.0	3.6
Hex-Hex-Xyl-R	-1	798.3877	803.4191	798.3856	803.4171	2.6	2.5
Hex-Xyl(P)-R	-1	716.3012	721.3326	716.2997	721.3301	2.1	3.5
NeuAc-Hex-Xyl-R	-1	927.4303	932.4617	927.4294	932.4594	1.0	2.5
Hex-Hex-Xyl(P)-R	-1	878.3541	883.3855	878.3537	883.3832	0.5	2.6
Hex(S)-Hex-Xyl(P)-R	-2	478.6518	481.1675	478.6514	481.1672	0.8	0.6
NeuAc-Hex-Hex-Xyl-R	-1	1089.4832	1094.5145	1089.4833	1094.5087	-0.1	5.3
NeuAc-Hex-Xyl(P)-R	-1	1007.3967	1012.4280	1007.3961	1012.4286	0.6	-0.6
NeuAc-Hex-(NeuAc)Hex-Xyl-R	-2	689.7856	692.3013	689.7868	692.3014	-1.7	-0.1
HexA-Hex-Hex-Xyl-R	-1	974.4198	979.4512	974.4195	979.4492	0.3	2.0
HexA(S)-Hex-Hex-Xyl-R	-1	1054.3766	1059.4080	1054.3760	1059.4059	0.6	2.0
HexNAc-HexA-Hex-Hex-Xyl-R	-1	1177.4992	1182.5306	1177.4988	1182.5303	0.3	0.3
HexA(S)-Hex-Hex-Xyl(P)-R	-1	1134.3430	1139.3744	1134.3407	1139.3711	2.0	2.9
NeuAc-Hex-Hex-Xyl(P)-R	-1	1169.4495	1174.4809	1169.4504	1174.4777	-0.8	2.7
S+HexNAc-HexA-Hex-Hex-Xyl-R_1	-2	628.2244	630.7401	628.2227	630.7375	2.7	4.1
S+HexNAc-HexA-Hex-Hex-Xyl-R_2	-2	628.2244	630.7401	628.2248	630.7397	-0.6	0.6
S+HexNAc-HexA-Hex-Hex-Xyl-R_3	-2	628.2244	630.7401	628.2233	630.7394	1.8	1.1
S+HexNAc-HexA-Hex-Hex-Xyl-R_4	-2	628.2244	630.7401	628.2253	630.7392	-1.4	1.4
NeuAc-NeuAc-Hex-Hex-Xyl(P)-R	-2	729.7688	732.2845	729.7670	732.2830	2.5	2.0
HexNAc-HexA-Hex-Hex-Xyl(P)-R	-2	628.2291	630.7448	628.2291	630.7444	0.0	0.6
HexA-HexNAc-HexA-Hex-Hex-Xyl-R	-2	676.2620	678.7777	676.2629	678.7742	-1.3	5.2
$(HexNAc\text{-}HexA)_2$-Hex-Hex-Xyl-R_HS[a]	-2	777.8017	780.3174	777.8030	780.3184	-1.7	-1.3
$(HexNAc\text{-}HexA)_2$-Hex-Hex-Xyl-R_CS[b]	-2	777.8017	780.3174	777.8023	780.3177	-0.8	-0.4
S+HexNAc-HexA-HexNAc-HexA-Hex-Hex-Xyl-R	-2	817.7801	820.2958	817.7810	820.2961	-1.1	-0.4
S+$(HexNAc\text{-}HexA)_2$-Hex-Hex(S)-Xyl-R_1	-2	857.7585	860.2742	857.7580	860.2659	0.6	9.6
S+$(HexNAc\text{-}HexA)_2$-Hex-Hex(S)-Xyl-R_2	-2	857.7585	860.2742	857.7587	860.2715	-0.2	3.1
HexA(S)-Hex-(NeuAc)Hex-Xyl-R	-2	672.2324	674.7481	672.2327	674.7485	-0.4	-0.6
HexNAc+NeuAc+NeuAc+Hex+Hex+Xyl-R_1	-2	791.3253	793.8410	791.3264	793.8411	-1.4	-0.1
HexNAc+NeuAc+NeuAc+Hex+Hex+Xyl-R_2	-2	791.3253	793.8410	791.3270	793.8436	-2.1	-3.3
NeuAc-Hex-HexNAc-(NeuAc)Hex-Hex-Xyl-R	-2	872.3517	874.8674	872.3527	874.8679	-1.1	-0.6
NeuAc-Hex-(NeuAc)HexNAc-HexA-Hex-Hex-Xyl-R	-2	960.3678	962.8835	960.3654	962.8807	2.5	2.9
NeuAc-Hex-HexNAc-HexA-Hex-Hex-Xyl-R	-2	814.8201	817.3358	814.8212	817.3329	-1.3	3.5

[a] The product digested by heparitinases.

[b] The product digested by C-ABC.

Some glycosylated products were successfully analyzed using MS/MS and enzymatic digestion; however, some structural features such as glycoside bond linkages or sulfation position have not been determined. For example, four peaks were detected in sulfated pentasaccharides (S+HexNAc-HexA-Hex-Hex-Xyl-R), and their MS/MS spectra implied that their sulfation positions were different (Figure 4-2, Figure 4-3, Figure 4-4, and Figure 4-5). To understand the GAG biosynthesis mechanism of individual cells and tissues, structural analysis including these structural features of glycosylated products are needed.

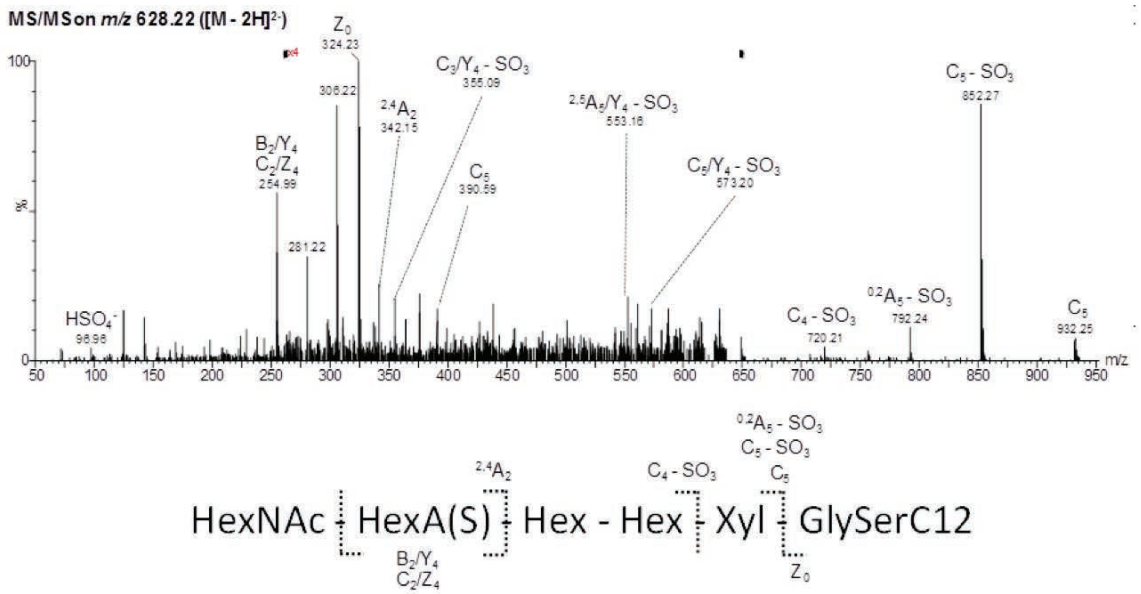

Figure 4-2 MS/MS spectrum of S + HexNAc-HexA-Hex-Hex-Xyl-GlySerC12_1.

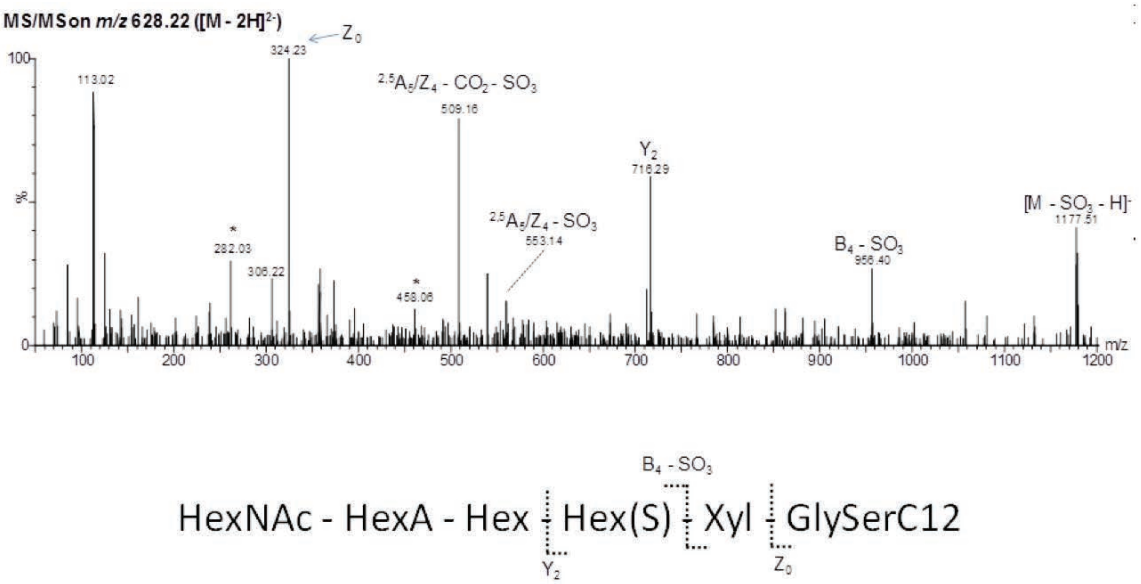

Figure 4-3 MS/MS spectrum of S + HexNAc-HexA-Hex-Hex-Xyl-GlySerC12_2.

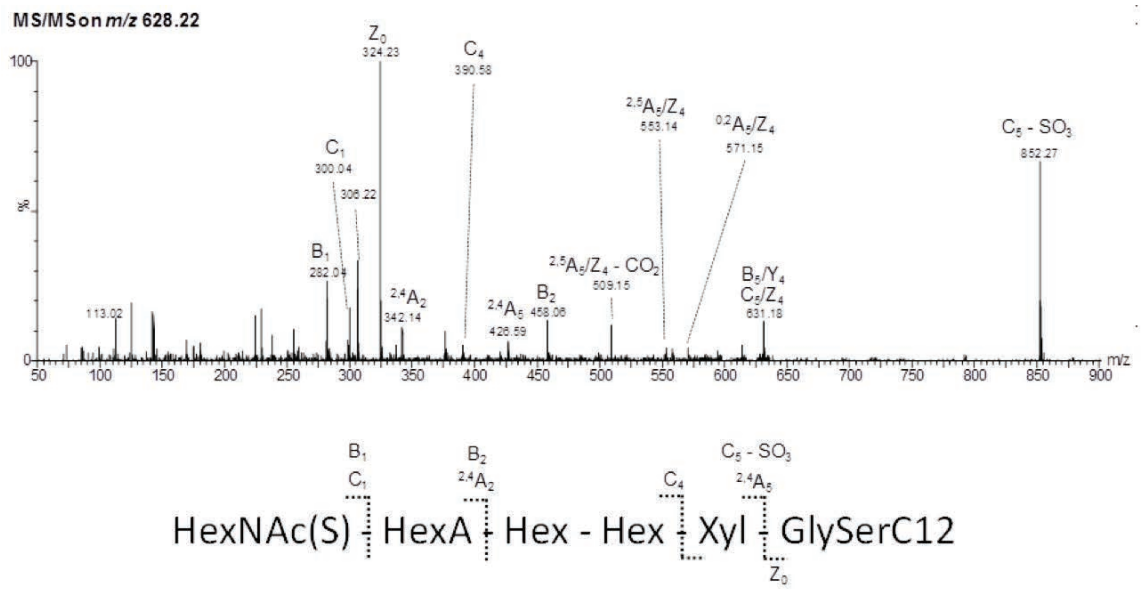

Figure 4-5 MS/MS spectrum of S + HexNAc-HexA-Hex-Hex-Xyl-GlySerC12_3.

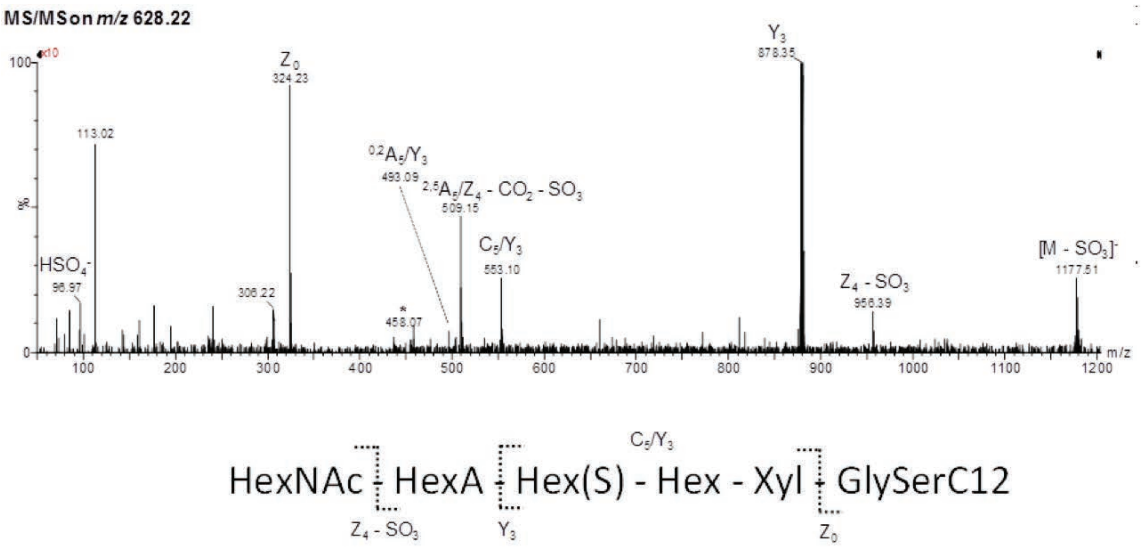

Figure 4-4 MS/MS spectrum of S + HexNAc-HexA-Hex-Hex-Xyl-GlySerC12_4.

4.3.3 Method verification

Although deuterium labeling is the first choice for stable isotope labeling in LC–MS quantification, there are some drawbacks using deuterium-labeled compounds as internal standards. Foremost, deuterium-labeled compounds could be separated from the originals in LC analysis.[81] This separation might cause miss-assignment of the pairs and introduce bias in the quantification result. The composition of the mobile phase and

the conditions of the MS equipment could affect retention times, and this instability may affect the ionization efficiencies of the examined compounds. Hence, we first confirmed the retention times of both glycosylated products elongated on light and heavy primers.

Table 4-4 shows retention times and differences in retention times (ΔRT) of the glycosylated products obtained from the light and heavy primers. Surprisingly, most of the glycosylated product pairs showed the same retention times and ΔRTs were obviously small; the largest ΔRT was 0.03 ± 0.03 min. In addition, to investigate retention behavior in detail, the peak shapes of the pairs of glycosylated products were compared. Figure 4-6 illustrates example pairs of EIC chromatograms elongated on the primers. The retention times and peak shapes of each pair appeared identical. These results mean that the deuterium group in the heavy primer does not affect the retention time of HILIC separation. This might be because the hydrophilic moiety, the saccharide chain in this case, is the main contributor to the interaction with the HILIC stationary phase, whereas the hydrophobic moiety of the primers does not contribute to the interaction. This information may expand the utility of deuterium-labeled compounds as stable isotope-labeled standards by coupling with HILIC separation. In light of this result, we proposed the use of the glycosylated products of the heavy primer as internal standards of those of the light primer.

Table 4-4 Retention times and ΔRT of the glycosylated products. ΔRT values represent the means ± standard deviations (S. D.) of three independent experiments.

Glycosylated products	Retention times		ΔRT
	Light	Heavy	
Hex-Xyl-R	8.45	8.45	0.00 ± 0.00
Hex-Hex-Xyl-R	12.31	12.32	0.00 ± 0.01
Hex-Xyl(P)-R	13.87	13.87	0.01 ± 0.01
NeuAc-Hex-Xyl-R	13.89	13.89	0.00 ± 0.00
Hex-Hex-Xyl(P)-R	15.93	15.94	0.01 ± 0.01
Hex(S)-Hex-Xyl(P)-R	16.64	16.65	0.01 ± 0.01
NeuAc-Hex-Hex-Xyl-R	16.27	16.27	0.00 ± 0.01
NeuAc-Hex-Xyl(P)-R	17.31	17.32	0.00 ± 0.01
NeuAc-Hex-(NeuAc)Hex-Xyl-R	19.22	19.23	0.01 ± 0.01
HexA-Hex-Hex-Xyl-R	17.84	17.84	0.00 ± 0.00
HexA(S)-Hex-Hex-Xyl-R	17.97	17.97	0.00 ± 0.00
HexNAc-HexA-Hex-Hex-Xyl-R	18.97	18.97	0.00 ± 0.00
HexA(S)-Hex-Hex-Xyl(P)-R	20.71	20.71	0.00 ± 0.01
NeuAc-Hex-Hex-Xyl(P)-R	19.11	19.11	0.00 ± 0.01
S+HexNAc-HexA-Hex-Hex-Xyl-R_1	18.63	18.63	0.00 ± 0.00
S+HexNAc-HexA-Hex-Hex-Xyl-R_2	19.04	19.02	0.03 ± 0.03
S+HexNAc-HexA-Hex-Hex-Xyl-R_3	19.14	19.14	0.00 ± 0.01
S+HexNAc-HexA-Hex-Hex-Xyl-R_4	19.43	19.43	0.00 ± 0.00
NeuAc-NeuAc-Hex-Hex-Xyl(P)-R	21.23	21.23	0.00 ± 0.01
HexNAc-HexA-Hex-Hex-Xyl(P)-R	21.36	21.36	0.00 ± 0.00
HexA-HexNAc-HexA-Hex-Hex-Xyl-R	22.76	22.77	0.01 ± 0.01
$(HexNAc\text{-}HexA)_2$-Hex-Hex-Xyl-R_HS	22.75	22.76	0.01 ± 0.01
$(HexNAc\text{-}HexA)_2$-Hex-Hex-Xyl-R_CS	23.15	23.15	0.00 ± 0.01
S+HexNAc-HexA-HexNAc-HexA-Hex-Hex-Xyl-R	23.33	23.33	0.00 ± 0.00
S+$(HexNAc\text{-}HexA)_2$-Hex-Hex(S)-Xyl-R_1	23.69	23.69	0.00 ± 0.01
S+$(HexNAc\text{-}HexA)_2$-Hex-Hex(S)-Xyl-R_2	24.06	24.06	0.00 ± 0.01
HexA(S)-Hex-(NeuAc)Hex-Xyl-R	20.79	20.79	0.00 ± 0.00
HexNAc+NeuAc+NeuAc+Hex+Hex+Xyl-R_1	19.45	19.45	0.00 ± 0.00
HexNAc+NeuAc+NeuAc+Hex+Hex+Xyl-R_2	20.29	20.29	0.00 ± 0.00
NeuAc-Hex-HexNAc-(NeuAc)Hex-Hex-Xyl-R	21.23	21.23	0.00 ± 0.01
NeuAc-Hex-(NeuAc)HexNAc-HexA-Hex-Hex-Xyl-R	24.04	24.04	0.00 ± 0.01
NeuAc-Hex-HexNAc-HexA-Hex-Hex-Xyl-R	22.54	22.54	0.01 ± 0.01

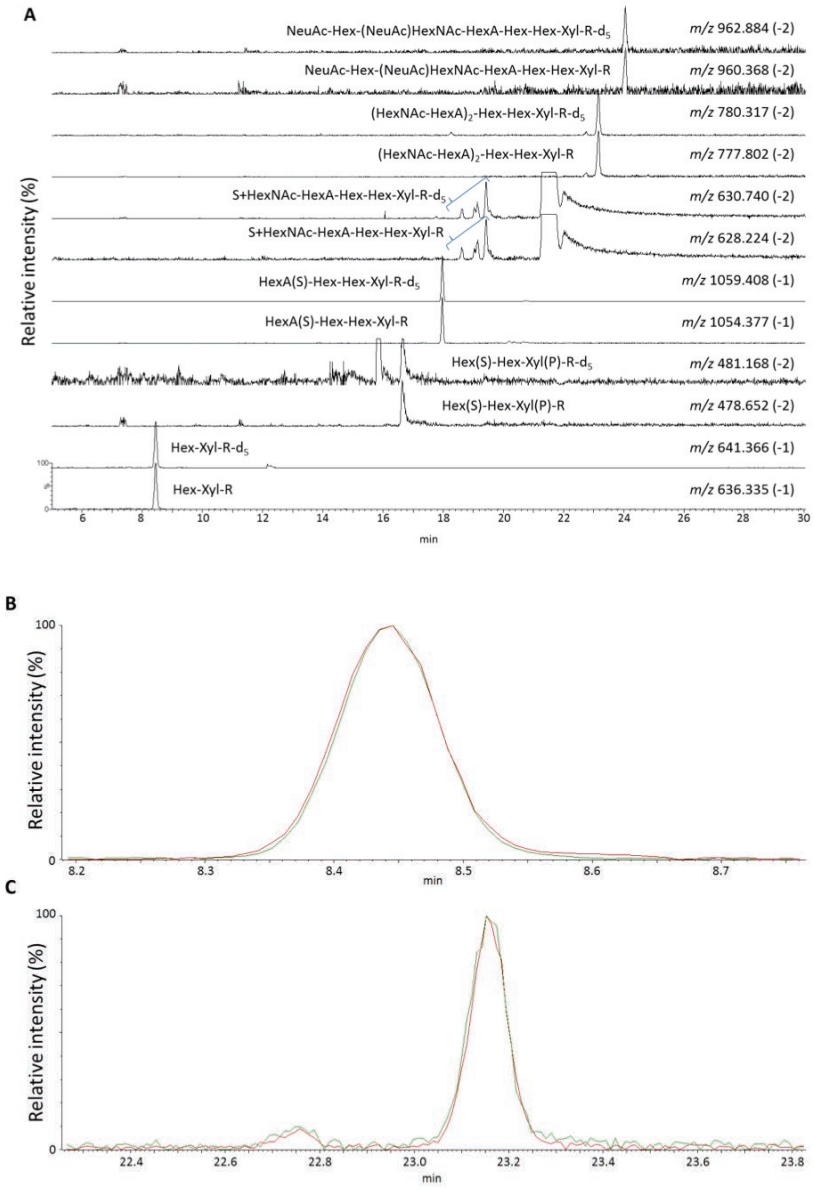

Figure 4-6 EIC chromatograms of glycosylated products. (A) The EIC chromatograms of Hex-Xyl-R, Hex(S)-Hex-Xyl(P)-R, HexA(S)-Hex-Hex-Xyl-R, S+HexNAc-HexA-Hex-Hex-Xyl-R, $(HexNAc-HexA)_2$-Hex-Hex-Xyl-R, and NeuAc-Hex-(NeuAc)HexNAc-HexA-Hex-Hex-Xyl-R. *m/z* values and charges of the precursor ions are described in the figure. (B) The EIC chromatograms of Hex-Xyl-R enlarged at 8.45 min and (C) those of $(HexNAc-HexA)_2$-Hex-Hex-Xyl-R at 23 min. The green and red lines indicate products of the light and heavy primers, respectively.

Next, the priming abilities of the primers were confirmed because differences in priming abilities may represent a bias in the quantification results. The same volumes of "light" and "heavy" media were mixed, processed and analyzed by LC–MS. In Figure 4-7, peak areas of several glycosylated products observed in "light" medium were plotted relative to those of "heavy" medium. The graph shows good linearity, with a slope of about 0.99. This result indicates that the primers have very similar priming abilities. Taking into consideration that the heavy products are used as internal standards, the priming abilities do not affect the quantification results.

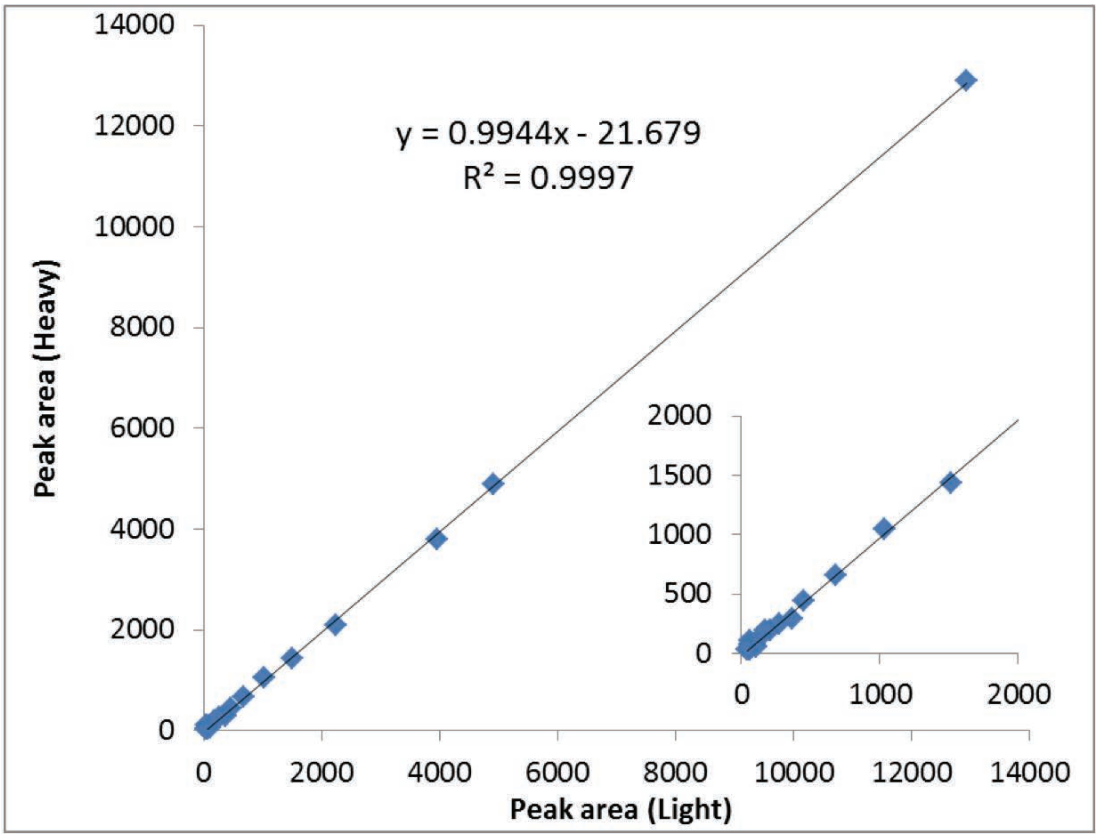

Figure 4-7 Correlation of the peak areas of light products to heavy products. The inset enlarges the region with small peak areas.

Moreover, the linearity and quantification accuracy of the method were examined using mixtures of light and heavy media at ratios of 1:1, 1:2.5, 1:5, 1:7.5 and 1:10. The mixed medium was subjected to solid phase extraction and then analyzed by LC–MS. Figure 4-8 shows graphs of the relative peak areas (light/heavy) of some

glycosylated products relative to the theoretical ratio. The graphs show good linearity over the tested range, although the observed ratios were somewhat smaller than the theoretical ratios. The result is probably attributable to the differences in the total concentrations of glycosylated products, since when the media were harvested, the plates or wells were washed with a small amount of PBS and the solution was pooled with the media. Given that the glycosylated products elongated on the heavy primer would be used as internal standards, the plot showed sufficient linearity for comparative quantification of glycosylated products.

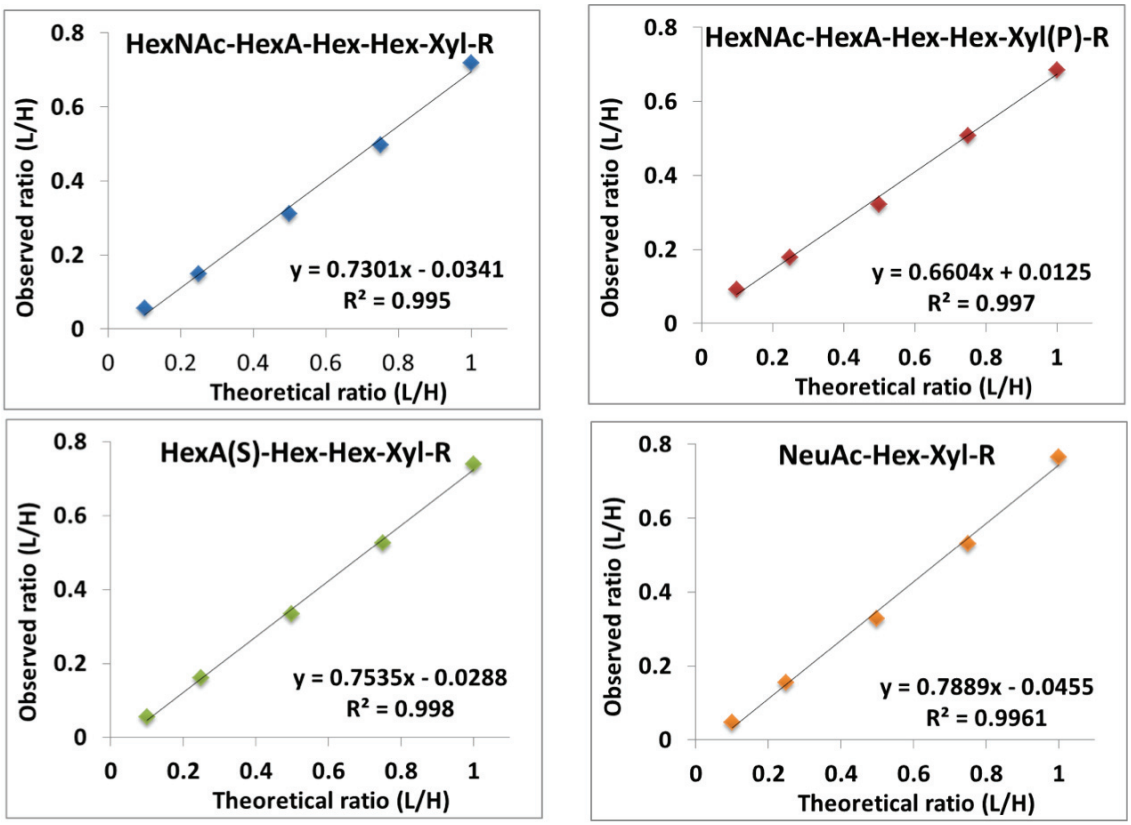

Figure 4-8 Linearity of the method at ratios of 1:1, 1:2.5, 1.5, 1:7.5, and 1:10. (A) Pentasaccharides (HexNAc-HexA-Hex-Hex-Xyl-R). (B) Phosphorylated pentasaccharides (HexNAc-HexA-Hex-Hex-Xyl(P)-R). (C) Sulfated tetrasaccharides (HexA(S)-Hex-Hex-Xyl-R). (D) Sialylated trisaccharides (NeuAc-Hex-Xyl-R).

4.3.4 Method validation using GAG biosynthesis inhibitors

To validate the method, a GAG inhibition assay was carried out to estimate the relative amounts of glycosylated products elongated in NHDF cells incubated with

GAG biosynthesis inhibitors. As GAG biosynthesis inhibitors, azaserine, brefeldin A, genistein, and rhodamine B were chosen. Azaserine is an inhibitor of glutamine:fructose-6-phosphate amidotransferase, which is a key enzyme in the hexosamine biosynthetic pathway (HBP).[82,83] Brefeldin A is an inhibitor that interferes with glycoprotein transport from the ER to the Golgi apparatus during glycan biosynthesis.[53] Rhodamine B is a nonspecific inhibitor that reduces the expression of glycosyltransferases related to GAG biosynthesis.[84,85] Genistein is a tyrosine kinase inhibitor for the epidermal growth factor receptor, which regulates downstream gene expression related to GAG biosynthetic enzymes.[86]

As shown in Figure 4-1C, NHDF cells were incubated in medium containing each inhibitor (10 μM or 100 μM) and light primer (25 μM). NHDF cells were also incubated with medium containing the heavy primer (25 μM). After 3 days, the media were collected and equal volumes of both media were mixed. The glycosylated products were extracted, and then analyzed by LC–MS. Individual peak areas of the elongated products on the light primer were normalized to those on the heavy primer.

Figure 4-9 shows the comparison of the relative amounts of the heptasaccharide ($(HexNAc\text{-}HexA)_2$-Hex-Hex-Xyl-R_2). Without correction by the internal standard, the relative amounts of the heptasaccharide between the control and GAG biosynthesis inhibitors were not significantly different (Figure 4-9A), which was attributable to the large standard deviation of the control sample. In contrast, the relative amounts of the heptasaccharide between the control and GAG biosynthesis inhibitors were significantly different when corrected by the internal standard (Figure 4-9B). This result indicates that the established method can effectively reveal differences in GAG biosynthesis activity using GAG inhibitors.

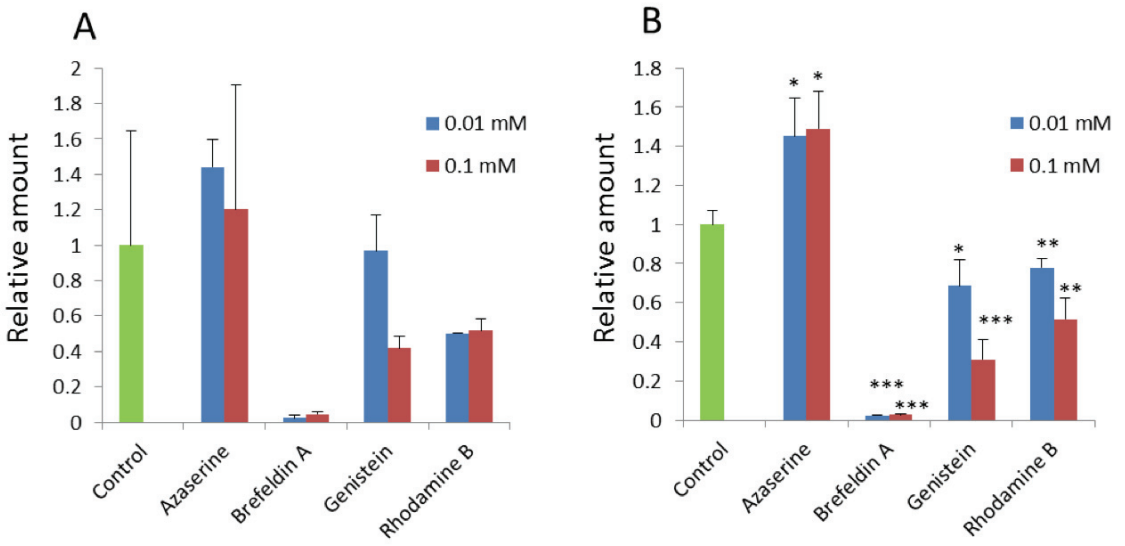

Figure 4-9 Comparison of the relative amounts of the heptasaccharide ((HexNAc-HexA)$_2$-Hex-Hex-Xyl-R_2). (A) The relative amounts were compared based on the peak area of the heptasaccharide elongated on the light primer. The individual relative amounts were calculated by dividing the peak area of each GAG inhibitor by the average of the peak areas of control samples. (B) The relative amounts were compared based on the relative peak areas, which were calculated by dividing the peak areas of the light primer products by those of the heavy primer products. Relative amounts indicated in both graphs represent the mean values ± S. D. Asterisks indicate $p < 0.05$ (*), < 0.01 (**), < 0.001 (***) versus the control (n = 3 per condition).

The comparative results of the detected oligosaccharides are shown in Table 4-5 and Figure 4-10. The result was able to clarify differences in the relative amounts of glycosylated products obtained from each medium containing the GAG inhibitors. As expected, the relative amounts of most glycosylated products were decreased in the genistein- or rhodamine B-added medium in a dose-dependent manner. This indicates that the method can detect the inhibition of GAG biosynthesis using these two inhibitors.

Table 4-5 Comparative quantification of glycosylated products elongated with each GAG inhibitor. The relative amounts indicate the mean values obtained from three individual experiments, and those that are significantly different from that of the control sample are heatmapped ($p < 0.05$).

Glycosylated products	Relative amount							
	Azaserine		Brefeldin A		Genistein		Rhodamine B	
	10 μM	100 μM	10 μM	100 μM	10 μM	100 μM	10 μM	100 μM
Hex-Xyl-R	1.19	1.28	2.08	1.78	1.56	1.04	0.76	0.27
Hex-Hex-Xyl-R	1.39	1.54	0.04	0.04	0.69	0.23	0.61	0.18
Hex-Xyl(P)-R	1.44	1.29	2.09	2.84	0.89	0.55	0.87	0.50
NeuAc-Hex-Xyl-R	0.34	0.39	0.00	0.00	0.63	0.18	0.73	0.44
Hex-Hex-Xyl(P)-R	1.09	1.22	0.01	0.06	0.63	0.21	0.85	0.71
Hex(S)-Hex-Xyl(P)-R	4.96	5.11	0.00	0.00	1.05	0.95	0.68	0.48
NeuAc-Hex-Hex-Xyl-R	1.28	1.60	0.02	0.02	0.55	0.28	0.57	0.29
NeuAc-Hex-Xyl(P)-R	0.29	0.31	0.17	0.16	0.45	0.15	0.83	0.79
NeuAc-Hex-(NeuAc)Hex-Xyl-R	0.32	0.35	0.05	0.05	0.63	0.60	0.62	0.34
HexA-Hex-Hex-Xyl-R	1.97	2.05	7.44	10.35	0.83	0.44	0.87	0.63
HexA(S)-Hex-Hex-Xyl-R	1.66	1.57	0.01	0.01	0.56	0.08	0.79	0.28
HexNAc-HexA-Hex-Hex-Xyl-R	1.51	1.65	0.02	0.03	0.72	0.39	0.78	0.43
HexA(S)-Hex-Hex-Xyl(P)-R	1.33	1.25	0.02	0.04	0.55	0.11	0.76	0.30
NeuAc-Hex-Hex-Xyl(P)-R	0.69	0.82	0.05	0.14	0.50	0.24	0.56	0.37
S+HexNAc-HexA-Hex-Hex-Xyl-R_1	1.54	1.26	0.19	0.19	0.51	0.05	0.91	0.16
S+HexNAc-HexA-Hex-Hex-Xyl-R_2	1.89	1.07	0.01	0.00	1.44	0.86	1.14	0.86
S+HexNAc-HexA-Hex-Hex-Xyl-R_3	1.80	1.53	0.03	0.00	0.78	0.43	0.85	0.53
S+HexNAc-HexA-Hex-Hex-Xyl-R_4	1.09	1.07	0.00	0.00	0.91	0.44	0.73	0.37
NeuAc-NeuAc-Hex-Hex-Xyl(P)-R	0.28	0.27	0.07	0.06	0.74	0.53	0.91	0.49
HexNAc-HexA-Hex-Hex-Xyl(P)-R	1.09	1.00	0.09	0.06	0.64	0.20	0.71	0.40
HexA-HexNAc-HexA-Hex-Hex-Xyl-R	1.50	1.59	0.07	0.08	0.53	0.30	0.72	0.46
$(HexNAc\text{-}HexA)_2$-Hex-Hex-Xyl-R_1	1.37	1.42	0.00	0.00	0.77	0.53	0.76	0.60
$(HexNAc\text{-}HexA)_2$-Hex-Hex-Xyl-R_2	1.45	1.49	0.02	0.03	0.69	0.31	0.78	0.52
S+HexNAc-HexA-HexNAc-HexA-Hex-Hex-Xyl-R	1.57	1.51	0.00	0.00	0.67	0.19	0.82	0.46
S+$(HexNAc\text{-}HexA)_2$-Hex-Hex(S)-Xyl-R_1	2.17	2.07	0.00	0.00	0.70	0.36	0.63	0.48
S+$(HexNAc\text{-}HexA)_2$-Hex-Hex(S)-Xyl-R_2	1.16	1.09	0.00	0.00	0.76	0.22	1.00	0.36
HexA(S)-Hex-(NeuAc)Hex-Xyl-R	0.50	0.46	0.01	0.01	0.60	0.15	0.80	0.27
HexNAc+NeuAc+NeuAc+Hex+Hex+Xyl-R_1	0.32	0.36	0.00	0.00	0.70	0.17	0.90	0.22
HexNAc+NeuAc+NeuAc+Hex+Hex+Xyl-R_2	0.33	0.42	0.00	0.00	0.66	0.55	0.79	0.86
NeuAc-Hex-HexNAc-(NeuAc)Hex-Hex-Xyl-R	0.44	0.47	0.00	0.00	0.74	0.24	0.76	0.17
NeuAc-Hex-(NeuAc)HexNAc-HexA-Hex-Hex-Xyl-R	0.79	0.85	0.00	0.00	0.88	0.80	0.75	0.53
NeuAc-Hex-HexNAc-HexA-Hex-Hex-Xyl-R	2.70	3.12	0.00	0.00	0.79	0.70	0.79	0.66

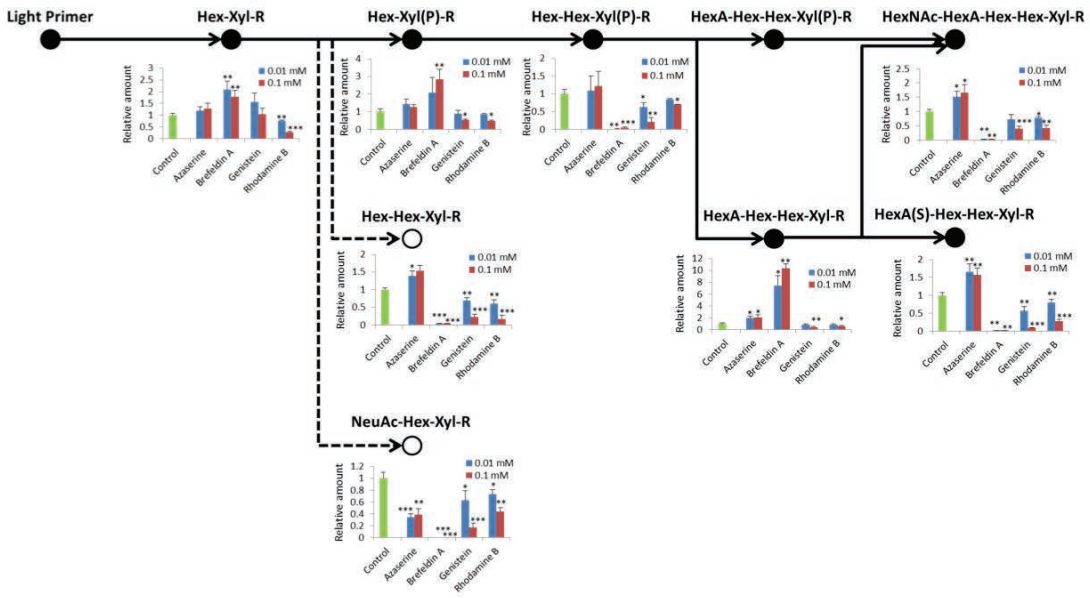

Figure 4-10 Linkage tetrasaccharide biosynthetic pathway elongated on the light primer. The closed circles and bold arrows indicate the GAG intermediates biosynthesis pathway. The open circles and dashed arrows indicate the competitive pathway to synthesize sialylated and other glycosylated products. The bar graphs placed under the circles show the relative amounts of glycosylated products. Relative amounts indicated in the graphs represent the mean values ± S. D. Asterisks indicate $p < 0.05$ (*), < 0.01 (**), < 0.001 (***) versus the control (n = 3 per condition).

The relative amounts of products found in the brefeldin A-added medium showed a characteristic change. Disaccharides (Hex-Xyl-R and Hex-Xyl(P)-R) and a tetrasaccharide (HexA-Hex-Hex-Xyl-R) were clearly increased, although glycosylated products longer than pentasaccharides were obviously decreased (Figure 4-10). This result indicates that brefeldin A inhibits certain steps in the GAG biosynthesis pathway. For example, the accumulation of disaccharides indicates that brefeldin A inhibits secondary Gal addition catalyzed by GalT-II. Also, the accumulation of HexA-Hex-Hex-Xyl-R indicates inhibition of the HexNAc addition step. On the other hand, our result indicates that brefeldin A inhibited the synthesis of HexA-Hex-Hex-Xyl(P)-R. This phenomenon is consistent with the mode of action of brefeldin A, which inhibits anterograde vesicular transportation through the Golgi apparatus.[50,53,87] It has been reported that brefeldin A inhibited CS/DS biosynthesis but not HS biosynthesis.[88] The report concluded that HS biosynthetic enzymes are localized in the ER and proximal Golgi apparatus. Hence, the tetrasaccharide

HexA-Hex-Hex-Xyl-R could be considered as an HS biosynthesis precursor, indicating the reason for HexA-Hex-Hex-Xyl-R accumulation by brefeldin A. In contrast, HexA-Hex-Hex-Xyl(P)-R is considered to be a CS/DS biosynthesis precursor and is suppressed by brefeldin A, because it has been demonstrated that xylose phosphatase and chondroitin *N*-acetylgalactomaminidase-1 are co-localized and work in harmony.[15] In this context, our results are consistent with the mode of action of brefeldin A.

Unlike the above three inhibitors, azaserine exhibited a completely different effect on GAG chain elongation. Surprisingly, azaserine increased most of the GAG related oligosaccharides in a dose-dependent manner. In addition, the relative amounts of sialylated oligosaccharides were decreased in azaserine-added medium. These two results cannot be explained by the known mode of action of azaserine. One hypothesis to explain this effect is that azaserine might specifically inhibit certain steps in sialylation. Specific inhibition of sialylation would reduce adenosine triphosphate (ATP) consumption, and more ATP could be utilized for GAG biosynthesis. If sufficient amounts of hexosamine had been supplied, GAG chain elongation might be increased even in azaserine-added medium. Supporting this hypothesis, it has been reported that GAG biosynthesis inhibition by 6-diazo-5-oxonorleucine, an HBP inhibitor, was rescued by glucosamine addition.[89] This point can be clarified by confirming the amount of hexosamine in the medium and the rate-limiting step for GAG production in NHDF cells.

According to this result, the comparative quantification method could demonstrate differences in the mode of action between the four GAG biosynthesis inhibitors, and is thus considered applicable to investigate the GAG biosynthetic mechanism and its regulation.

4.4 Conclusion

In this chapter, a novel quantitative method for glycomics using a stable isotope-labeled saccharide primer was demonstrated. The heavy saccharide primer, which is deuterium-labeled in its alkyl chain, primed glycosaminoglycan-type oligosaccharides the same as the light primer, and the pairs of elongated oligosaccharides were not resolved in HILIC separation. In applying this method, four

GAG biosynthesis inhibitors were examined and their effects on GAG biosynthesis were compared. The result clearly indicated that this method could identify differences in the mode of action of the GAG inhibitors.

In this study, some positional isomers of sulfated GAGs were detected, even though the sulfation position of these isomers has not been determined. The sulfation position in GAG biosynthesis is considered to be an important factor in determining the GAG type, length and number attached to PGs. Therefore, quantitative and qualitative analyses of the sulfated isomers will contribute to the investigation of the GAG biosynthetic mechanism.

The saccharide primers can be applied to comparative glycomics study as well as to the preparation of analytical standard libraries to examine the activities of various enzymes related to GAG catabolism. These libraries could be applied to the diagnosis of GAG metabolic diseases like mucopolysaccharidosis (MPS), since the activity of GAG degradation enzymes can be easily measured by comparison of the glycosylated products with or without GAG enzymatic treatment. Therefore, the quantification strategy represents a new tool for comparative glycosaminoglycomics using cultured cells and tissues, not only in the search for GAG biomarkers, but also to construct GAG oligosaccharide libraries for MPS diagnostics.

Chapter 5
Evaluation of Exogenous GAG Effects on GAG Biosynthesis

5.1 Introduction

Exogenously administration of GAGs has been used in therapeutic applications such as visco-supplementations for knee osteoarthritis. It is well-known that GAGs not only work as shock absorber or lubricant in synovial fluid, but also directly affect chondrocytes through their specific receptors such as CD44 and ICAM-I.[1,90,91] In addition, there are some studies that demonstrate that exogenous GAG affects endogenous GAG production in several cells and tissues.[92–95] These results suggest that GAGs work as signaling molecules that regulate ECM components autocrinally. Since the structures of GAGs generally affect the affinity to their receptors, it is also assumed that the autocrinal effect is regulated by the structural feature of the exogenous GAGs. In most cases, the effects of exogenous GAGs have been examined by metabolic labeling experiment using radioisotopes. Although both the sensitivity and selectivity of the experiments were sufficiently high, the structural elucidation of the endogenously synthesized GAG had been conducted insufficiently. As described in chapter 1, GAG biosynthesis is closely related to the production of the intermediates including the phosphorylated linkage tetrasaccharide. Therefore, exogenously added GAGs are assumed to control the endogenously produced GAG intermediates.

In chapter 4, the comparative quantification method for GAG intermediates elongated on the saccharide primers was established. In this chapter, the comparative quantification method was applied to confirm the effect of exogenous GAGs on the biosynthetic ability of NHDF cells for GAGs and GAG intermediates.

5.2 Materials and methods

5.2.1 Materials

CS-C and CS-E were purchased from Seikagaku Corporation (Tokyo, Japan). Heparin was purchased from Wako Pure Chemical Industries (Osaka, Japan). Cells, media, and other reagents were the same as described in Chapter 4. Unless otherwise stated, reagents and solvents were used without purification.

5.2.2 Comparative quantification of elongated oligosaccharides

Priming of elongated oligosaccharides, relative quantification of the elongated oligosaccharides, LC–MS/MS analysis, and data analysis were carried out according to the method described in Chapter 4. In brief, NHDF cells (4×10^5) were seeded onto the wells of a six-well plate and cultured for 18 h to 80 % confluence. After the cells were washed with PBS, they were incubated for 3 days with 1 mL of DMEM without phenol red and containing both 25 μM of the light primer and 500 μg/mL of each GAG. The media and cells were then harvested, the cells were removed by centrifugation, and then the medium was transferred to a 5 mL tube. The internal standards, glycosylated products elongated on the heavy primer, were obtained from the medium that was harvested from the NHDF cells (1×10^6) and incubated in a 15 cm dish with the heavy primer. The collected medium was stored at −80 °C until use. A 0.75-mL aliquot of the "heavy" medium was added to the same volume of the "light" medium collected from a well and then mixed. The mixed media were subjected to the SPE, and then analyzed by LC–MS.

5.3 Results and discussion

To confirm the effects of exogenous GAGs, CS-C, CS-E, and heparin were chosen as samples for examination. CS-C, mainly sulfated on 6-O-groups on GalNAc residues, is easily available because of its wide commercialization. CS-E is a highly sulfated CS and has demonstrated many biological activities such as interaction with growth factors.[10,96,97] Heparin was chosen as a positive control since it is a typical highly sulfated GAG and is well-known for its biological activity. Structural features of these GAGs are described in Table 5-1.

Table 5-1 Weight-average molecular weight (Mw) and sulfur content of GAGs examined in the study. (*) Determined by gel filtration chromatography. (**) Determined by an in-house established method using capillary electrophoresis. (***) Quoted from Lin *et al.* [98]

GAGs	Mw* (kDa)	Sulfur contents (%)
CS-C	45.5	7.42**
CS-E	97.6	9.43**
Heparin	15.6	12.20***

The result of comparative quantification is shown in Table 5-2 and Figure 5-1. Compared with those of the control samples, the relative amounts of elongated glycans in exogenous added GAG samples increased. In particular, CS-E considerably increased the relative amounts of the glycosylated products. This result indicates that certain exogenous GAGs could stimulate the biosynthesis of glycans including GAGs in fibroblasts. Kawamura *et al*. documented how exogenous CS-E enhanced endogenous GAG production and how it promoted chondrogenic differentiation of ATDC5, which is a chondrogenic cell line derived from mouse teratocarcinoma.[92] They reported in the paper that CS-A and CS-C, which are low-sulfated GAGs, did not show significant enhancement of endogenous GAG production. The result indicates that the sulfated pattern could strongly affect the enhancement of endogenous GAG production. Albeit the cells used in the studies were different, the results are consistent with those in previous studies. Therefore, the comparative quantification method using stable-isotope saccharide primer is applicable to the evaluation of the effect of exogenous GAGs on endogenous GAG production.

In contrast, heparin did not significantly increase the glycosylated products, although the sulfur content of heparin was much higher than that of CS-E. This indicates that the effect observed in this study mainly depends on certain structural features, such as sulfation pattern and molecular weight, rather than on the polyanionic nature of GAG. To clarify the structure–activity relationship of the exogenous and endogenous GAG, more studies using structurally determined GAGs are needed.

Table 5-2 Comparative quantification of glycosylated products elongated with each GAG. The relative amounts indicate the mean values obtained from three individual experiments, and those that are significantly different from that of the control sample are heatmapped ($p < 0.05$).

Glycosylated products	Relative amounts		
	CS-C	CS-E	Hep
Hex-Xyl-R	1.19	1.34	1.24
Hex-Hex-Xyl-R	1.24	1.42	1.26
Hex-Xyl(P)-R	1.20	1.29	1.68
NeuAc-Hex-Xyl-R	1.39	1.65	1.40
Hex-Hex-Xyl(P)-R	1.32	1.43	1.60
Hex(S)-Hex-Xyl(P)-R	1.62	1.41	1.50
NeuAc-Hex-Hex-Xyl-R	1.37	1.44	1.30
NeuAc-Hex-Xyl(P)-R	1.18	1.48	2.59
NeuAc-NeuAc-Hex-Hex-Xyl-R	1.28	1.34	1.23
HexA-Hex-Hex-Xyl-R	1.77	2.58	2.05
HexA(S)-Hex-Hex-Xyl-R	1.19	1.35	1.28
HexNAc-HexA-Hex-Hex-Xyl-R	1.24	1.41	1.24
S+HexA-Hex-Hex-Xyl(P)-R	1.23	1.57	1.79
NeuAc-Hex-Hex-Xyl(P)-R	1.13	1.12	1.18
S+HexNAc-HexA-Hex-Hex-Xyl-R_1	1.22	1.54	1.10
S+HexNAc-HexA-Hex-Hex-Xyl-R_2	1.17	1.28	0.87
S+HexNAc-HexA-Hex-Hex-Xyl-R_3	1.31	1.25	1.21
S+HexNAc-HexA-Hex-Hex-Xyl-R_4	1.23	1.28	1.24
NeuAc-NeuAc-Hex-Hex-Xyl(P)-R	1.70	1.86	1.85
HexNAc-HexA-Hex-Hex-Xyl(P)-R	1.24	1.45	1.43
HexA-HexNAc-HexA-Hex-Hex-Xyl-R	0.93	1.00	1.07
$(HexNAc\text{-}HexA)_2$-Hex-Hex-Xyl-R_1	1.12	1.29	1.15
$(HexNAc\text{-}HexA)_2$-Hex-Hex-Xyl-R_2	1.25	1.41	1.39
HexNAc(S)-HexA-HexNAc-HexA-Hex-Hex-Xyl-R	1.16	1.28	1.32
2S+$(HexNAc\text{-}HexA)_2$-Hex-Hex-Xyl-R_1	1.13	1.30	1.26
2S+$(HexNAc\text{-}HexA)_2$-Hex-Hex-Xyl-R_2	1.38	1.40	1.24
S+NeuAc-HexA-Hex-Hex-Xyl-R	1.17	1.32	1.25
HexNAc+NeuAc+NeuAc+Hex-Hex-Xyl-R_1	1.07	1.34	0.94
HexNAc+NeuAc+NeuAc+Hex-Hex-Xyl-R_2	1.34	1.54	1.29
Hex+HexNAc+NeuAc-NeuAc-Hex-Hex-Xyl-R	1.17	1.60	1.22
NeuAc+NeuAc-Hex-HexNAc-HexA-Hex-Hex-Xyl-R	1.27	1.52	1.23
NeuAc+Hex-HexNAc-HexA-Hex-Hex-Xyl-R	1.17	1.39	1.18

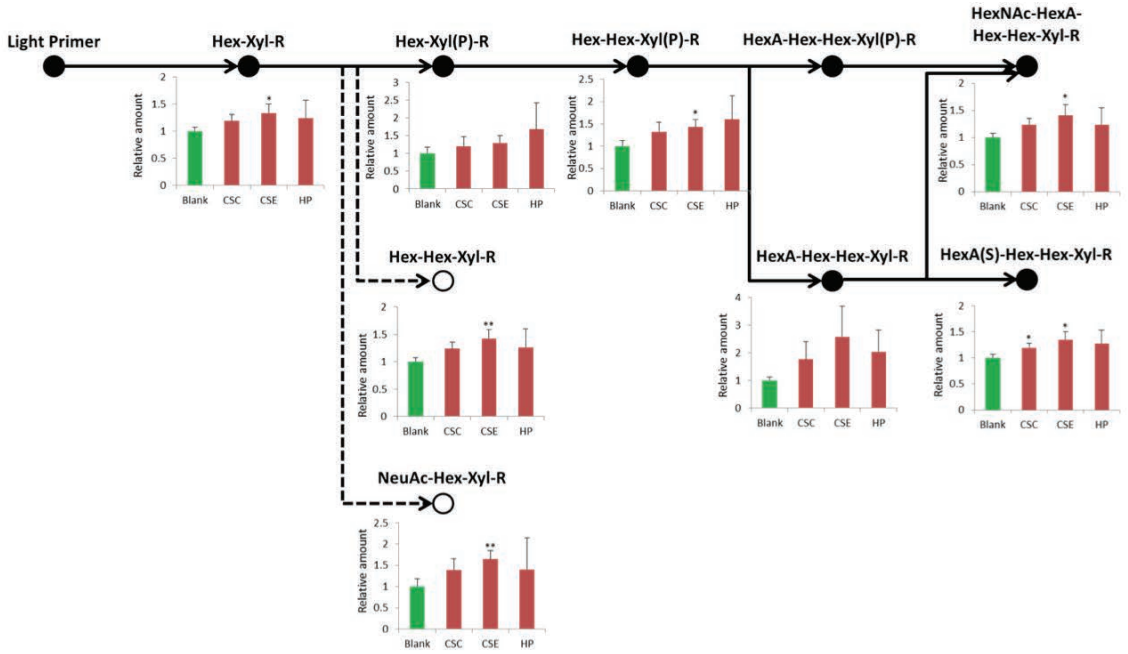

Figure 5-1 CS-E increases GAG biosynthetic intermediates elongated on the primer. The closed circles and bold arrows indicate the GAG intermediates in the biosynthetic pathway. The open circles and dashed arrows indicate the competitive pathway for the synthesis of sialylated and other glycosylated products. The bar graphs placed under the circles show the relative amounts of glycosylated products. Relative amounts indicated in the graphs represent the mean values ± S. D. Asterisks indicate $p < 0.05$ (*), < 0.01 (**).

5.4 Conclusion

By applying relative quantification strategy using an isotope-labeled saccharide primer, the effect of exogenous GAG on endogenous GAG production could be evaluated. Endogenous GAG production was increased with highly sulfated GAGs such as CS-E. Compared with CS-C and heparin, CS-E significantly increased the relative amounts of oligosaccharides elongated on the primer. This result indicates that the sulfur contents, which represents the anion charge amounts in the GAG chain, as well as the structure of GAGs including repeating disaccharide units and sulfated positions, affects GAG biosynthesis. Further investigation on the relationship between exogenous and endogenous GAG would lead to an understanding of both proliferation and differentiation behaviors due to the GAG autocrine mechanism.

Chapter 6
Concluding remarks

The glycomics research field has expanded in recent decades in line with the development of quantitative and qualitative analysis technologies for glycans. Although GAGs, which are one of the main components of ECM and pericellular matrices, have been reported to play key roles in a wide variety of biological phenomena, glycomics techniques for GAGs are still in their infancy. The aim of this study is to discover a β-xyloside suitable for in-depth analysis of GAG biosynthetic intermediates in cells and to establish a comparative quantification method for applying the saccharide primer method.

In chapter 1, the structures, biological activities, and analytical methods for GAGs were summarized. Additionally, the aim of the study was described.

In chapter 2, the synthetic scheme for β-xylosides that have O-xylosyl amino acid residues was established using chemoemzymatic condensation.

In chapter 3, the priming ability of the four β- xylosides in NHDF cells was studied. By optimization of sample preparation and LC–MS/MS conditions, the difference in the priming ability and GAG intermediate oligosaccharides was clarified.

In chapter 4, a comparative quantification method for elongated oligosaccharides using stable-isotope-labeled saccharide primer was established. The method was validated using GAG biosynthesis inhibitors. The result clearly indicates that the method could reveal differences in the mode of action of the examined GAG inhibitors.

In chapter 5, the effect of exogenous sulfated GAGs on endogenous GAGs production was examined by the comparative quantification method. The result reveals that certain sulfated GAGs stimulate NHDF cells to increase endogenous GAG production.

In the thesis, the feasibility of saccharide primer method for quantitative and qualitative GAG-omics study was demonstrated. To enable convenient synthesis and

expand the versatility of structural development of β-xylosides, chemical synthesis using chemoenzymatic condensation was established. The four derivatives could be synthesized through protocols of only three steps, and the relationship between the GAG chain priming ability and aglycone structure of the β-xylosides was clarified. In addition, the relative quantification method using the stable-isotope-labeled β-xyloside was established. This method made it possible to reveal the inhibition mechanisms of the GAG biosynthesis inhibitor and to clarify a novel effect of azaserine, which inhibit sialic acid biosynthesis without GAG biosynthesis inhibition. Finally, the method was applied to evaluate the effect of exogenous GAGs on endogenous GAG production. The effect of exogenous CS-E on endogenous GAG production was successfully confirmed by the established method. The result indicates that the exogenous sulfated GAGs up-regulate GAG biosynthesis including GAG intermediates.

GAGs contribute to various biological events related to cell–cell interactions. Understanding GAG biosynthesis mechanisms and the structure–activity relationship of the GAGs on the GAG autocrine system will open a new avenue for GAG-driven drug discovery. I believe that the method developed in the study will shed new light on the GAG-omics research field.

References

(1) Volpi, N. *Curr. Med. Chem.* **2006**, *13* (15), 1799–1810.

(2) Yamada, S.; Sugahara, K.; Ozbek, S. *Commun. Integr. Biol.* **2011**, *4* (2), 150–158.

(3) Casu, B.; Naggi, A.; Torri, G. *Carbohydr. Res.* **2015**, *403* (11), 60–68.

(4) Sasisekharan, R.; Raman, R.; Prabhakar, V. *Annu. Rev. Biomed. Eng.* **2006**, *8* (1), 181–231.

(5) Rek, A.; Krenn, E.; Kungl, A. J. *Br. J. Pharmacol.* **2009**, *157* (5), 686–694.

(6) Nugent, M. A.; Zaia, J.; Spencer, J. L. *Biochem.* **2013**, *78* (7), 726–735.

(7) Lindahl, U.; Li, J. In *International review of cell and molecular biology*; Elsevier: Oxford, 2009; Vol. 276, pp 105–159.

(8) Yamada, S.; Sugahara, K. *Curr. Drug Discov. Technol.* **2008**, *5* (4), 289–301.

(9) Uyama, T.; Ishida, M.; Izumikawa, T.; Trybala, E.; Tufaro, F.; Bergström, T.; Sugahara, K.; Kitagawa, H. *J. Biol. Chem.* **2006**, *281* (50), 38668–38674.

(10) Bergefall, K.; Trybala, E.; Johansson, M.; Uyama, T.; Naito, S.; Yamada, S.; Kitagawa, H.; Sugahara, K.; Bergström, T. *J. Biol. Chem.* **2005**, *280* (37), 32193–32199.

(11) Cooke, B. M.; Rogerson, S. J.; Brown, G. V; Coppel, R. L. *Blood* **1996**, *88* (10), 4040–4044.

(12) Cattaruzza, S.; Perris, R. *Macromol. Biosci.* **2006**, *6* (8), 667–680.

(13) Uyama, T.; Kitagawa, H.; Sugahara, K. In *Comprehensive Glycoscience*; Elsevier: Oxford, 2007; pp 79–104.

(14) Wen, J.; Xiao, J.; Rahdar, M.; Choudhury, B. P.; Cui, J.; Taylor, G. S.; Esko, J. D.; Dixon, J. E. *Proc. Natl. Acad. Sci.* **2014**, *111* (44), 15723–15728.

(15) Izumikawa, T.; Sato, B.; Mikami, T.; Tamura, J.; Igarashi, M.; Kitagawa, H. *J. Biol. Chem.* **2015**, *290* (9), 5438–5448.

(16) Gomez Toledo, A.; Nilsson, J.; Noborn, F.; Sihlbom, C.; Larson, G. *Mol. Cell. Proteomics* **2015**, *14* (12), 3118–3131.

(17) Wakabayashi, H.; Natsuka, S.; Mega, T.; Otsuki, N.; Isaji, M.; Naotsuka, M.; Koyama, S.; Kanamori, T.; Sakai, K.; Hase, S. *J. Biol. Chem.* **1999**, *274* (9), 5436–5442.

(18) Nakagawa, N.; Izumikawa, T.; Kitagawa, H.; Oka, S. *Biochem. Biophys. Res. Commun.* **2011**, *415* (1), 109–113.

(19) Hart, G. W.; Copeland, R. J. *Cell* **2010**, *143* (5), 672–676.

(20) Kasuya, M. C. Z.; Wang, L. X.; Lee, Y. C.; Mitsuki, M.; Nakajima, H.; Miura, Y.; Sato, T.; Hatanaka, K.; Yamagata, S.; Yamagata, T. *Carbohydr. Res.* **2000**, *329* (4), 755–763.

(21) Kato, T.; Hatanaka, K. *J. Lipid Res.* **2008**, *49* (11), 2474–2478.

(22) Sato, T.; Takashiba, M.; Hayashi, R.; Zhu, X.; Yamagata, T. *Carbohydr. Res.* **2008**, *343* (5), 831–838.

(23) Okayama, M.; Kimata, K.; Suzuki, S. *J. Biochem.* **1973**, *74* (5), 1069–1073.

(24) Izumi, J.; Takagaki, K.; Nakamura, T.; Shibata, S.; Kojima, K.; Kato, I.; Endo, M. *J. Biochem.* **1994**, *116* (3), 524–529.

(25) Lugemwa, F. N.; Esko, J. D. *J. Biol. Chem.* **1991**, *266* (11), 6674–6677.

(26) Abrahamsson, C. O.; Ellervik, U.; Eriksson-Bajtner, J.; Jacobsson, M.; Mani, K. *Carbohydr. Res.* **2008**, *343* (9), 1473–1477.

(27) Jacobsson, M.; Mani, K.; Ellervik, U. *Bioorg. Med. Chem.* **2007**, *15* (15), 5283–5299.

(28) Siegbahn, A.; Aili, U.; Ochocinska, A.; Olofsson, M.; Rönnols, J.; Mani, K.; Widmalm, G.; Ellervik, U. *Bioorg. Med. Chem.* **2011**, *19* (13), 4114–4126.

(29) Jacobsson, M.; Ellervik, U.; Belting, M.; Mani, K. *J. Med. Chem.* **2006**, *49* (6), 1932–1938.

(30) Vassal-Stermann, E.; Duranton, A.; Black, A. F.; Azadiguian, G.; Demaude, J.; Lortat-Jacob, H.; Breton, L.; Vivès, R. R. *PLoS One* **2012**, *7* (10), e47933.

(31) Pineau, N.; Carrino, D. A.; Caplan, A. I.; Breton, L. *Eur. J. Dermatol.* **2011**, *21* (3), 359–370.

(32) Kuberan, B.; Ethirajan, M.; Victor, X. V; Tran, V.; Nguyen, K.; Do, A. *Chembiochem* **2008**, *9* (2), 198–200.

(33) Victor, X. V.; Nguyen, T. K. N.; Ethirajan, M.; Tran, V. M.; Nguyen, K. V.; Kuberan, B. *J. Biol. Chem.* **2009**, *284* (38), 25842–25853.

(34) Tran, V. M.; Kuberan, B. *Bioconjug. Chem.* **2014**, *25* (2), 262–268.

(35) Kalita, M.; Quintero, M. V; Raman, K.; Tran, V. M.; Kuberan, B. In *Methods in molecular biology*; Humana Press: New York, 2015; Vol. 1229, pp 517–528.

(36) Freeze, H. H.; Etchison, J. R. *Trends Glycosci. Glycotechnol.* **1996**, *8* (40), 65–77.

(37) Wang, Y.; Kumazawa, T.; Shiba, K.; Osumi, K.; Mizuno, M.; Sato, T.

Carbohydr. Res. **2012**, *361* (1), 33–40.

(38) van Rantwijk, F.; Woudenberg-van Oosterom, M.; Sheldon, R. A. *J. Mol. Catal. B Enzym.* **1999**, *6* (6), 511–532.

(39) Kadi, N.; Crouzet, J. *Food Chem.* **2006**, *98* (2), 260–268.

(40) Kadi, N.; Belloy, L.; Chalier, P.; Crouzet, J. C. *J. Agric. Food Chem.* **2002**, *50* (20), 5552–5557.

(41) Eneyskaya, E. V; Brumer, H.; Backinowsky, L. V; Ivanen, D. R.; Kulminskaya, A. A.; Shabalin, K. A.; Neustroev, K. N. *Carbohydr. Res.* **2003**, *338* (4), 313–325.

(42) Saito, M.; Shinoyama, H.; Saito, A.; Chiku, K.; Ando, A. *Chiba Univ. Fac. Hortic.* **2010**, *64*, 35–41.

(43) Groll, M.; Götz, M.; Kaiser, M.; Weyher, E.; Moroder, L. *Chem. Biol.* **2006**, *13* (6), 607–614.

(44) Prydz, K.; Vuong, T. T.; Kolset, S. O. *Glycoconj. J.* **2009**, *26* (9), 1117–1124.

(45) Vassal-Stermann, E.; Duranton, A.; Black, A. F.; Azadiguian, G.; Demaude, J.; Lortat-Jacob, H.; Breton, L.; Vivès, R. R. *PLoS One* **2012**, *7* (10), e47933.

(46) Mani, K.; Havsmark, B.; Persson, S.; Kaneda, Y.; Yamamoto, H.; Sakurai, K.; Ashikari, S.; Habuchi, H.; Suzuki, S.; Kimata, K.; Malmstrom, A.; Westergren-Thorsson, G.; Fransson, L.-A. *Cancer Res.* **1998**, *58* (6), 1099–1104.

(47) Brusa, C.; Muzard, M.; Rémond, C.; Plantier-Royon, R. *RSC Adv.* **2015**, *5* (110), 91026–91055.

(48) Johnsson, R.; Mani, K.; Ellervik, U. *Bioorganic Med. Chem. Lett.* **2007**, *17* (8), 2338–2341.

(49) Abrahamsson, C.-O. O.; Ellervik, U.; Eriksson-Bajtner, J.; Jacobsson, M.; Mani, K. *Carbohydr. Res.* **2008**, *343* (9), 1473–1477.

(50) Prydz, K.; Dalen, K. T. *J. Cell Sci.* **2000**, *113*, 193–205.

(51) Sugahara, K.; Tsuda, H.; Yoshida, K.; Yamada, S.; de Beer, T.; Vliegenthart, J. F. G. *J. Biol. Chem.* **1995**, *270* (39), 22914–22923.

(52) Cheng, F.; Heinegârd, D.; Fransson, L.; Bayliss, M.; Bielicki, J.; Hopwood, J.; Yoshida, K. *J. Biol. Chem.* **1996**, *271* (45), 28572–28580.

(53) Silbert, J. E.; Sugumaran, G. *IUBMB Life* **2002**, *54* (8), 177–186.

(54) Ogiso, H.; Suzuki, T.; Taguchi, R. *Anal. Biochem.* **2008**, *375* (1), 124–131.

(55) Asakawa, Y.; Tokida, N.; Ozawa, C.; Ishiba, M.; Tagaya, O.; Asakawa, N. *J.*

Chromatogr. A **2008**, *1198–1199* (11), 80–86.

(56) Myint, K. T.; Uehara, T.; Aoshima, K.; Oda, Y. *Anal. Chem.* **2009**, *81* (18), 7766–7772.

(57) Antonopoulos, A.; Favetta, P.; Jacquinet, J.-C.; Lafosse, M. *J. Mass Spectrom.* **2005**, *40* (12), 1628–1636.

(58) Kenny, D. T.; Issa, S. M. A.; Karlsson, N. G. *Rapid Commun. Mass Spectrom.* **2011**, *25* (18), 2611–2618.

(59) Wen, J.; Xiao, J.; Rahdar, M.; Choudhury, B. P.; Cui, J.; Taylor, G. S.; Esko, J. D.; Dixon, J. E. *Proc. Natl. Acad. Sci.* **2014**, *111* (44), 15723–15728.

(60) Nilsson, J.; Noborn, F.; Gomez Toledo, A.; Nasir, W.; Sihlbom, C.; Larson, G. *J. Am. Soc. Mass Spectrom.* **2017**, *28* (2), 229–241.

(61) Wang, Y.; Yang, X.; Yamagata, S.; Yamagata, T.; Sato, T. *Mol. Cell. Biochem.* **2013**, *373* (1–2), 63–72.

(62) Kato, T.; Miyagawa, A.; Kasuya, M. C. Z.; Ito, A.; Hatanaka, K. *J. Chromatogr. A* **2008**, *1178* (1–2), 154–159.

(63) Victor, X. V; Nguyen, T. K. N.; Ethirajan, M.; Tran, V. M.; Nguyen, K. V; Kuberan, B. *J. Biol. Chem.* **2009**, *284* (38), 25842–25853.

(64) Damager, I.; Olsen, C. E.; Blennow, A.; Denyer, K.; Møller, B. L.; Motawia, M. S. *Carbohydr. Res.* **2003**, *338* (2), 189–197.

(65) von Bergen, M.; Jehmlich, N.; Taubert, M.; Vogt, C.; Bastida, F.; Herbst, F.-A.; Schmidt, F.; Richnow, H.-H.; Seifert, J. *ISME J.* **2013**, *7* (10), 1877–1885.

(66) Chokkathukalam, A.; Kim, D.; Barrett, M. P.; Breitling, R.; Creek, D. J. *Bioanalysis* **2014**, *6* (4), 511–524.

(67) Li, J.; Hoene, M.; Zhao, X.; Chen, S.; Wei, H.; Häring, H.-U.; Lin, X.; Zeng, Z.; Weigert, C.; Lehmann, R.; Xu, G. *Anal. Chem.* **2013**, *85* (9), 4651–4657.

(68) Ong, S.-E. *Mol. Cell. Proteomics* **2002**, *1* (5), 376–386.

(69) Müller, S. A.; van der Smissen, A.; von Feilitzsch, M.; Anderegg, U.; Kalkhof, S.; von Bergen, M. *J. Mater. Sci. Mater. Med.* **2012**, *23* (12), 3053–3065.

(70) Kliemt, S.; Lange, C.; Otto, W.; Hintze, V.; Möller, S.; Von Bergen, M.; Hempel, U. *J. Proteome Res.* **2013**, *12* (1), 378–389.

(71) Graumann, J.; Hubner, N. C.; Kim, J. B.; Ko, K.; Moser, M.; Kumar, C.; Cox, J.; Schöler, H.; Mann, M. *Mol. Cell. Proteomics* **2008**, *7* (4), 672–683.

(72) Kailemia, M. J.; Ruhaak, L. R.; Lebrilla, C. B.; Amster, I. J. *Anal. Chem.* **2014**,

86 (1), 196–212.

(73) Lawrence, R.; Olson, S. K.; Steele, R. E.; Wang, L.; Warrior, R.; Cummings, R. D.; Esko, J. D. *J. Biol. Chem.* **2008**, *283* (48), 33674–33684.

(74) Xia, B.; Feasley, C. L.; Sachdev, G. P.; Smith, D. F.; Cummings, R. D. *Anal. Biochem.* **2009**, *387* (2), 162–170.

(75) Yang, S.; Wang, M.; Chen, L.; Yin, B.; Song, G.; Turko, I. V; Phinney, K. W.; Betenbaugh, M. J.; Zhang, H.; Li, S. *Sci. Rep.* **2015**, *5* (1), 17585.

(76) Tao, S.; Orlando, R. *J. Biomol. Tech.* **2014**, *25* (4), 111–117.

(77) Kang, P.; Mechref, Y.; Kyselova, Z.; Goetz, J. A.; Novotny, M. V. *Anal. Chem.* **2007**, *79* (16), 6064–6073.

(78) Orlando, R.; Lim, J.-M.; Atwood, J. A.; Angel, P. M.; Fang, M.; Aoki, K.; Alvarez-Manilla, G.; Moremen, K. W.; York, W. S.; Tiemeyer, M.; Pierce, M.; Dalton, S.; Wells, L. *J. Proteome Res.* **2009**, *8* (8), 3816–3823.

(79) Ceroni, A.; Maass, K.; Geyer, H.; Geyer, R.; Dell, A.; Haslam, S. M. *J. Proteome Res.* **2008**, *7* (4), 1650–1659.

(80) Domon, B.; Costello, C. E. *Glycoconj. J.* **1988**, *5* (4), 397–409.

(81) Ong, S. E.; Foster, L. J.; Mann, M. *Methods* **2003**, *29* (2), 124–130.

(82) Tannock, L. R.; Little, P. J.; Wight, T. N.; Chait, A. *J. Lipid Res.* **2002**, *43* (1), 149–157.

(83) Hull, R. L.; Zraika, S.; Udayasankar, J.; Kisilevsky, R.; Szarek, W. A.; Wight, T. N.; Kahn, S. E. *AJP Cell Physiol.* **2007**, *293* (5), C1586–C1593.

(84) Roberts, A. L. K.; Thomas, B. J.; Wilkinson, A. S.; Fletcher, J. M.; Byers, S. *Pediatr. Res.* **2006**, *60* (3), 309–314.

(85) Derrick-Roberts, A. L. K.; Marais, W.; Byers, S. *Mol. Genet. Metab.* **2012**, *106* (2), 214–220.

(86) Piotrowska, E.; Jakóbkiewicz-Banecka, J.; Barańska, S.; Tylki-Szymańska, A.; Czartoryska, B.; Węgrzyn, A.; Węgrzyn, G. *Eur. J. Hum. Genet.* **2006**, *14* (7), 846–852.

(87) Sugumaran, G.; Katsman, M.; Silbert, J. E. *J. Biol. Chem.* **1992**, *267* (13), 8802–8806.

(88) Uhlin-Hansen, L.; Yanagishita, M.; Uhlin-hansens, L.; Yanagishitag, M. *J. Biol. Chem.* **1993**, *268* (23), 17370–17376.

(89) Telser, A.; Robinson, H. C.; Dorfman, A. *Proc. Natl. Acad. Sci. U. S. A.* **1965**, *54*

(3), 912–919.

(90) Solursh, M.; Hardingham, T. E.; Hascall, V. C.; Kimura, J. H. *Dev. Biol.* **1980**, *75* (1), 121–129.

(91) Altman, R. D.; Dasa, V.; Takeuchi, J. *Cartilage* **2018**, *9* (1), 11–20.

(92) Kawamura, D.; Funakoshi, T.; Mizumoto, S.; Sugahara, K.; Iwasaki, N. *J. Orthop. Sci.* **2014**, *19* (6), 1028–1035.

(93) Anastassiades, T.; Chopra, R.; Wood, A. *Mol. Cell. Biochem.* **1979**, *158* (1), 25–32.

(94) Meier, S.; Hay, E. D. *Proc. Natl. Acad. Sci. U. S. A.* **1974**, *71* (6), 2310–2313.

(95) Evangelisti, R.; Stabellini, G.; Becchetti, E.; Carinci, P. *Cell Biol. Int. Rep.* **1989**, *13* (5), 437–446.

(96) Hikino, M.; Mikami, T.; Faissner, A.; Vilela-Silva, A.-C. C. E. S.; Pavão, M. S. G.; Sugahara, K. *J. Biol. Chem.* **2003**, *278* (44), 43744–43754.

(97) Pantazaka, E.; Papadimitriou, E. *Biochim. Biophys. Acta* **2014**, *1840* (8), 2643–2650.

(98) Lin, K. H.; Maeda, S.; Inagaki, H.; Saito, T. *Biosci. Biotechnol. Biochem.* **1997**, *61* (6), 971–974.

Abbreviation list

Apo B/E	apolipoprotein B/E
ATP	adenosine triphosphate
BSA	bovine serum albumin
C-ABC	chondroitinase ABC
C-ACII	chondroitinase ACII
CE	collision energy
CMP	cartilage matrix protein
cps	count per second
CS	chondroitin sulfate
DBAA	dibutylammonium acetate
DIEA	*N,N*-diisopropylethylamine
DMEM	Dulbecco's modified Eagle's medium
DMF	*N,N*-dimethylformamide
DMT-MM	4-(4,6-dimethoxy-1,3,5-triazin-2-yl)-4-methylmorpholinium chloride
DS	dermatan sulfate
ECM	extracellular matrix
EDCI	1-(3-dimethylaminopropyl)-3-ethylcarbodiimide hydrochloride
EDTA	ethylenediaminetetraacetic acid
EGF	epidermal growth factor
EIC	extracted ion chromatogram
ER	endoplasmic reticulum
ESI	electrospray ionization
Ext	exostosin
Extl-1/2/3	exostosis-like gene 1/2/3
FA	formic acid
FAM20B	GAG xylosylkinase-named family with sequence similarity 20, member B
FGF	fibroblast growth factor
FGFR	fibroblast growth factor receptor

GAG	glycosaminoglycan
Gal	galactose
GalNAc	*N*-acetylgalactosamine
GalT	galactosyltransferase
GlcA	glucuronic acid
GlcNAc	*N*-acetylglucosamine
Gly	glycine
Gly-(Xyl)Thr-C12	N^{α}-lauroyl -*O*-*β*- D-xylopyranosyl-L-threonyl glycinamide
Gly-(Xyl)Ser-C12	N^{α}-lauroyl -*O*-*β*- D-xylopyranosyl-L-serinyl glycinamide
GM-CSF	granulocyte macrophage colony-stimulating factor
GRIP-1	GDSL esterase/lipase 1
HB-EGF	heparin-binding EGF-like growth factor
HB-GAM	heparin-binding growth-associated molecule
HBP	hexosamine biosynthetic pathway
HDL	high density lipoprotein
Hep	heparin
Hex	hexose
HexA	hexuronic acid
HexNAc	*N*-acetylhexosamine
HGF	hepatocyte growth factor
HILIC	hydrophilic interaction chromatography
HOBt	1-hydroxybenzotriazole
HPLC	high-performance liquid chromatography
HRMS	high resolution mass spectrometory
HS	heparan sulfate
ICAM-1	intercellular adhesion molecule-1
IdoA	iduronic acid
IGF	insulin-like growth factor
IP-10	IFN-γ-inducible protein of 10 kDa
KS	keratan sulfate
LC	liquid chromatoraphy
LDL	low density lipoprotein

MAC-1	macrophage-1 antigen
MMP7	matrix metalloproteinase-7
MPS	mucopolysaccharidosis
MS	mass spectrometry
MS/MS	tandem mass spectrometry
MT3-MMP	membrane-type-3 matrix metalloproteinase
N-CAM	neural cell adhesion molecule
NDST	*N*-deacetylase-*N*-sulfotransferase
NeuAc	*N*-acetylneuraminic acid
NHDF	normal human dermal fibroblasts
NMR	nuclear magnetic resonance
PDGF	platelet-derived growth factor
PECAM-1	platelet endothelial cell adhesion molecule-1
PF-4	platelet factor 4
PG	proteoglycan
*p*NP	para-nitrophenol
PTN	pleiotrophin
PyBOP	(benzotriazol-1-yloxy)tripyrrolidinophosphonium hexafluorophosphate
RANTES	regulated on activation, normal T cell expressed and secreted
SD	standard deviation
SDF	stromal cell derived factor
Ser	serine
SF	scatter factor
SLC	solute carrier
SPE	solid phase extraction
TBA	tetrabutylammonium
TFA	trifluoroacetic acid
TGFβ	transforming growth factor β
THF	tetrahydrofuran
Thr	threonine
TMSOTf	trimethylsilyl trifluoromethanesulfonate

TNF	tumor necrosis factor
TPA	tissue plasminogen activator
VEGF	vascular endothelial growth factor
Xyl	xylose
Xyl-C12	dodecyl xyloside
Xyl-Thr-C12	N^{α}-lauroyl-*O*-β-D-xylopyranosyl-L-threonamide
Xyl-Ser-C12	N^{α}-lauroyl-*O*-β-D-xylopyranosyl-L-serinamide

Publications

6.1 Articles related to the thesis

1. Otsuka Y.; Sato T. Saccharide Primers Comprising Xylosyl-Serine Primed Phosphorylated Oligosaccharides Act as Intermediates in Glycosaminoglycan Biosynthesis. *ACS Omega*. **2017**, *2* (7), 3110-3122. doi: 10.1021/acsomega.7b00073.

2. Otsuka Y.; Sato T. Comparative Quantification Method for Glycosylated Products Elongated on β-Xylosides Using a Stable Isotope-Labeled Saccharide Primer. *Anal. Chem.*, **2018**, *90* (8), 5201–5208. doi: 10.1021/acs.analchem.7b05438

6.2 Other articles

1. Otsuka Y.; Minamisawa T. Evaluation of Intermolecular Association of Glycosaminoglycan Oligosaccharides Using Nanoelectrospray Ionization Mass Spectrometry. *Eur. J. Mass Spectrom*. **2015**, *21* (4), 669-678. doi: 10.1255/ejms.1376.

6.3 Presentations at international conferences

1. Otsuka Y.; Sato T. GAG Structure Analysis of Glycosaminoglycan Intermediate Oligosaccharides Elongated on β-xylosides, 65th ASMS Conference on Mass Spectrometry and Allied Topics, Indianapolis, IN, US, June 4-8, 2017

2. Otsuka Y.; Sato T. Structure Analysis of Glycosaminoglycan-Type Oligosaccharides Elongated on Saccharide Primers and Investigation of Their Priming Abilities, Pacifichem 2015, Honolulu, HA, US, Dec. 15-20, 2015

3. Ohashi Y.; Otsuka Y.; Minamisawa T.; Hirano T. Reconfirmation of the "Charge-Localization Isomers" of Dibasic Acids Using Another GAG Disaccharide. 62th ASMS Conference on Mass Spectrometry, Baltimore, MD, US, June 15-19, 2014

4. Ohashi Y.; Otsuka Y.; Minamisawa T.; Hirano T. Confirming the Presence of "Charge-Localization Isomers" in the Disulfated GAG-Type Disaccharide. 61th

ASMS Conference on Mass Spectrometry, Minneapolis, MN, US. June 9-13, 2013

5. Otsuka Y.; Minamisawa T. Evaluation of Intermolecular Association of Glycosaminoglycan Oligosaccharides Using Nanoelectrospray Ionization Mass Spectrometry. International Society for Hyaluronan Science 9th International Conference, Oklahoma City, OK, US, June 2-7, 2013

Acknowledgements

First, I would like to deeply acknowledge my supervisor, Prof. Toshinori Sato, for his considerable guidance and cooperation during my graduate studies at the Keio University. His great knowledge, insight, and experience in glycoscience have helped me to achieve this work. Additionally, his professional attitude on scientific research has taught me how I should be as a scientist.

I wish to convey great gratitude for the thesis committee members: Prof. Masaya Imoto, Prof. Yukari Fujimoto, and Associate Prof. Daisuke Takahashi for their valuable suggestions.

I am also grateful to my colleagues at Seikagaku Corporation. Dr. Toshikazu Minamisawa has encouraged and supported me to achieve this work. Without his help, I would have never thought to pursue a Ph.D. degree. I would like to express my appreciation to Dr. Hiroshi Fujita for his support on GAG analyses. I also received much helps from Mr. Hiroshi Maeda and Kiyoshi Suzuki in carrying out experiments at the company. I also deeply thank Mr. Tetsuya Hirayama for his technical advices on chemical synthesis.

I would like to thank Dr. Yoko Ohashi of RIKEN for the very fruitful discussions. Her sincere comments have motivated me to accomplish the publications in relation to this thesis.

Finally, I would like to thank my wife and two sons for their patience, encouragements, kind support, and understanding.